2018

Engineering Surface Properties to Modulate Inflammation and Stem Cell Recruitment through Macrophage Activation

Kelly M. Hotchkiss
Biomedical Engineering

Engineering Surface Properties to Modulate Inflammation and Stem Cell Recruitment through Macrophage Activation

A dissertation submitted in partial fulfillment of the requirements for the degree of

Doctor of Philosophy at Virginia Commonwealth University

by

Kelly Morgan Hotchkiss

B.S. Materials Science and Engineering, Virginia Tech 2013

Advisor: René Olivares-Navarrete, D.D.S, Ph.D.

Assistant Professor, Biomedical Engineering

Committee Members:
Barbara D. Boyan, Ph.D.
Henry Donahue, Ph.D.
Bruce K. Rubin, M.Engr., M.D., M.B.A., FRCPC
John J. Ryan, Ph.D.

Virginia Commonwealth University
Richmond, VA
April, 2018

Acknowledgements

I would like to thank my friends, family, and boyfriend Ethan Lotz, for their continuous support and encouragement throughout my time as a Ph.D. student at VCU. I would also like to thank my committee members, specifically my advisor Dr. Olivares-Navarrete and Dr. Boyan for their advice and guidance throughout my studies and for my future as a successful researcher.

Table of Contents

List of Tables

List of Figures

List of Abbreviations and Symbols

ELISA	Enzyme linked immunosorbent assay
DPBS	Dulbecco's modified phosphate buffered saline
FBS	Fetal Bovine Serum
IL-1β	Interleukin 1 beta
IL-4	Interleukin 4
IL-6	Interleukin 6
IL-10	Interleukin 10
LPS	Lipopolysaccharide, model gram-negative bacteria
MΦ	Naïve macrophage
M1	Pro-inflammatory macrophage activated by bacteria
M2a	Anti-inflammatory macrophage activated by IL4/IL13
M2c	Anti-inflammatory macrophage activated by IL10
M-CSF	Macrophage colony stimulating factor
mSLA	Modified SLA surface, micro-nano-rough hydrophilic surface
PBS	Phosphate buffered saline
PCR	Polymerase chain reaction
PT	Pretreatment, smooth hydrophobic Ti surface
RPMI 1640	Roswell Park Memorial Institute medium
RPMI FM	RPMI 1640 media + 10% FBS + 1% Sodium Pyruvate + 1% Penicillin Streptomycin
S_a	Average surface roughness
S_{dr}	Developed surface area ration
S_{ku}	Kurtosis
S_{sk}	Skewness
SLA	Sandblasted large-grit, acid etched. Microrough hydrophobic Ti surface
TCPS	Tissue Culture Polystyrene
Th1	T helper 1 cells
Th2	T helper 2 cells
Th17	T helper 17 cells
Ti	Titanium
Treg	T helper regulatory cells
TNFα	Tumor Necrosis Factor alpha

Abstract

ENGINEERING SURFACE PROPERTIES TO MODULATE INFLAMMATION AND STEM CELL RECRUITMENT THROUGH MACROPHAGE ACTIVATION

By: Kelly Morgan Hotchkiss, Ph.D.

A dissertation submitted in partial fulfillment of the requirements for the degree of Doctor of Philosophy at Virginia Commonwealth University

Virginia Commonwealth University 2018

Major Director: René Olivares-Navarrete, D.D.S., Ph.D.

Biomaterials are becoming the most commonly used therapeutic method for treatment of lost or damaged tissue in the body. Metallic materials are chosen for high strength orthopaedic and dental applications. Titanium (Ti) implants are highly successful in young, healthy patients with the ability to fully integrate to surrounding tissue. However the main population requiring these corrective treatments will not be healthy or young, therefore further research into material modifications have been started to improve outcomes in compromised patients. The body's immune system will generate a response to any implanted material, and control the final outcome. Among the first and most influential, cells to interact with the implant will be macrophages. Throughout this study we have 1) established the ability of macrophages to recognize and differentially activate in response to material surface properties, 2) investigated the role of integrin binding in macrophage activation to material properties, and 3) confirmed the importance of macrophage activation in vivo following Ti implant placement. The generation of a hydrophilic implant surface promoted the greatest anti-inflammatory and pro-regenerative macrophage activation. Surface wettability will control protein adsorption which can activated different integrin binding on macrophages and may be responsible for changes in activation. When integrin β3 subunit binding was prevented hydrophilic surfaces no

longer promoted an anti-inflammatory macrophage activation. Additionally, when macrophage levels were reduced using two separate ablation models, MaFIA mice and clodronate liposomes, hydrophilic surfaces no longer promoted anti-inflammatory T-cell populations and cytokine profiles. There were also fewer stem cells adhered to implant surfaces at 1, 3, and 7 days when macrophage populations were compromised.

Chapter 1 | Introduction

Biomaterials are implanted into the body to treat lost or damaged tissue by replacement or as templates to facilitate regeneration. In orthopaedic or dental implants, high levels of new bone contact with the material surface resulting in high stability and lack of movement under loading will be markers of success. The immune system will determine the fate of implanted materials by a cascade of events starting with initial protein adsorption and cell interactions. This host response can lead to successful integration or encapsulation and necrosis of healthy tissue surrounding the material. Cells of the innate immune system, specifically macrophages, will be the first to respond to biomaterials. Macrophages can be activated to further promote inflammation (M1) or to modulate the immune response and lead to tissue regeneration (M2). Recent studies have focused on surface modification procedures to instruct stem cell differentiation to promote tissue regeneration, however, the ability of these surface modifications to instruct inflammation and recruit stem cells to the implant site should be considered first. The **overall goal** of this study is to determine how material surface properties can alter macrophage activation in inflammation and control healing following implantation of biomaterials. The **general hypothesis** is that surface wettability will control protein adsorption and ultimately rate of healing. Hydrophilic surfaces will promote protein adsorption resulting in anti-inflammatory macrophage activation and hydrophobic surfaces generating an elevated inflammatory response. Changes in levels of inflammation can promote or prevent the progression of the healing process and regulate tissue regeneration. By designing implant surface properties to control inflammation and

promote regeneration, the success of implants in impaired healing cases can be achieved. Success of biomaterial implantation is reduced in patients with increasing age and elevated basal levels of inflammation.

Significance

The implantation of synthetic materials as a treatment for injury and disease has become increasingly popular in recent years. Engineering design concepts led to the selection of these biomaterials being focused on how their bulk properties could best mimic characteristics of natural tissues. With metals, high stiffness polymers, and ceramics being selected for bone tissue implantation, soft polymers or hydrogels used for muscle, brain or skin, and degradable polymers for temporary and drug delivery applications. This strategy resulted in a range of outcomes from success to failure and further damage to the patient. Successful biomaterial outcomes consist of integration with surrounding tissue, regeneration, or full degradation without damage to surrounding tissue. An orthopeadic or dental implant will be considered a success with high levels of new bone in contact with the material surface resulting in high stability and lack of movement under loading. One of the most well-known failures being seen in the fibrous encapsulation of silicone breast implants, which results in a dense scar tissue forming around the material. A fibrous capsule will wall off the material from surrounding tissue[1]. Each material may have different surface properties, but most original designs consist of a smooth outer surface. While the structural properties are important for the ultimate function of the implant, the initial host response should also be considered. If a material is not first accepted by the body, it will not interact long enough to fulfil its ultimate function. New strategies in tissue engineering and regeneration have aimed to control cell

response to improve host response to the material. It has been hypothesized that the increased stem cell differentiation is the cause of the improved integration of the material, however these cells will not be the first to interact with the material. Controlling the levels of initial inflammation will allow for the process of osseointegration to begin. Success rates of around 95% have been shown clinically in titanium (Ti) implants with surface modifications to generate roughness and increased wettability in healthy patients [2] without added medical considerations. Success rates are reduced in patients with reduced healing and increased inflammation, such as the elderly and smokers. By understanding how materials surface modifications alter immune response we can select implants to improve patient healing outcome.

Chapter 2 | Specific Aims

Specific Aim 1: Determine if material surface properties can modulate macrophage activation. The ability of macrophages to differentially respond to changes in surface properties will allow them to modulate inflammation and healing following implantation. *The objective is to determine if macrophages will respond to different surface properties and if this response will affect surrounding cell types. The hypothesis is that chemical surface properties will have a stronger effect on macrophage activation.* Surface properties such as roughness, wettability, and chemistry were tested on clinically relevant materials in a cell culture model to determine macrophage activation.

Specific Aim 2: To elucidate the mechanism of macrophage activation in response to different material surface properties. The traditional methods of classification of these cells is considered a spectrum from pro-inflammatory M1 to anti-inflammatory M2. The cells will not interact directly with the material surface, but rather with an assembled layer of protein at the interface. *The hypothesis is that integrin binding to ECM domains will be the main modulator of macrophage activation in response to surface properties.* Additionally, shRNA silencing of Intb1 and Intb3 in RAW 264.7 cells and blocking antibodies (ITGB1, ITGB2, and ITGB3) were used to determine influence of integrin signaling.

Specific Aim 3: To determine the role of material surface induced macrophage activation in the response to implanted materials. An interfemoral implant model will be used to test macrophage activation and cell recruitment during initial healing response. *We hypothesize that activated macrophages will secrete soluble factors to recruit other*

cells to material surface and be important in regulating immune events over the first week following implant placement. The role of macrophage response to Ti implants was tested through control C57B/l6 mice compared to two models of macrophage reduction clodronate liposome injections and MaFIA mice. Immune cell populations were characterized by flow cytometry in bone marrow surrounding the implant and spleen of each animal. Levels of systemic inflammatory markers were measured by ELISA in circulating plasma.

Chapter 3 | Background

3.1 Biomaterials

The use of implantable artificial materials in the body is becoming increasingly used in medicine as the population ages and medical treatments advance. The initial choice of which material to use in the body was based on matching the mechanical properties of the lost or damaged tissue while also being minimally toxic. Some first generation biomaterials used in high strength bone and tooth applications included metals and ceramics such as gold, platinum, aluminum, and porcelain [3], which were assumed to be mostly “bioinert”, or to elicit little response from the body. The inflammation and fibrous encapsulation of these materials led to the introduction of additional metals, such as titanium (Ti), Ti alloys and stainless steel. As the field progressed, second generation biomaterial designs were developed which aimed to achieve successful integration of materials with the host through improved cell interaction at the bio interface. These materials applied surface coatings such as heparin to improve cell response and biocompatibility. The third generation has sought to not only improve cell response, but to stimulate a specific response through changes in surface or bulk properties as well as the addition of bioactive molecules and coatings[4], [5].

Biomaterials may be implanted in the body for many different clinical applications including cell transplantation[6], drug release[7], and tissue regeneration[8]–[10]. The success of these implanted materials is usually determined several months after collocation, which may be too late to determine the cause of a failed implant. Implanting synthetic materials into the body can result in a range of outcomes from complete success

to failure. Success of the material is characterized based on its intended application. For structural implants, success is determined by the ability of the construct to promote tissue regeneration and lack of adverse effects to the surrounding healthy tissue. Successfully regenerated tissue should replace natural tissue in both function and appearance. Failure of an implanted biomaterial may result in death of surrounding tissue or a fibrous capsule forming around the implant preventing interaction with the body and secretion of factors from an implanted device. The encapsulation of a material can prevent the ability to integrate with surrounding tissues [1], which is extremely important in structurally important materials such as bone applications, and the ability for factors to diffuse out of a material in cases of drug delivery devices.

3.1.1 Dental and Orthopaedic Implants

Metals are commonly implanted in high strength tissues such as bone to replace or repair damaged tissues and restore function for both orthopaedic and dental applications[11], [12]. A metallic implant must be able to fully integrate with surrounding bone tissue, termed osseointegration, to allow for the necessary support and to prevent micro motion that could result in particle release. Titanium (Ti) or titanium alloy dental implants are a common therapeutic means to treat edentulous individuals [13], [14] and are highly successful in healthy patients. The application of surface modification procedures to increase surface roughness and wettability have further increased implant stability and reduced healing times.

3.2 Surface Modifications

Surface properties of biomaterials can be altered by either additive or subtractive methods. The additive methods consist of material being added to the surface in an effort

to improve biocompatibility. Coatings can be added by methods such as plasma spraying of a thermally melted material onto the surface of another material which can build up surface topography and add functional groups to promote a beneficial cell response [15]. Prolonged exposure to simulated body fluid has been shown to breakdown the bonding between the original material and coating [16], which can result in shedding or shearing off of surface layers and creation of debris.

Subtractive modification methods will remove a portion of the outermost layer at the surface. The most common subtractive techniques applied to metals are blasting with sands or ceramic particles, acid etching, [17] and anodization. Blasting treatments, considered physical modifications, mechanically remove surface oxide layers to expose the core material and typically generate a macro or micron sized topography based on blasting parameters such as particle size and pressure. Chemical treatments etch away the surface layer using either alkaline or acidic solutions which react with the surface and remove contaminants, sand particles, and the surface layer. These modifications typically alter the nano-topography of the material. Application of these procedures will result in changes in the topography, chemistry, and wettability of the material [18].

3.3 Previous Studies with Titanium

The increased surface roughness generated by sandblasting and acid etching Ti to create micro rough Ti (SLA) has been shown to promote stem cell differentiation toward an osteoblastic lineage compared to smooth Ti (PT) and classical tissue culture polystyrene (TCPS) substrates [19], [20]. Additional modifications have resulted in a hydrophilic surface (mSLA) by storage in a saline solution following the sand-blasting and acid-etching procedure. This storage method maintains the surface hydrophilicity as well

as promotes the formation of nanostructures on the micro-rough SLA surface. The increased wettability and generation of nanostructures is consistent between Ti and alloys with metals having similar α and β structure transitions, such as TiZr [21]–[23]. *In vitro* assessment has shown an increase in osteogenic and angiogenic factors released from osteoblasts and stem cells cultured on micro structured, hydrophilic Ti surfaces (mSLA) [20], [22]. *in vivo* studies have found reduced healing times and increased bone-implant contact in high-energy, micro-rough Ti [24]–[29].

3.4 Immune System

The immune system consists of two separate but interconnected branches, the innate and adaptive. The innate immune system protects the body through physical barriers and phagocytic cells including macrophages, neutrophils and dendritic cells. Innate immune cells react to a perceived threat in two ways, protein release and microenvironment conditioning or direct contact to destroy pathogens and instruct other cells. Following interaction with foreign objects, macrophages will be activated toward an anti- or pro-inflammatory phenotype or along the gradient between the two. Anti-inflammatory activated macrophages will release high levels of immunomodulatory factors to attenuate the response such as interleukins (IL) and chemokines [30], [31]. Pro-inflammatory macrophage activation triggers the release of ILs and other proteins that promote inflammatory cell recruitment and prolong the response [32], [33]. If the innate system is not able to control the response alone, it can activate the adaptive immune response through factor release and antigen presentation. Antigens presented to the adaptive system typically result from the degradation products of an object that has been engulfed and broken down by dendritic cells or macrophages [34].

Antigen presenting cells (APC), like macrophages and dendritic cells, are responsible for activating T cells of the adaptive immune system. T cell activation, specifically CD4+ helper-T cells, can result in a prolonged response. T-helper cells are the most influential in directing the continued immune response to foreign elements in the body. There are several phenotypes of T-helper cell subpopulations, the most prevalent being type 1 helper cells (Th1), type 2 helper cells (Th2), type 17 helper cells (Th17), and T regulatory cells (Tregs). Each subtype of T-helper cells can specifically alter the immune response through the secretion of cytokines. Classically, Th1 cells activate macrophages and promote inflammation via secretion of interferon gamma (IFN-γ) and commonly characterized by the expression of T-bet [34], [35]. Th2 cells are capable of alternatively activating macrophages to reduce inflammation through production of IL-4 and IL-13. This alternative Th2 activation is marked by increased expression of the Gata3 transcription factor [35], [36]. Th17 cells are characterized by the production of IL-17, IL-21, and IL-22, as well as the induced expression of retinoid-related orphan receptor γt (RORγt) [37]. While Tregs are known for regulating inflammation through the release of increased levels of immunomodulatory IL-10 and characterized by increased expression of transcription factor forkhead box 3 (Foxp3). Th2 and Treg helper cells are considered the most important for tissue regeneration [9], [38], [39].

It is well established that the adaptive immune system determines how xenografts and allografts are accepted after implantation. However, it is not clear whether elements of the adaptive immune system, particularly T-helper cells, contribute to the healing and regenerative response after biomaterial implantation. While it is known that biological implants may be rejected if the immune system becomes activated after antigen

processing and presentation, many of these principles have been under-represented when considering synthetic biomaterials.

3.5 Immune Response to Injury

The surgical procedures to place metallic implants in the body cause trauma that initiates a cascade of immune events. Tissue healing following this injury depends on a multitude of tightly regulated biological processes controlled by various cells and molecules in the immune system [40]. The body's defense to the material is based on signals produced by the first cells to enter the site following the surgical procedure and to interact with the implant material [9]. These cells not only mount the initial response but control the recruitment of tissue regenerating stem cells. Macrophages are be among the first cells to arrive and begin to clean up the damaged tissue [41], [42]. Once at the site cells produce growth factors, chemokines, and cytokines that recruit additional immune cells to the site, and in a normal wound healing response, induce phagocytosis of the damaged cells/tissue and stimulate the wound healing process. Macrophages are responsible for the initial immune response, inflammation, and maintaining tissue homeostasis [43]–[45]. Control of the levels of inflammation can either promote or prevent the progression of the healing process and the regulate tissue regeneration.

3.6 Macrophage Activation

The ability of macrophages to be activated by bacteria, viruses, and danger signals has been studied for many years. An immune response may be activated by danger associated molecular patterns (DAMPs). These are molecules released by non-apoptotic cell death and signal tissue damage and danger to the body [23]. Examples of DAMPs, also known as alarmins, include high mobility group box 1 (HMGB1), S100 proteins, heat

shock proteins, IL-1α, and uric acid. These molecules are released when cell membranes are ruptured and allowed to enter into the extracellular environment. One of the more potent and studied alarmins is HMGB1, which signals through the receptor of advanced glycation end-products (RAGE) [24], [25]. This molecule is known to facilitate the maturation of myeloid derived immune cells as well as the recruitment and proliferation of mesenchymal stem cells (MSCs) [26]–[28]. These molecules will be present due to damage occurring in the initial surgery and may become trapped in the assembled matrix on the material surface to produce a continue signaling.

Macrophages may be activated to different phenotypes that are characterized by the cytokine release profile of the cells. This activation may be to a “classical” pro-inflammatory M1 or “alternative” anti-inflammatory M2 response, or somewhere between the two extremes. The M1 response is an acute, destructive, clearing response characterized by high levels of the three most common inflammatory interleukins: interleukin (IL)1β, IL6, and tumor necrosis factor alpha (TNFα) [45]–[47]. Typical M1 macrophages appear as round and flattened in shape [48]. The anti-inflammatory M2 response is characterized by high levels of IL4, IL10, and transforming growth factor beta-1 (TGFβ1) [20], [49], [50] and more recently expression of genes Ym1 (Chil3) and Fizz1 (Retnla). The M2 activation has also been characterized by its elongated shape [48]. This “alternative” activation controls and/or suppresses the immune response and facilitates blood vessel formation and wound healing [51], [52]. The ability of a material surface to control the reaction of these cells will influence the host’s initial response to the device, and ultimately decide the integration of the material.

Our group has shown that macrophages respond to differences in titanium (Ti) surface properties like roughness, wettability, and chemistry [53], [54]. Changes in these properties can control the polarization of naïve macrophages towards either a pro-inflammatory phenotype (M1-like) or an anti-inflammatory phenotype (M2-like) [45]–[47], [50]. Anti-inflammatory macrophage activation was generated on rough-hydrophilic implants, which correlate with high success rates and reduced healing times of rough-hydrophilic metallic implants in clinical settings. These same materials promote stem cell osteogenesis *in vitro* [2], [19], [28], [55].

3.7 Immune Cells in Fracture Healing

Healing occurs differently in highly stabilized and non-ridged fractures. Mechanically stabilized breaks are healed with inflammation, anabolic repair, followed by a prolonged remodeling phase. Non-ridged fracture healing occurs through endochondral ossification [30]. This process also begins with inflammation, followed by soft callus and hard callus formation, and finally remodeling. Macrophages are responsible for promoting initial levels of inflammation to clear the wound site of tissue debris and apoptotic neutrophils [31]. Too great a reduction of this critical step has been shown to impair the full repair of a wound site. Additionally, a prolonged immune response will prevent the progression of healing. Following the first stage of inflammation, macrophages release matrix metalloproteinases (MMPS) required for the breakdown of the initial collagen formation allowing for reorganization of the matrix [30], [56]. Without the initial immune response led by macrophages, normal bone formation cannot occur, as demonstrated in fracture healing studies with delayed callus formation following macrophage ablation [30], [57]–[59].

3.8 Cell-Material Interactions

In order to improve the immune response of a material it is important to understand how cells are able to recognize and respond. Immediately following implantation, proteins from blood and interstitial fluids adsorb to the material surface [60]. The performance of an implanted biomaterial is dependent on its interaction with the host immune system [60], [61] and the foreign body reaction generated. These interactions can lead to persistent inflammation, the formation of foreign body giant cells, fibrosis, and damage to the surrounding tissue. The formation of fibrosis surrounding the material can occur within 1 month and completely segregate the material from surrounding tissue. Normal wound healing occurs in four overlapping phases: hemostasis, inflammation, proliferation and remodeling [62]. Upon initial contact cells will not interact directly with a material surface, but with the layer of proteins adsorbed to the surface [63], [64]. Material properties have been shown to control the type and arrangement of proteins on the surface [65]. This initial response can increase or reduce the rate of osseointegration of the implant [44], [60].

3.9 Extracellular Matrix Binding

Cells interact with extracellular matrix (ECM) proteins through integrin binding. Integrins are heterodimer transmembrane molecules responsible for cell interaction with proteins in the extracellular matrix and other cells. These receptors consist of non-covalently associated α and β subunits [49], [66]–[68]. The binding of two associated subunits can activate intracellular signaling pathways to promote differentiation or activation of cells. Cells of the innate immune systems have been shown to express β-subunits 1, 2, 3 and 7 [69]. Differing levels of these molecules are expressed on immune

cells based on the degree of differentiation and location of the cell. Immune cells rely on integrin binding to migrate through tissue to sites of inflammation. The β_1 integrin is the dominant adhesion mechanism to extracellular matrix ligands for many mesenchymal cell types including connective, muscular, neural, and epithelial cells [67], [68]. In addition to supporting adhesion, spreading, and migration, these binding units activate various intracellular signaling pathways controlling gene expression and protein activity responsible for higher order cellular functions [70]. The function of leukocytes is highly dependent on integrin units containing the β2 subunit (CD18), particularly $\alpha_M\beta_2$ (Mac-1), control monocyte and macrophage binding to ligands including fibrinogen, fibronectin, and IgG. Binding of $\alpha_M\beta_2$ integrin to fibrinogen adsorbed to material surface controls initial recruitment and accumulation of immune cells to the site of implantation [10], [67], [71].

3.10 FAK vs Podosome

Macrophages travel through tissues to sights of infection or tissue damage and are responsible for regulating the host rapid response. Due to the need for rapid migration through ECM, macrophage do not form well defined actin stress filaments as are seen in stem cells or osteoblasts [72]. Therefore, while each cell type binds to surrounding extracellular matrix through integrins, the more mobile immune cells don't form the distinct focal adhesion bundles seen in stem cells. These cells sense the surface through podosomes which appear as less defined rings. Podosomes appear as rings of tightly bundled surface and intracellular proteins. They allow for macrophages to resorb small footholes out of the ECM to pull themselves forward through matrix. Interaction between Arp2/3 and N-WASP proteins are essential for the formation of podosomes. Immune cells from children with Wiskott Aldrich Syndrome (WAS) have a mutation in the WASP gene

and display abnormal cytoskeletal structures, including a lack of podosome formation [73]. This prevention of podosome formation leads to inadequate infection control. Podosomes not only allow immune cells to sense the surface, but also secrete factors to dissolve through ECM to reach sites of interest.

3.11 Reduced Healing

Optimal healing following an injury consists of a series of events including rapid hemostasis, inflammation, mesenchymal stem cell migration and differentiation, angiogenesis, re-epithelialization and synthesis of collagen. A breakdown or inappropriate response at any of these events can lead to impaired healing. Increased age will impair healing and regeneration in patients both healthy and with other complications. Clinical and animal studies have examined age-related changes in delayed wound healing. A delay in healing with ultimate successful healing[74] is seen in healthy elderly individuals [75]. This delay is thought to be due to an altered inflammatory response and reduced cell infiltration and reduced phagocytic activity by macrophages at sites of damage.

3.12 Macrophage Ablation Models

Several different animal models have been developed to study the role of macrophages in different bodily processes. Each model can be used to remove a specific subset of macrophages, but will also eradicate other cells sharing characteristics or surface markers to macrophages. Cells possessing the CSF1R can be removed in the macrophage Fas-induced apoptosis (MaFIA) transgenic mouse by injection of a synthetic dimerizer (AP20187). The coupling of multiple CSF1Rs will induce apoptosis in all myeloid lineage cells, monocytes, macrophages, dendritic cells and osteoclasts. The

synthetic molecule can be delivered through intravenous or intraperitoneal injection to achieve up to 80% target cell ablation[76], [77].

Mature phagocytic cells can be ablated by injecting clodronate filled phospholipid liposomes ranging from 30-200um[56], [78]–[80]. These cells include both macrophages and neutrophils but may be limited to more “pro-inflammatory” activated macrophages triggered to phagocytize particles in the microenvironment. The liposome size is designed to be too large to diffuse through the cell membrane, therefore the clodronate can only be taken up by phagocytic cells. Clodronate is a bisphosphonate that is known to induce apoptosis at elevated intracellular concentrations.

Chapter 4 | Standard Methodologies

Similar metallic materials were used throughout the following studies and were characterized by standard methods presented here.

4.1 Surface Creation

Titanium (Ti) and Ti alloy disks were provided by Institut Straumann AG (Basel, Switzerland) for these studies. Each disk was created by a 15 mm punch from 1 mm thick sheets of grade 2 unalloyed Ti. The disks were sized to fit securely in a 24 well plate for *in vitro* cell culture. Disks were cleaned and degreased by acetone bath, and then processed in a 2% ammonium fluoride/2% hydrofluoric acid/10% nitric acid solution at 55°C for 30 seconds to produce the pretreatment (PT) smooth Ti surfaces. Rough Ti surfaces were created by coarse-grit sand blasting smooth disks with 0.25-0.50 mm corundum followed by acid etching in a mixture of HCl and H_2SO_4 to create surface structures and roughness at the macro and micro scale (SLA). Hydrophilic rough Ti (mSLA) disks were created using the same procedure as rough Ti but were rinsed under nitrogen protection to prevent air exposure and immediately stored in an isotonic NaCl solution in sealed glass tubes until use. This process results in a hydrophilic surface with roughness at the micro-, submicron-, and nano-scale. Disks were sterilized by γ-irradiation.

4.2 Surface Characterization

4.2.1 Laser Scanning Confocal Microscopy

The roughness generated under each surface condition was determined by laser scanning confocal microscopy (LSCM, Zeiss LSM 710, Carl Zeiss). Measurements were taken with a scan size of 600 µm x 600 µm with a 20-x lens. Roughness values (average roughness over area: S_a, skewness: S_{sk}, kurtosis: S_{ku}, and developed interfacial area ratio: S_{dr}) were calculated with a 100 µm threshold. Measurements were taken at three different points on each disk.

4.2.2 Scanning Electron Microscopy

Qualitative assessments of macro-, micro-, and nanostructure of each surface were acquired by scanning electron microscopy (SEM, Zeiss Auriga, Carl Zeiss, Jena, Germany) at 1kx and 100kx magnifications. Disks were analyzed without the addition of a conductive coating with a secondary electron detector at 5kV, under vacuum and a distance of approximately 2mm.

4.2.3 Contact Angle

The wettability of each surface type was indirectly measured by sessile drop contact angle (ramé-hart contact angle goniometer 250, model 100-25a, ramé-hart instrument co., Succasunna, NJ). Measurements using 1µL drops of deionized water were taken at three locations of six disks per surface condition. A contact angle of 0° considered hydrophilic and greater than 80° considered hydrophobic.

4.2.4 X-ray Photo Spectroscopy

The chemical composition of the surface was determined by X-ray photoelectron spectroscopy (XPS, ESCALAB 250, Thermo Scientific, Waltham MA) under ultra-high

vacuum (10^{-9} Torr or below) with a microfocused monochromatic AlKa x-ray source. The focus of the XPS was to assess differences in carbon levels; therefore, disks were secured to the mount with stainless steel clips in order to remove potential carbon readings from the adhesive tape. Prior to analysis clips and mount were sonicated in acetone to remove contaminants. Survey scans were completed at each region, followed by high-resolution scans for C1s, Ti2p, Zr3d, O1s, Na1s, and Cl2p. Scans were aligned to the binding energy of the C1s peak at 284.8 eV. Thermo Advantage software was used to evaluate spectrum results. Each surface characterization procedure was performed on three regions of six disks per surface condition. modSLA surfaces were rinsed in ultrapure water prior to each surface characterization procedure.

4.3 Cell culture

In each study, primary murine macrophages were isolated from femurs of 6-8 week-old male C57BL/6 mice (The Jackson Laboratory, Bar Harbor, ME) under VCU IACUC approval (AD10001108) using published methods [17]. Briefly, bone marrow cells were flushed from the femurs using Dulbecco's phosphate-buffered saline (Life Technologies, Carlsbad, CA). Red blood cells were lysed from bone marrow extract with ACK Lysing Buffer (Quality Biological, Inc., Gaithersburg, MD). Cells were counted (TC20™ Automated Cell Counter, Bio-Rad Laboratories, Hercules, CA) and plated in a 75 cm^2 flask at a density of 500,000 cells/mL in 10mL RPMI 1640 media (Life Technologies) supplemented with 10% fetal bovine serum (Life Technologies), 50U/mL penicillin-50 µg/mL streptomycin (Life Technologies), and 30ng/mL macrophage colony-stimulating factor (M-CSF, PeproTech, Rocky Hill, NJ). Cells were cultured at 37°C, 5% CO_2, and 100% humidity. Fresh media supplemented with M-CSF was added after four days. After

differentiation cells were passaged with Accutase and plated on surfaces for 1 and 3 days in a 24 well plate with 6 cultures per group (n=6).

4.4 Gene Expression

To assess changes in gene expression, supernatant was removed and TRIzol (Invitrogen, Life Technologies) added to extract mRNA of cells adherent to the surface and 1µg cDNA generated for quantification of gene expression of pro- and anti-inflammatory cell markers through quantitative polymerase chain reaction (qPCR).

4.5 Protein Analysis

In each study, differentiated, un-activated macrophages were plated at a density of 50,000cells/cm^2 RPMI 1640 culture medium without M-CSF. Cells plated on tissue culture polystyrene (TCPS) served as a control of naïve macrophages. Conditioned media were harvested from cell cultures 24 and 72 hours after plating. Medium was changed 24 hours prior to harvest. Levels of IL1β, IL4, IL6, IL10, and TNFα in the conditioned media were measured by enzyme-linked immunosorbent assays (ELISA, PeproTech) following the manufacturer's protocol. Immunoassay results are presented as normalized to dsDNA content in cell lysates. Cell monolayers were washed in PBS, lysed in 0.05% Triton X-100, and homogenized by sonication. DNA levels were quantified in cell lysates using the Quant-iT™ PicoGreen dsDNA Assay Kit (Invitrogen, Life Technologies) as per manufacturer protocol.

4.6 Statistical Analysis

Surface characterization experiments were conducted on a minimum of three regions of six separate disks per surface condition. Each cell study experiment was conducted with six independent cultures per surface. Experiments were performed at least twice to ensure consistent results; presented data are from one experiment. A one-factor, equal-variance analysis of variance (ANOVA) was used to test the null hypothesis that the group

means are equal, against an alternative hypothesis that at least two of the group means are different, at the α=0.05 significance level. Upon determination of a *p*-value less than 0.05 from the overall ANOVA model, multiple comparisons between the group means were made using the Tukey-HSD method. All statistical analysis was completed using JMP pro11 or GraphPad V5 software.

Chapter 5 | Aim 1

Modulation of Macrophage Activation by Material Surface Properties

5.1| Introduction

The main focus in innovation for metallic biomaterials has been the application of surface modification procedures. The effect of different surface properties on stem cell differentiation and osteoblastic maturation has been previously demonstrated *in vitro* and *in vivo.* Clinically, the used of hydrophilic implants have shown faster healing times compared to hydrophobic implants. However, cells of the immune system, specifically macrophages, will arrive at the site of implantation prior to stem cell differentiation and control the healing cascade. To compare the effect of each surface property on macrophages, first the differences in surface properties of clinically used materials were characterized. Followed by a comparison of macrophage response to each property (roughness, wettability, and chemistry) individually. *The overall objective is to determine if macrophages will respond to different surface properties.* Previous studies from our group and others have shown an increased osteoblastic differentiation in stem cells cultured on surfaces with increased roughness and wettability. *The hypothesis is that surface modifications affecting wettability will have a stronger effect on macrophage activation.*

5.2| Changes in Macrophage Activation due to Roughness

Results and Discussion

Surface Characterization

Disks modified by sandblasting and acid etching created a surface with a more similar topography to osteoclast conditioned bone than the smooth PT surfaces [18]. A qualitatively similar microstructured surface was seen in SEM images of the rough surfaces. We selected this imaging technique due to the high micron-scale roughness of the disk topography. While atomic force microscopy would allow for the assessment of nanostructures on a smooth surface, it may not accurately measure the large-scale roughness [19]. The tapping mechanism used for surface roughness assessment in AFM prevents the accurate perception of steep peaks and valleys, which may be generated as a result of sandblasting treatment. In addition, a sample height of greater than 20 μm and scan area of less than 150 μm x 150 μm is necessary to use this technique [20]. LSCM was selected as the optimal method for surface roughness measurements due to these limitations. This characterization method can select a larger scan area to give a better overall description of disk roughness. Smooth disks were determined to have a lower average roughness (S_a) value than both rough and hydrophilic rough surfaces. No difference was detected between the average roughness of either rough surface.

Cell Response

Initial studies showed similar levels of DNA present on each Ti surface and the TCPS control which indicates the ability of macrophages to attach to and interact with the surfaces being tested. Increased levels of both pro- and anti-inflammatory associated cytokines from macrophages cultured on micro-rough surfaces (SLA) compared to

smooth Ti (PT). Alternatively, macrophages cultured on the micro-submicron rough hydrophilic mSLA surface released reduced levels of pro-inflammatory and further increased levels of anti-inflammatory factors. These results were consistent with previous results from our lab considering the release of inflammatory factors from stem cells cultured on Ti surfaces. An additional study was conducted to establish a time line of macrophage activation in response to material surface properties (Figure 5.2.1). The level of pro-inflammatory factors showed a steep increase from 6 to 12 hours, at which point SLA continued to increase and mSLA began to reduce levels and result in lowest level at 24 hours. The highest level of anti-inflammatory factors were released from macrophages on mSLA at each time point, ultimately resulting in the highest level at 24 hrs (Figure 5.2.2).

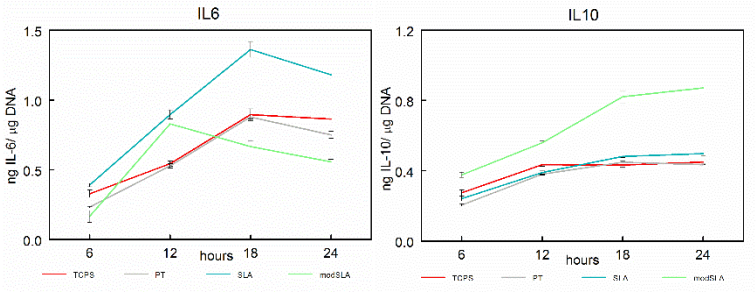

Figure 5.2.1: Time course of cytokine release profile of macrophages cultured on Ti PT, SLA, and mSLA for 24 hours.

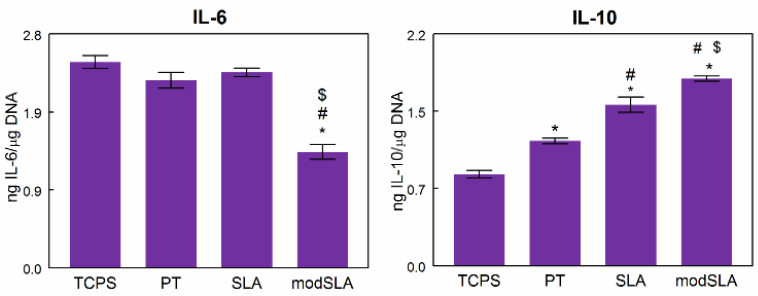

Figure 5.2.2: Increased surface roughness results in elevated levels of pro and anti-inflammatory factors. *p<0.05 vs. TCPS, # vs. PT, $ vs. SLA

Previous studies have shown an improved implant success rate in correlation with the increase in surface roughness and wettability. An increase in the differentiation of MSCs and their production of osteogenic and angiogenic microenvironment has been shown to occur with increased roughness and wettability of a Ti surface [24]. High success rates of bone substitute materials such as beta tri-calcium

phosphate with microstructure have also been studied [25, 26]. However, the resorption of these materials makes it difficult to determine if the success is due to activation of macrophages or osteoclasts in the remodeling of material and bone following implantation. The importance of the interaction of immune cells and biomaterial surface has been previously established [27]. Successful implant integration relies on a balance of classically activated (M1) macrophages to clear the wound site coupled with anti-inflammatory (M2) activated macrophages to promote wound healing and regeneration. A consistently high M1 response will recruit additional immune cells to the site, and this chronic inflammation can lead to fibrous encapsulation instead of successful tissue integration. The ability to control the ratio of M1 and M2 macrophages at the host-biomaterial interface will allow damaged tissue to be removed without a prolonged immune response that can lead to the creation of foreign body giant cells and inhibition of healing and integration.

5.3| Changes in Macrophage Activation due to Wettability

A second study was designed to determine if the different cell response measured between cells cultured on SLA and mSLA was due to the presence of submicron structures on the surface or the increase in wettability. Cells were cultured on two different sets of commercially pure Ti surfaces with matching surface topography and opposite surface wettability.

Study Specific: Materials and Methods

A set of hydrophilic, smooth and rough disks were created by oxygen plasma cleaning (pPT, pSLA) as established in prior experiments [15, 16]. Disks were treated in an oxygen plasma cleaner (PDC-32G, Harrick Plasma, NY) at a medium radio frequency for 2

minutes per side. A hydrophobic surface was created by sonicating hydrophilic rough Ti surfaces in ultrapure water for 10 minutes in two cycles to remove the residual saline solution and aged by exposure to air for two weeks under sterile conditions.

Results and Discussion

Surface Characterization

The wettability was successfully altered by our treatments. pPT, pSLA, and hydrophilic-rough Ti (mSLA) were hydrophilic with water droplets spreading completely on the surfaces and a contact angle of 0°, while smooth PT (93.6°), rough SLA (120.9°), and aged hydrophilic-rough(mSLA) (110.4°) surfaces were hydrophobic (Figure 5.3.1).

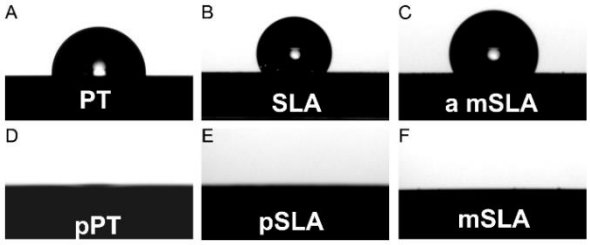

Figure 5.3.1: Surface modification procedures were successful in generating surfaces with matching surface topography and opposite wettability.

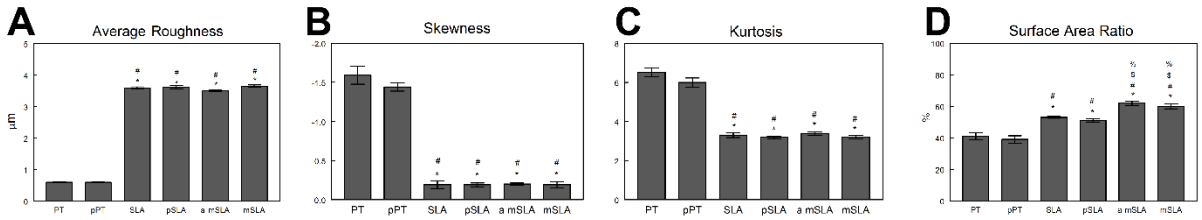

Figure 5.3.2: Surface modification procedures did not alter roughness profiles of surfaces. *p<0.05 vs. PT, # vs. pPT, $ vs. SLA, % vs. pSLA, & vs. a mSLA

The surface roughness was characterized using parameters of average roughness (S_a), skewness (S_{sk}), kurtosis (S_{ku}) and developed interfacial area ratios (S_{dr}). The

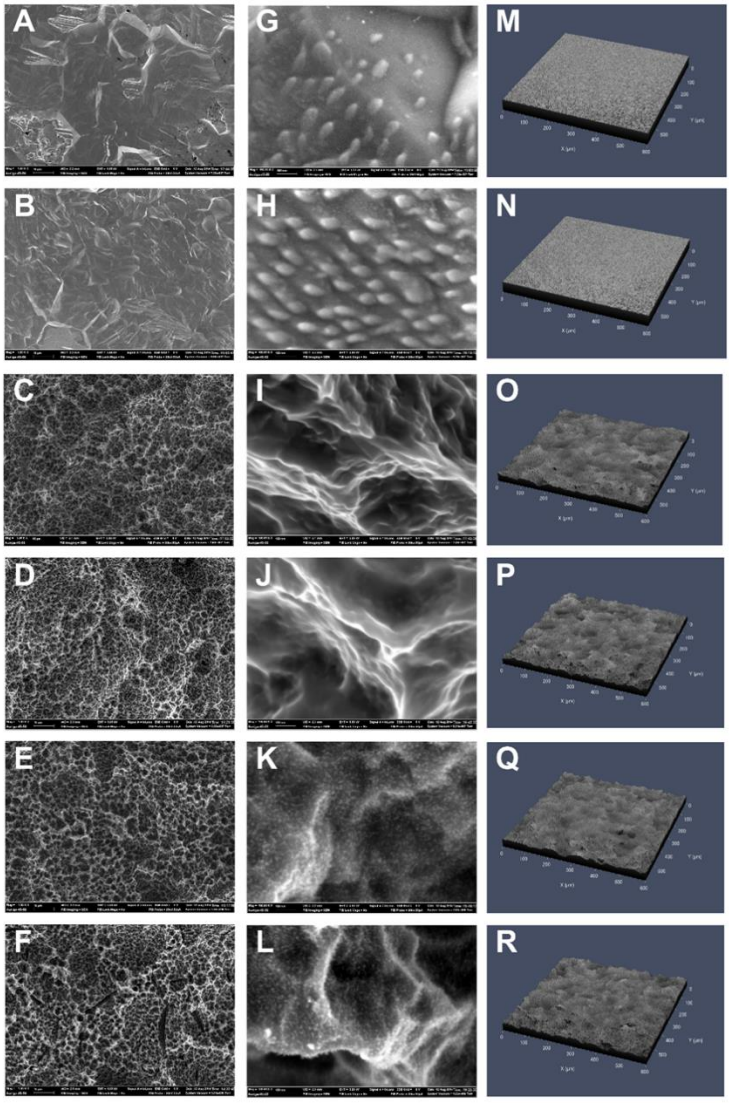

Figure 5.3.3: Qualitative SEM low magnification A-F, and high magnification G-L, and topographical Z-stack LSCM M-R images on Ti surfaces.

application of wettability modifications did not change the surface roughness of the disks in any of the three parameters measured. The average roughness of smooth was found to be 0.59 µm ± 0.019 µm and the average roughness of pPT was 0.59 µm ± 0.023 µm. Both were significantly less rough than all micro structured surfaces. The roughness values of the four micro-rough surfaces were not significantly different. The average roughness of SLA Ti was 3.58 µm ± 0.042 µm and pSLA Ti was 3.61 µm ± 0.047 µm, hydrophilic-rough was 3.64 µm ± 0.029 µm and aged hydrophilic-rough was 3.49 µm ± 0.029 µm. Skewness values are a ratio between peaks and valleys present throughout the surface microstructure, which represents the symmetry between peaks and valleys. A negative value is indicative of more distinct valleys and positive is more distinct peaks about the average plane. Skewness measurements were -1.59 ± 0.114 on PT and -1.44 ± 0.053 on pPT while

rough surfaces displayed skewness of rough Ti -0.19 ± 0.048, pSLA Ti -0.19 ± 0.024, aged hydrophilic-rough Ti -0.20 ± 0.014, and hydrophilic-rough Ti -0.19 ± 0.042. The kurtosis value assigns a number to the relative steepness of each peak. Kurtosis values were 6.52 ± 0.218 for PT Ti, 5.99 ± 0.231 for pPT and 3.30 ± 0.125 on SLA Ti, 3.19 ± 0.067 pSLA, 3.39 ± 0.088 aged hydrophilic-rough, and 3.19 ± 0.086 hydrophilic-rough Ti indicating smaller but sharper peaks present on smooth surfaces in comparison to the rough (Figure 5.3.2 and Figure 5.3.3). The developed interfacial area ratios were similar between both smooth Ti surfaces (41% ± 2.2% and 39% ± 2.3%), between the two rough Ti surfaces (53% ± 0.6% and 51% ± 1%) and finally the two micro and nano rough Ti surfaces (62% ± 1.3% and 60% ± 1.5%). Near positive skewness values (S_{Sk}) on each microrough surface indicated a greater number of peaks present on sandblasted surfaces compared to smooth. Similarities in developed interfacial area ratio (S_{dr}) between disks pre- and post-wettability modification demonstrate our ability to maintain matching surface topography. This ratio represents the amount of textured area on the surface. The highest percent of textured area was quantified on surfaces with both micro- and nanostructure (aged mSLA and mSLA).

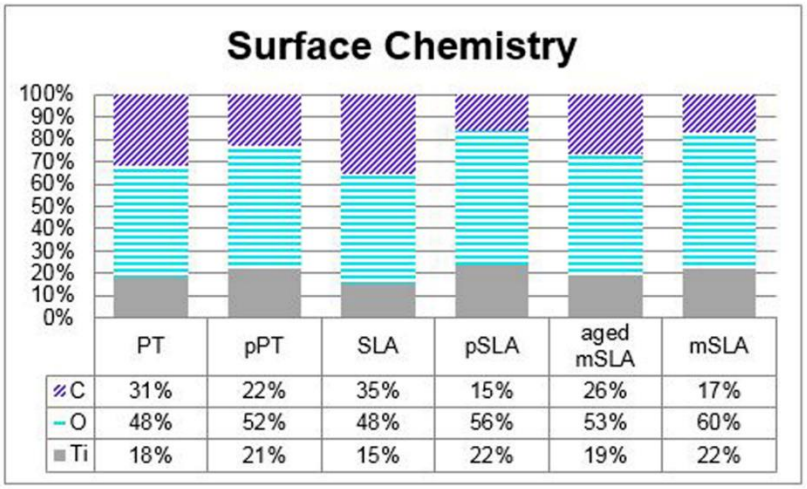

	PT	pPT	SLA	pSLA	aged mSLA	mSLA
C	31%	22%	35%	15%	26%	17%
O	48%	52%	48%	56%	53%	60%
Ti	18%	21%	15%	22%	19%	22%

Figure 5.3.4: XPS analysis of Ti oxide layer following O2 plasma modification treatment

XPS analysis revealed more carbon was present on hydrophobic surfaces in comparison to hydrophilic surfaces. Trace elements of nitrogen were present on some disks. More oxygen was present on the plasma-treated and modified surfaces compared

Table 5.3.1: Binding Energies determined from high resolution XPS scans of C1s, Ti2p, and O1s. Values are mean ± standard error of three regions of six disks per surface.

	C1s						Ti2p				O1s			
	C-C or C-H		C-O		C=O		TiO_2		Ti(M)		C-O or OH		TiOx	
Groups	mean	SEM	mean	SEM	mean	SEM	mean	SEM	mean	SEM	mean	SEM	mean	SEM
PT	67	2.8	10	2.2	8	1.1	88	0.1	5	0.5	37	0.7	63	0.7
pPT	100	0.0	0	0.0	0	0.0	88	0.5	5	0.6	31	1.4	69	1.4
SLA	67	4.9	20	6.9	17	2.0	87	0.2	5	0.2	39	0.6	61	0.6
pSLA	100	0.0	0	0.0	0	0.0	89	0.3	3	0.1	29	1.0	71	1.0
aged modSLA	75	0.9	1	0.5	24	0.5	93	0.4	ND	ND	30	4.3	68	3.6
modSLA	76	1.2	1	0.7	23	1.2	88	0.9	3	0.5	27	1.0	73	1.0

to untreated surfaces. Similar levels of carbon and oxygen were measured on smooth and rough surfaces with similar surface wettability. Plasma treated surfaces had the highest percent of binding at 284.8 eV, which is representative of C-C or C-H binding. These surfaces only displayed this peak and did not show C-O (286 eV) or C=O (288 eV) binding. Untreated smooth and rough Ti had similar levels of each form of carbon binding between them. Both mSLA and aged mSLA surfaces showed the highest amount of C=O binding compared to the other surfaces. No differences were measured in Ti_{2p} measurements at the TiO_2 (peaks at 458.5 eV and 465 eV) on any surface. Levels of Ti metal were not detected on the aged mSLA surface. The greatest portion of O_{1s} binding was present in the TiO_x oxide layer of each of the surfaces.

The hydrophilic surfaces used in this study had less carbon contamination and more oxygen, consistent with studies comparing SLA and mSLA by our group and others [18,21, 22]. The application of an oxygen plasma treatment successfully modified the oxide layer of each hydrophobic disk by the removal of hydrocarbon contamination, thus

generating a hydrophilic surface. Reduced levels of carbon present in the XPS scans were due to clean sample preparation and the use of metallic clips instead of carbon adhesive tape. These reduced levels resulted in only minor differences between the surfaces. Surfaces treated with oxygen plasma did not show any carbon bound to oxygen, suggesting the successful removal of hydrocarbons bound to the oxide layer (Figure 5.3.4). This surface modification may have altered surface chemistry in addition to the surface energy. These changes in surface features may have altered protein adsorption to the surfaces [23], which can change the cell response to a material.

Cell Response

The increased surface wettability resulted in a greater anti-inflammatory cell response in comparison to hydrophobic surfaces with matching roughness characteristics. DNA content on each of the surfaces was similar to levels on TCPS, showing that macrophages can interact with Ti surfaces. The reduced number of cells at 72 hours on all surfaces may correlate with the fast acting and short lifespan of macrophages [28]. The reduced cell number also suggests that the cause of chronic immune responses may be due to recruitment of new immune cells to the injury site and not because of a single constant inflammatory cell population [28].

Surface topography and wettability may control the attachment of cells in different ways. Smooth surfaces may allow the cells to attach and spread more than on rough surfaces. The configuration of the cells may alter the cytokines produced [29]. Increased levels of DNA were present on smooth PT surfaces in this study. A surface similar to that present in natural tissue, such as those with microroughness and hydrophilicity, may be able to stimulate the cells to switch activation and prevent a chronic immune response. A

switch in cell activation can lead to the resolution of a previously chronic immune microenvironment. Interestingly, most of the research performed on macrophage activation has been done on TCPS or glass substrates that lack biological relevance or similarity with any tissue in our body. The wettability of a material surface will control the proteins able to adsorb to the surface and the formation of a blood clot and fibrin network [30]. Cells such as macrophages will then interact with the adsorbed proteins through integrin complexes. These interactions may activate different pathways and allow various factors to be produced by the cell.

After 24 hours, IL1β was significantly lower on rough hydrophilic surfaces (plasmaSLA and mSLA) compared to rough hydrophobic SLA and aged mSLA, with no difference on smooth (PT and plasmaPT). IL6 was reduced on Ti, with the exclusion of SLA, in comparison to the TCPS control, and levels were similar between PT, pPT, pSLA, and mSLA surfaces. Hydrophobic microrough surfaces (SLA and aged mSLA) produced increased IL6 levels. TNFα was reduced on smooth surfaces (PT and pPT) and hydrophilic micro rough surfaces (pSLA and mSLA) compared to TCPS, and greater on hydrophobic rough surfaces than hydrophilic (Figure 5.. At 72 hours, there was

approximately twice the amount of protein present in media collected from each of the test surfaces per μg DNA in comparison to 24 hours. There was again no significant difference in IL1β secreted by cells on PT or plasmaPT compared to TCPS.

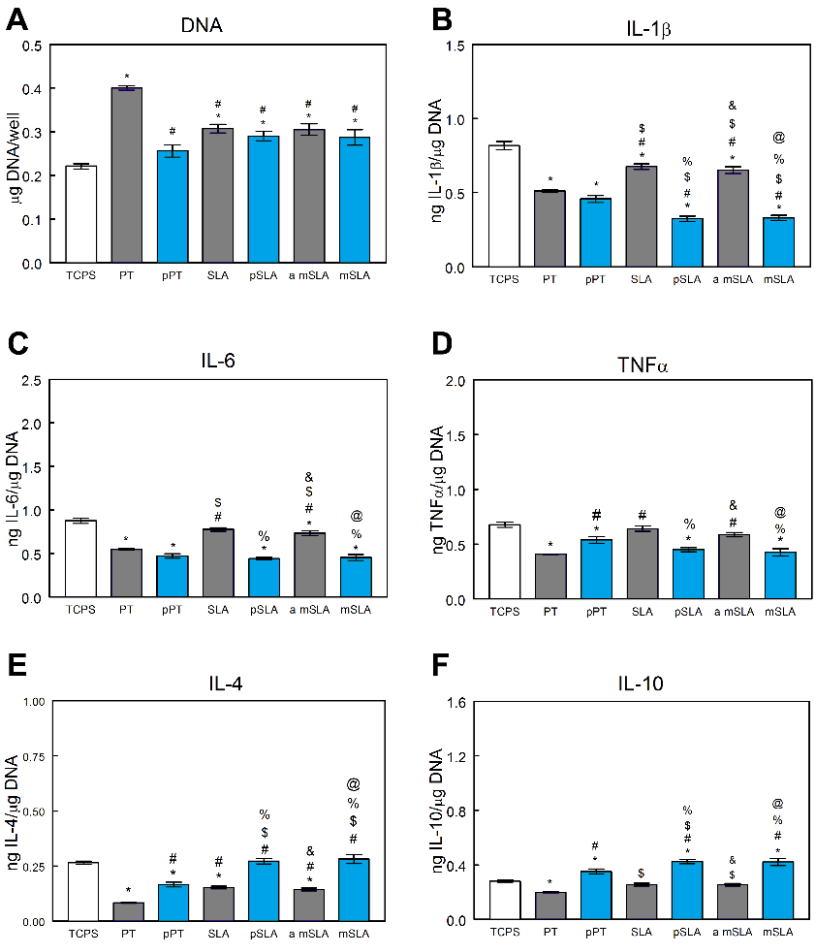

Figure 5.3.5: DNA and protein quantification of media harvested from primary macrophages cultured on Ti surfaces for 24 hours. A) DNA B) IL-1β, C) IL-6, D) TNFα, E) IL-4, F) IL-10 *p<0.05 vs. TCPS, # vs. PT, $ vs. pPT, % vs. SLA, & vs. pSLA, @ vs. a mSLA.

Secretion of pro-inflammatory IL1β, IL6, and TNFα was lower in cells cultured on rough hydrophilic surfaces (plasmaSLA and mSLA) in comparison to rough hydrophobic surfaces (SLA and aged mSLA). Reduced levels of IL6 were measured in cultures on plasmaPT compared to PT. No difference was detected between the plasmaSLA and mSLA surfaces or the SLA and aged mSLA surfaces in the three pro-inflammatory factors measured, suggesting no effect of the presence of submicron structures.

After 24 hours, levels of anti-inflammatory IL4 and IL10, characteristic of an M2 phenotype, were upregulated on rough hydrophilic plasmaSLA and mSLA in comparison to both smooth and rough hydrophobic surfaces. IL4 was significantly reduced on PT, plasmaPT, SLA, and aged mSLA as compared to the TCPS control and was significantly higher in cells on plasmaPT compared to PT. An increase in the level of both IL4 and IL10 was measured on both plasmaSLA and mSLA compared to the matching hydrophobic surfaces (SLA and aged mSLA, respectively). IL10 levels were significantly higher on hydrophilic Ti surfaces in comparison to the TCPS control. Overall, levels of IL10 were higher in cells on hydrophilic Ti surfaces than those on their hydrophobic counterparts. Within 72 hours, secretion of anti-inflammatory IL4 and IL10

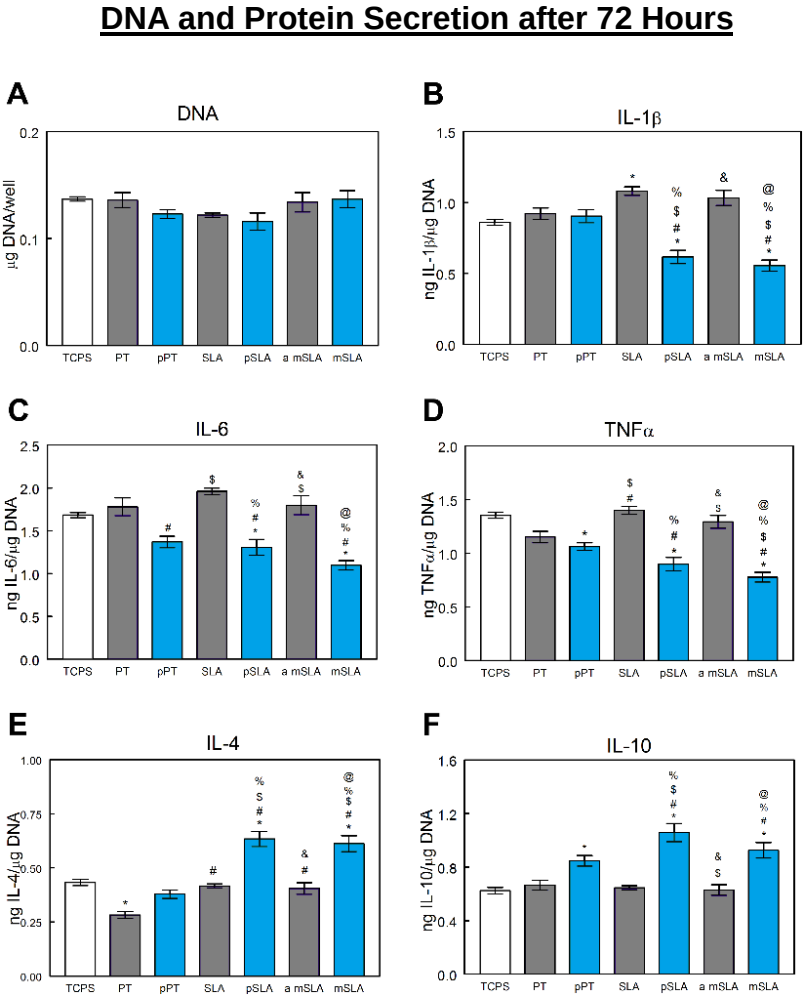

Figure 5.3.6: DNA and protein quantification of media harvested from primary macrophages cultured on Ti surfaces for 72 hours. A) DNA B) IL-1β, C) IL-6, D) TNFα, E) IL-4, F) IL-10 *p<0.05 vs. TCPS, # vs. PT, $ vs. pPT, % vs. SLA, & vs. pSLA, @ vs. a mSLA.

were similar on the PT and plasmaPT surfaces. Levels increased in cells on hydrophilic plasmaSLA and mSLA in comparison to hydrophobic SLA and aged mSLA. However, there was no difference between levels on the two rough hydrophilic surfaces (plasmaSLA and mSLA) or the rough hydrophobic (SLA and aged mSLA). (Figure 5.3.6)

The results of this study show that while wettability has the strongest effect on interleukin release, it may not be solely responsible for the increase in anti-inflammatory factors. The combination of hydrophilicity and the increase of both pro- and anti-inflammatory protein production due to increased surface roughness resulted in the greatest M2-activated macrophages. The reduction in pro-inflammatory cytokines here is consistent with observations from other studies, which have shown a decrease of gene expression of pro-inflammatory markers on hydrophilic rough Ti surfaces at 24 hours in comparison to rough hydrophobic surfaces [4, 21, 31]. Our study used primary bone-marrow-derived macrophages, whereas others have focused on the RAW 264.7 macrophage-like cell line [21]. Experiments conducted with both cell types have shown similar results, with an increase in pro-inflammatory factors secreted by macrophages cultured on hydrophobic surfaces. Studies focused on the macrophage cell line have quantified the effect of surface parameters on mRNA expression [21]. This study considers the next step in the actual production of proteins by the cells in contact with the surfaces and the microenvironment generated that will alter additional cell responses. Our results demonstrate the ability of rough, hydrophilic surfaces to produce initial levels of pro-inflammatory cytokines and ultimately produce the highest concentrations of anti-inflammatory and immunomodulatory factors. Additional studies have measured TFG-β as a marker for M2 activation. However, TFG-β is known to exist in three highly

conserved isoforms in mammals, 1, 2 and 3, each having slightly different effects on surrounding tissue.

5.4| Changes in Macrophage Activation due to Chemistry

Clinically, Ti alloys are used to increase implant strength and allow for smaller diameter implants. This is valuable in patients with reduced bucco-oral bone dimensions or limited mesio-distal length in order to maintain proper spacing[13], [81], [82]. An additional study was designed to determine if the different cell response measured between cells cultured on rough Ti (SLA) and rough-hydrophilic Ti (mSLA) was only a phenomena on pure Ti or if the response will be consistent on Ti alloys. In this study, we aimed to elucidate the different effects of surface energy and chemistry of rough surfaces on immune cell activation.

Results and Discussion

Surface Characterization

Next we wanted to determine if a difference in surface chemistry would affect macrophage response. Disks of 13-17 wt% Zr in Ti alloy were generated under the same manufacturing procedures as grade 2 Ti. Average surface roughness (S_a) was similar between three of the test surfaces (Ti SLA: 3.58 μm ± 0.04 μm, TiZr SLA: 3.58 μm ± 0.02

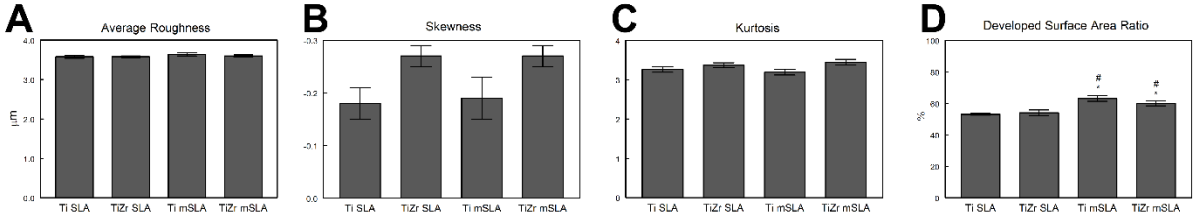

Figure 5.4.1: Characterization of surface topography. Roughness parameters A. average roughness, B. skewness, C. kurtosis, and D. developed surface area ratio of the test samples were quantified by laser scanning confocal microscopy. *p<0.05 vs. Ti SLA, # vs. TiZr SLA.

μm, Ti mSLA: 3.64 μm ± 0.04 μm, TiZr mSLA: 3.60 μm ± 0.03 μm), with no differences in surface roughness detected among the surfaces. Skewness was similar on the TiZr surfaces compared to the Ti surfaces (Ti SLA: -0.18 ± 0.03, TiZr SLA: -0.27 ± 0.02, Ti mSLA: -0.19 ± 0.04, and TiZr mSLA: -0.27 ± 0.02). A greater deviation from zero appears to be present on TiZr surfaces compared to Ti, but this was not found significant. There were no significant differences in the kurtosis values of Ti or TiZr substrates (Ti SLA: 3.26 ± 0.07, TiZr SLA: 3.37 ± 0.06, Ti mSLA: 3.19 ± 0.07, and TiZr mSLA: 3.45 ± 0.07), which

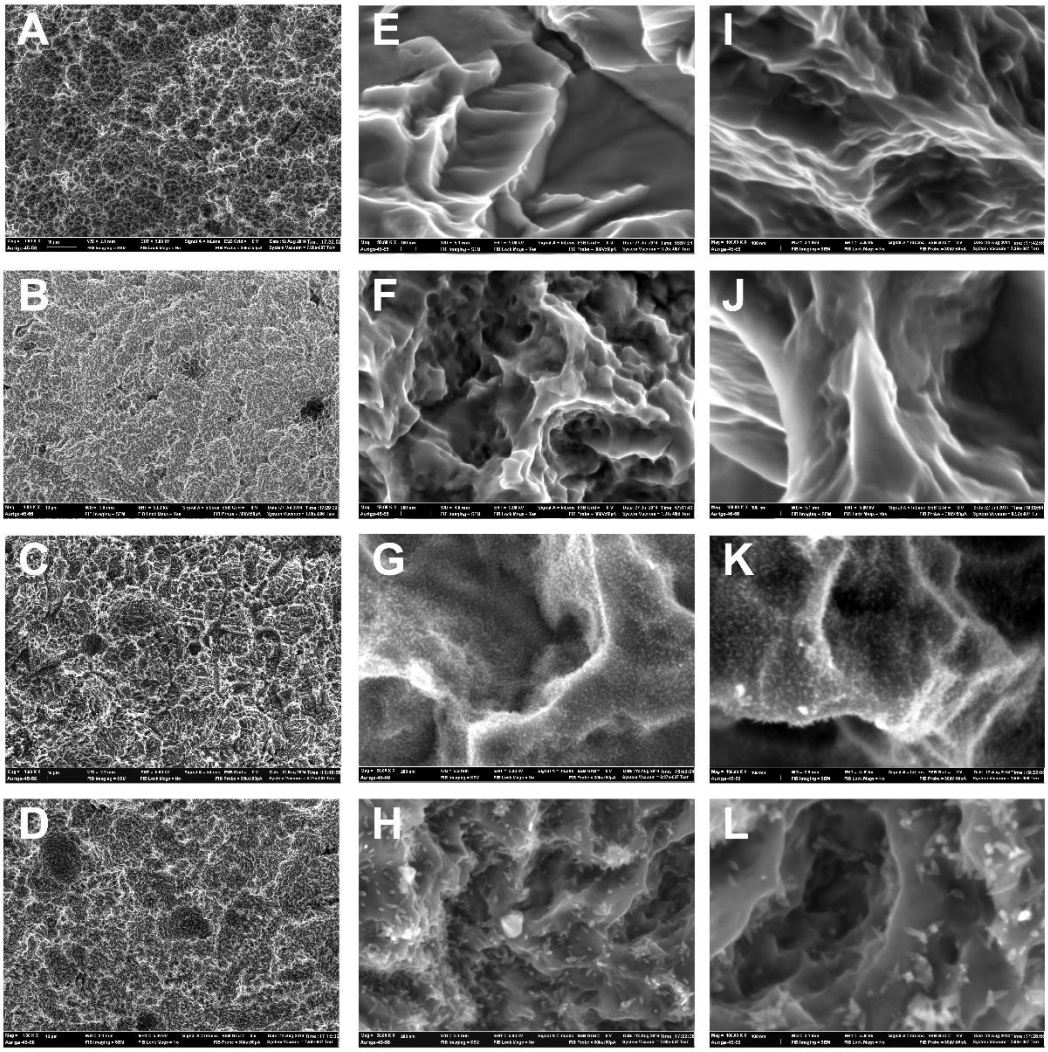

Figure 5.4.2: Qualitative scanning electron images of surface topography at 1kx (A. Ti SLA, B. TiZr SLA, C. Ti mSLA, D. TiZr mSLA), 50kx (E. Ti SLA, F. TiZr SLA, G. Ti mSLA, H. TiZr mSLA) and 100kx (I. Ti SLA, J. TiZr SLA, K. Ti mSLA, L. TiZr mSLA) magnification.

suggests similar microstructure on both Ti and TiZr surfaces. Both Ti and TiZr modified surfaces had higher developed surface area ratios, 63% ± 1.7% and 60% ± 1.5%, compared to unmodified SLA surfaces, 53% ± 0.6% and 54% ± 1.8%. (Figure 5.4.3)

Qualitatively, a similar microstructure was seen under SEM between both surface modifications of Ti (SLA, mSLA) and TiZr (SLA, mSLA) at low magnification (1kx). Nanostructures were visible on both mSLA surfaces under magnification of 50kx to 100kx. (Figure 5.4.2) Nanostructures on the Ti mSLA surface appeared as a dense coating of small dots covering the entire surface, and the nanostructures on TiZr mSLA surfaces appeared as thin, needle-like structures in a less dense covering of the surface.

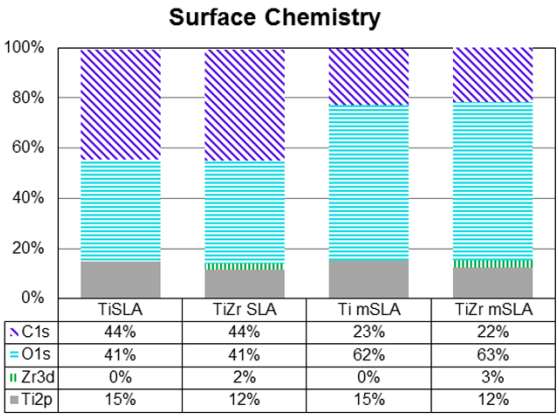

	TiSLA	TiZr SLA	Ti mSLA	TiZr mSLA
C1s	44%	44%	23%	22%
O1s	41%	41%	62%	63%
Zr3d	0%	2%	0%	3%
Ti2p	15%	12%	15%	12%

Figure 5.4.3: Elements present at material surface analyzed by x-ray photo spectroscopy.

Small amounts of Zr were detected on TiZr surfaces, but not on Ti surfaces. Lower carbon and higher oxygen contents were present on Ti mSLA and TiZr mSLA in comparison to their SLA counterparts. Surfaces with increased carbon content had higher contact angles (Ti SLA: 102°, TiZr SLA: 114°) than those with a reduced carbon content (Ti mSLA: 0°, TiZr mSLA: 0°). Contact angle measurements clearly show the two surfaces stored in saline post-modification are hydrophilic, with high surface energy, and the two groups stored dry were hydrophobic with low surface energy. Both low energy surfaces also showed a greater degree of carbon contamination compared to the high-energy surfaces. Qualitative and quantitative assessment of surface roughness properties showed each surface to have similar micro-

scale roughness values, thus allowing our comparisons to focus on surface energy and chemistry. (Figure 5.4.1) The presence of nanostructures on modified surfaces creates a difference between the low- and high-energy surfaces, and the difference in density and shape of the nanostructures distinguishes (Figure 5.4.2) Ti modSLA and TiZr modSLA [21].

TiZr implants have achieved similar levels of osseointegration in animal and clinical studies when compared to Ti materials. The high amount of success demonstrates the potential of this material and confirms the ability to undergo matching surface modification procedures and achieve matching results. Both materials promoted higher bone-to-implant contact values when compared to Ti6Al4V, in addition to a lower presence of foreign body giant cells [82]. A significantly higher removal torque values for TiZr over Ti implants in mini-pigs after 4 weeks has been found [23]. The higher removal force after one month may be due to a reduced healing time or differing bone quality being formed. The healing time and initial bone formation will be altered by the immune response to a material. Here we demonstrate these material surface properties can influence macrophage activation after one and three days.

Cell Response

After 12 hours, increased levels of mRNA anti-inflammatory macrophage markers, Il10 and Tgfb1 were detected on high-energy surfaces in comparison to low energy surfaces. Less pro-inflammatory Il1b, Il6, and Tnfa mRNA were measured on Ti and TiZr surfaces compared to TCPS. Mmp3, a gene for matrix remodeling, was significantly upregulated on TiZr SLA, Ti mSLA, and TiZr mSLA compared to TCPS. Il10 and Tgfb1

were highly upregulated, and Il1b and Il6 highly downregulated on TiZr mSLA surfaces in comparison to TCPS. (Figure 5.4.4)

The initial cell response to the surfaces was measured after 24 hours (Figure 5.4.5). A reduced level of pro-inflammatory cytokines IL1β, IL6, and TNFα released from macrophages on TiZr SLA surfaces was measured in comparison to the Ti SLA surface. The release of IL1β was reduced to levels similar to the hydrophilic Ti surface, mSLA. Less TNFα release was measured on the surfaces with increased surface energy (Ti and TiZr mSLA). Macrophages cultured for one day on the high-energy TiZr mSLA surface also resulted in the lowest levels of inflammatory cytokines IL1β and IL6, significantly reduced from all other groups at this time point. (Figure 5.4.6) Cells cultured for three days produced elevated protein levels in comparison to the initial response after one day. (Figure 5.4.7) In the cells cultured for three days, there was a reduction in IL6 detected on each of the metallic test

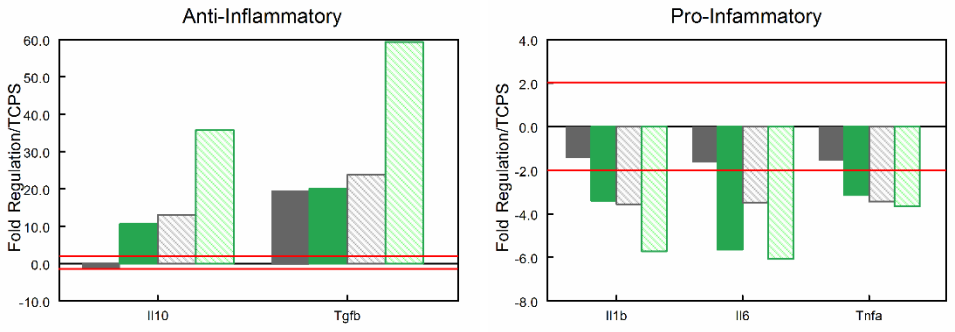

Figure 5.4.4: TiZr alloy resulted in increased anti- and reduction of pro-inflammatory gene expression compared to TCPS. p<0.05 vs. TCPS denoted by red line.

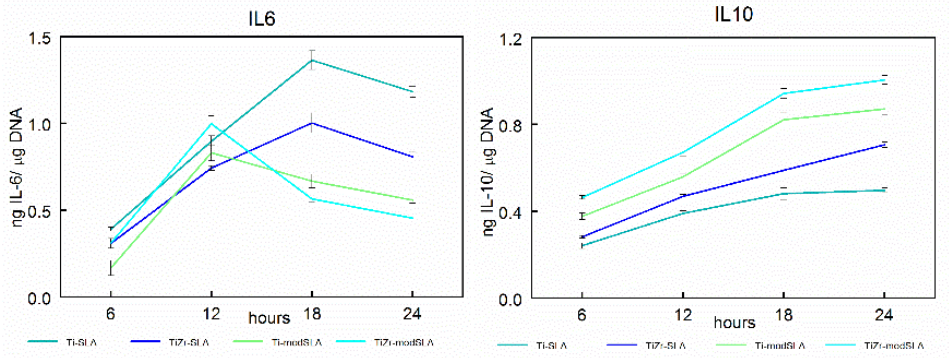

Figure 5.4.5: Cytokine release profile from macrophages over 24 hours on rough Ti and TiZr.

surfaces in comparison to the "naïve" cells grown on the TCPS control. Macrophages released a similar level of IL1β and TNFα on Ti SLA and TCPS and reduced levels on each other surface. Again, there was a reduction in pro-inflammatory cytokine production on the TiZr disks in comparison to the Ti disks with matching surface modifications. Levels of IL1β and TNFα were lowest on mSLA surfaces. The lowest level of IL6 release was measured on TiZr mSLA surfaces.

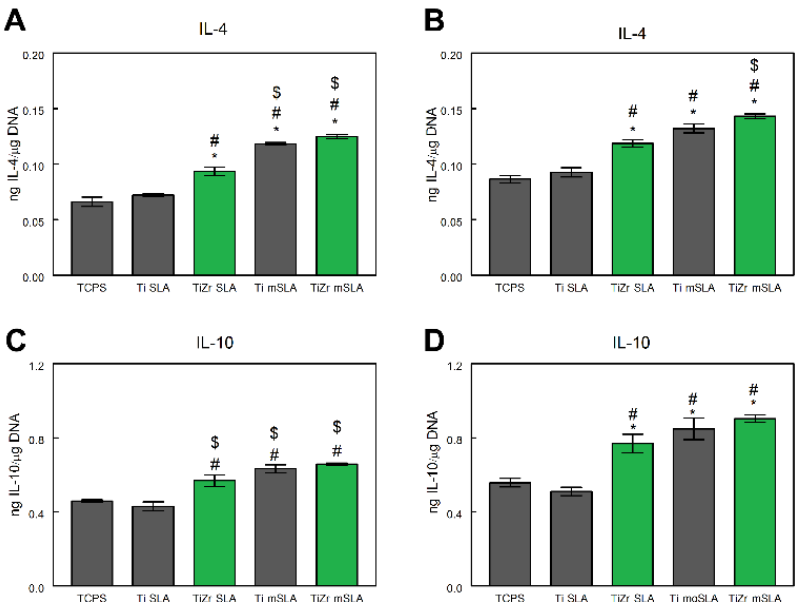

Figure 5.4.6: Anti-inflammatory protein quantification of media harvested from primary macrophages cultured on Ti and TiZr surfaces for 24 (A. IL-4, C. IL-10) and 72 (B. IL-4, D. IL-10) * p<0.05 vs. TCPS, # vs. TiSLA, $ vs. TiZr SLA, % vs. Ti mSLA

More anti-inflammatory IL4 and IL10 were detected on TiZr SLA, and both mSLA surfaces compared to the TCPS control after one day of culture. There was also a significant increase in the level of both IL4 and IL10 detected on TiZr SLA surfaces in comparison to the Ti SLA surface. After three days, the level of IL4 and IL10 released on TiZr SLA and both mSLA surfaces remained increased compared to the TCPS and Ti SLA surfaces. An increase in surface energy again resulted in the increase in anti-inflammatory cytokine levels. The levels of IL4 were further increased on TiZr mSLA in comparison to Ti mSLA.

Previous studies have shown hydrophilic surfaces to reduce the production of pro-inflammatory factors by osteoblasts [19]. In a similar fashion, our results showed that high-energy surfaces promote M2 activation and downregulate levels of pro-inflammatory factors from macrophage-like cells. *In vitro* studies have shown the effect of both roughness and energy on the activation of pro-inflammatory cytokine production in the RAW 264.7 macrophage cell line on unalloyed Ti surfaces [83].

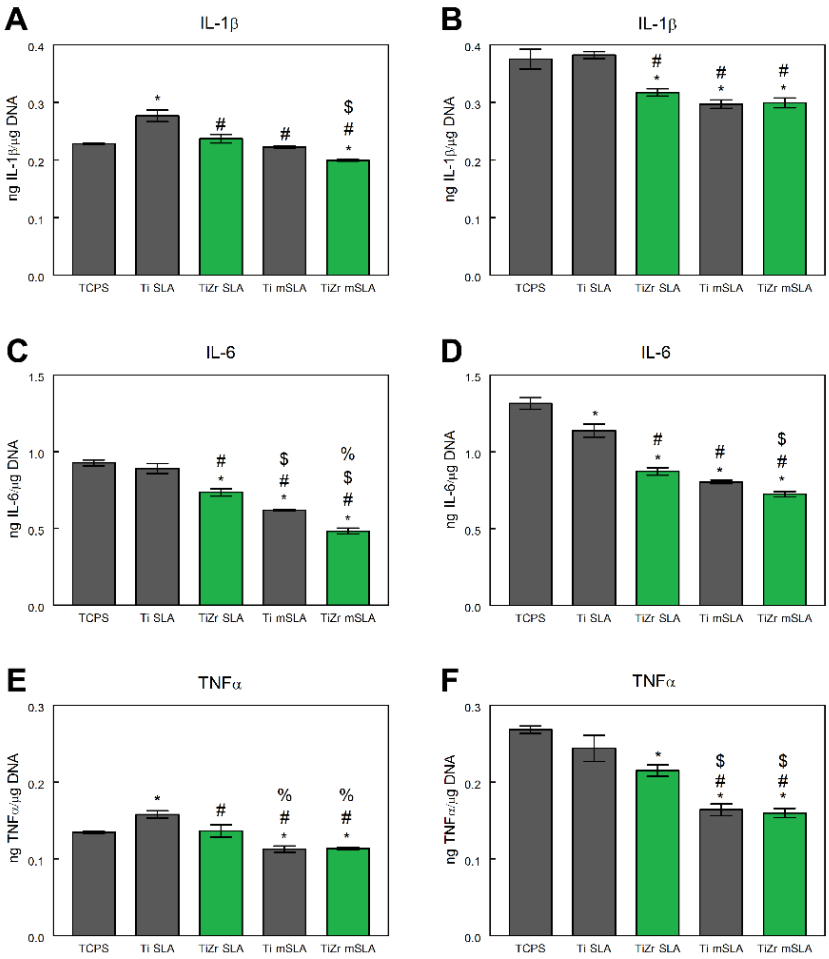

Figure 5.4.7: Pro-inflammatory protein quantification of media harvested from primary macrophages cultured on Ti and TiZr surfaces for 24 (A. IL-1β, C. IL-6, E. TNFα) and 72 (B. IL-1β, D. IL-6, F. TNFα) * p<0.05 vs. TCPS, # vs. TiSLA, $ vs. TiZr SLA, % vs. Ti mSLA

Here we first assessed macrophage activation at the mRNA level during the 24 hours of cell interaction with the surface. Both TiZr surfaces increased expression of M2 markers compared to the Ti with matching surface energy, suggesting differences in nanostructure density and shape or chemical composition of the oxide layer may act in concert with the high surface energy to modulate macrophage activation, but also on its own. The initial immune response to generate the microenvironment surrounding a wound

site or implanted material is the upregulation of messenger RNA, mRNA. Increased mRNA of Il10 and Tgfb1, measured in this study on alloyed metallic implant surfaces, promotes modulation of the immune response and stimulates wound healing around the implant site as suggested in previous studies [84]. Higher levels of Mmp3 on TiZr modSLA suggests a strong induction of tissue remodeling to replace damaged tissue with new, healthy, tissue. The greatest down regulation of pro-inflammatory markers, Il1b and Il6, were present on the TiZr surfaces. These factors will contribute to a state of inflammation by activating additional cells to a pro-inflammatory phenotype. The level of Il1b on TiZr SLA was reduced to a level matching the Ti modSLA surface, while levels of Il6 were lowered a greater amount than the high-energy Ti surface. This shows the potential for the altered surface chemistry to alter the immune response independently of surface energy. Additionally, the high-energy TiZr modSLA showed the highest down regulation of pro-inflammatory and the greatest increase in anti-inflammatory mRNA levels.

Macrophages produce different proteins to recruit or activate additional cells in response to an implanted material, such as a metallic dental implant. These factors modulate the immune cascade and begin the healing process [85], [86]. Based on protein secretion, TiZr surfaces appear to reduce levels of pro-inflammatory cytokines while simultaneously increasing levels of anti-inflammatory cytokines. Similar to results seen in mRNA expression levels, TiZr SLA reduced protein levels of each pro-inflammatory cytokine at both 24 and 72 hours of culture. Between the two low energy surfaces, TiZr also produced increased levels of anti-inflammatory cytokines IL4 and IL10. The greatest decrease in pro-inflammatory and increase in anti-inflammatory release between Ti and TiZr SLA was seen at 72 hours, where no difference in DNA level was measured. The

change in cytokine release with consistent cell numbers indicates a change in activation due to surface properties. This again suggests an immunomodulatory effect as an additional benefit of the TiZr alloy besides the improved mechanical properties. With the introduction of high surface energy in the mSLA surfaces, both the alloy and unalloyed Ti showed significantly reduced levels of pro-inflammatory and increased levels of anti-inflammatory factors compared to the SLA surfaces. High surface energy appears to have an overwhelming immunomodulatory effect. Though there seems to be a further improvement with the TiZr mSLA surface compared to the Ti mSLA surface, the results were not significant.

The ability of the surface to modulate the immune response may prevent the development of a chronic immune response once the cells have been in contact with the implant surface, aiding in the wound healing process and promoting osseointegration. *In vivo* studies comparing Ti mSLA and TiZr mSLA surfaces have shown little difference in the appearance of osseointegration [87], [88] but a greater quality of bone formation characterized by higher bone-implant contact (BIC) values and stronger required pullout forces surrounding TiZr implants [14]. Factors produced by macrophages on implant surfaces will not only affect cells in direct contact with the implant surface but also modulate the recruitment and activation of additional cells distal to the implant. The increased levels of IL4 and IL10 released from macrophages on Ti mSLA, TiZr SLA, and TiZr mSLA promote an M2 phenotype and control of the recruited immune response. The shortened immune response may allow osseointegration to begin at an earlier time point than the hydrophobic Ti SLA surface will. Previous studies from our lab demonstrated the ability of rough, high-energy surfaces to promote the differentiation of stem cells toward

the osteoblast lineage [49]. The previous results in combination with this study show promising evidence for the benefits of rough, high-energy TiZr surfaces in dental implantology. Macrophage activation and release of factors into the microenvironment surrounding an implant is a dominant factor in determining the nature of the healing response [89]. Control of macrophage response ultimately affects the recruitment and differentiation of stem cells and the process of osseointegration. Our results demonstrate an immunomodulatory property present with the TiZr alloy compared to the unalloyed Ti material. This surface was able to promote the release of anti-inflammatory factors by naïve macrophages to a greater extent than Ti. The levels of pro-inflammatory factors were also decreased on TiZr compared to Ti at each surface energy condition.

5.5| Conclusion

In this study, we examined the effect of surface roughness and wettability on activation of naïve macrophages as characterized by the production of cytokines released by the cells. The surface roughness and wettability were varied independently of each other to determine the effect of each property on macrophage activation. We found that increased surface wettability had a stronger immunomodulatory effect than increases in roughness.

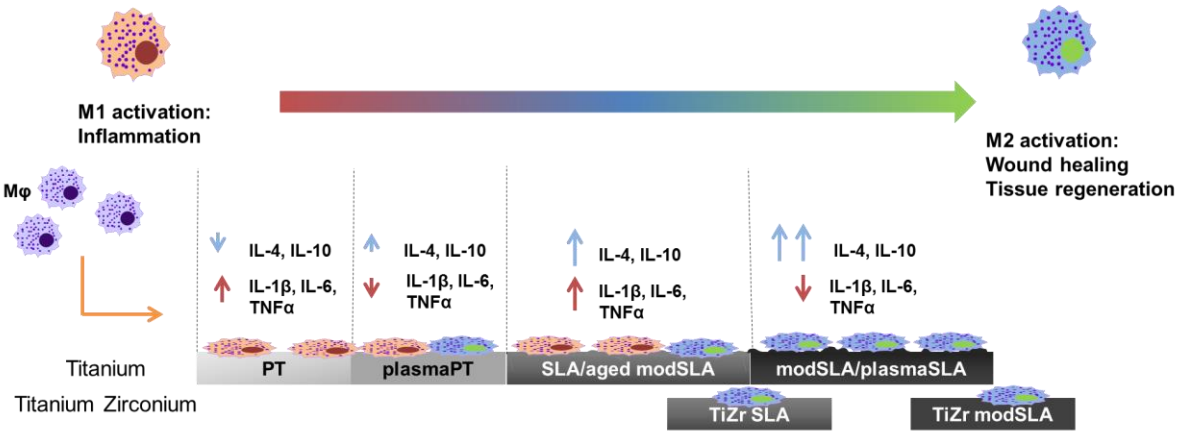

	PT	plasmaPT	SLA/aged modSLA	TiZr SLA	modSLA/plasmaSLA	TiZr modSLA
Roughness	-	-	+	+	+	+
Wettability	low	high	low	low	high	high

Figure 5.5.1: Summary figure of Aim 1. Hydrophilic Ti and Ti alloy materials promote a more anti-inflammatory, M2-like macrophage activation characterized by increased levels of anti-inflammatory cytokines and reduces pro-inflammatory cytokines.

Chapter 6 | Aim 2

Determine a potential mechanism for changes in macrophage activation with material surface properties.

6.1| Introduction

In Aim 1 we found a robust and repeatable phenomena of material surface properties to differentially activate macrophages. In each iteration, hydrophilic rough Ti promoted the greatest anti-inflammatory macrophage activation *in vitro*. The anti-inflammatory macrophage activation in response to rough-hydrophilic Ti resulted in higher release of IL10 and IL4 compared to macrophages on rough hydrophobic SLA. These cells also secreted lower levels of pro-inflammatory IL1β, IL6, and TNFα compared to other surfaces. There are many different potential factors that can affect how macrophages respond to a biomaterial, including cytokine interaction, cytoskeletal forces induced by substrate stiffness, protein binding interactions, and combination effects. Macrophages are classically known to be activated through binding of soluble factors such as bacteria or cytokines, but how macrophages recognize changes in material properties has not been established. A classically activated or pro-inflammatory macrophage activation can be induced by exposing cells to IFNγ and LPS, which will induce a round “pancake” phenotype. Alternatively activated macrophages are generated by exposure to cytokines IL4 and IL13 or IL10 and will adopt an elongated phenotype. *The objectives of this study are to determine how surface properties activate macrophages compared to soluble factors and what molecules are important for macrophage activation induced by*

biomaterials. The cells will not interact directly with the material surface, but rather with an assembled layer of protein at the interface. *Therefore, we hypothesize that integrin binding to ECM domains will be the main modulator of macrophage activation in response to surface properties.*

6.2| Classify surface induced macrophage activation along spectrum from M1-M2 activation.

Macrophages are known to be activated along a spectrum, with the classical LPS treated M1 at one pole and IL4/IL13 stimulated M2 at the other. The *objective* of this study is to determine what level of macrophage activation is induced by biomaterials compared to classical activation by cytokines and bacteria.

Materials and Methods

Ti disks of varying roughness (smooth PT, rough SLA, and rough-hydrophilic mSLA) were created and characterized as mentioned in Chapter 4.

Cell Activation

Naïve primary murine macrophages, isolated and differentiated as previously described (Chapter 4), were treated with 50ng/mL LPS (Sigma Aldrich), 20ng/mL IL4 and 20ng/mL IL13 (PeproTech), or 30ng/mL IL10 (PeproTech) to generate classically (M1) and alternative (M2a and M2c) macrophages respectively. These cells will be used as controls and compared to naïve macrophages in cultured on the modified Ti surfaces (PT, SLA, mSLA) and a TCPS control surface. Additionally, naïve macrophages were pre-treated with M1 and M2 stimuli for 12 hours prior to plating on surfaces to determine if surface properties could alter the established macrophage activation.

Macrophages were cultured in the presence of the ligands and on surfaces (n=6) for 24 hours. Supernatant was collected and a 0.05% Triton X100 solution added to each well to facilitate cell lysis. Levels of inflammatory factors released were quantified through ELISA and normalized to levels of DNA per well.

Results and Discussion

Classically activated M1 macrophages secreted the highest level of all cytokines measured, both pro- and anti-inflammatory, and M2 macrophages activated with IL4 and IL13 secreted the lowest levels. Macrophage activation induced by Ti surfaces were between the two ends of pro- and anti-inflammatory. Rough Ti SLA induced the greatest level of pro-inflammatory IL1β, IL6, and TNFα, while hydrophilic rough mSLA promoted macrophages to secrete the highest level of anti-inflammatory IL10 and IL4 among surface groups (Figure 6.2.1). This suggests the activation achieved through interaction with surface properties may be induced by different mechanisms than the classical bacteria or cytokine profiles.

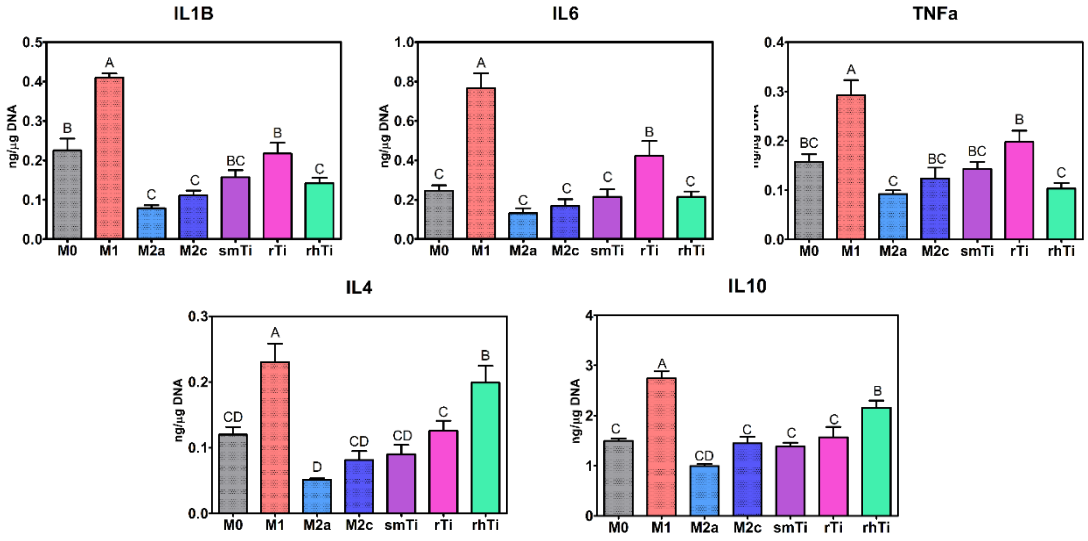

Figure 6.2.1: Comparison of macrophage cytokine profile after classical activation and in response to Ti biomaterials. Different letters denote $p<0.05$ significant difference

6.3| Determine the specific integrin heterodimers involved in macrophage activation on biomaterials.

Previous studies have shown the greatest effect on macrophage activation to be generated by changes in wettability. The wettability of the biomaterial surface will also govern the arrangement and type of proteins adsorbed to the surface. Cells will interact with the adsorbed proteins through integrin binding. The *objective* of this study is to establish which integrin binding unit is involved in surface induced activation of macrophages. We *hypothesize* that the $\alpha_m\beta_2$ (Mac-1) unit will be the most influential integrin binding in macrophage activation in response to biomaterial surface properties.

Materials and Methods

Protein coating

For this study, we will first coat plates with serum, fibronectin, fibrinogen, collagen I and vitronectin to induce binding through integrin $\alpha_m\beta_2$, $\alpha_4\beta_1$, $\alpha_{IIb}\beta_3$, $\alpha_{1/2}\beta_1$, and $\alpha_v\beta_3$, respectively. Human fibronectin (10µg/mL) (Sigma-Aldrich), collagen type 1 from calf skin (50µg/mL) (Sigma-Aldrich), laminin (5µg/mL) (Corning), human vitronectin (10µg/mL) (PeproTech), and human fibrinogen (10µg/mL) (Sigma-Aldrich), and 20% FBS protein concentrations were created in DPBS with calcium and magnesium (Life Technologies). Well plates and Ti disks were coated with 500 µL protein solution at 37C 5% CO_2 for 2 hours, at which point the solution was removed and surface rinsed with DPBS. Cells were then plated in RPMI media supplemented with 1% FBS, 1% sodium pyruvate, and 1% penicillin streptomycin in protein coated groups and RPMI FM in control groups.

Analysis of Integrin Subunit Changes

Naïve macrophages were cultured on surfaces for 12 (PCR) and 24 (flow cytometry) hours before being harvested for analysis of integrin β and α subunits. Changes in integrin subunits were quantified by qPCR, as described in chapter 4, and flow cytometry. For flow cytometry analysis cells were non-enzymatically passaged with Accutase and stained with conjugated antibodies against CD29 (ITGB1), CD18 (ITGB2), and CD61 (ITGB3) (BioLegend).

Antibody Blocking

To prevent binding of specific integrin subunits, naïve murine macrophages were incubated with blocking antibodies for 1 hour on ice prior to plating. Blocking antibodies against integrin beta 1 (anti-CD29), integrin beta 2 (anti-CD18), and integrin beta 3 (anti-CD61) (BioLegend) were added according to manufacturer's protocol.

shRNA Silencing

In order to determine which integrin subunit is most important in macrophage activation or if more than one is active in the response, integrin expression in the macrophage cell line RAW 264.7 gamma NO (-) (ATCC) were be silenced using short hairpin (sh)RNA. Cells were treated with 80ug/mL HEXA followed by lentiviral silencing particles for Itgb1, Itgb3 and control vector (Mission Lentiviral Particles, Sigma Aldrich). Transfected cells were selected by culture with 2.5µg/mL puromycin (Sigma-Aldrich) in RPMI FM for one week. Successful knockdown of integrin subunits was confirmed with qPCR.

Results and Discussion

Protein Coating

Protein coatings resulted in changes in pro-inflammatory and anti-inflammatory factor secretion from naïve macrophages. Both fibronectin and collagen 1 coatings elevated pro-inflammatory cytokine secretion from macrophages. The highest level of both IL6 and TNFα were secreted after 24 hours in contact with collagen 1. Lower levels of pro-inflammatory cytokines were released on vitronectin and fibrinogen coatings. Additionally, lower levels of anti-inflammatory IL10 and IL4 were secreted from macrophages in response to vitronectin and fibrinogen. These results suggest the ability of specific proteins to activate macrophages toward a pro-inflammatory phenotype (Figure 6.3.1).

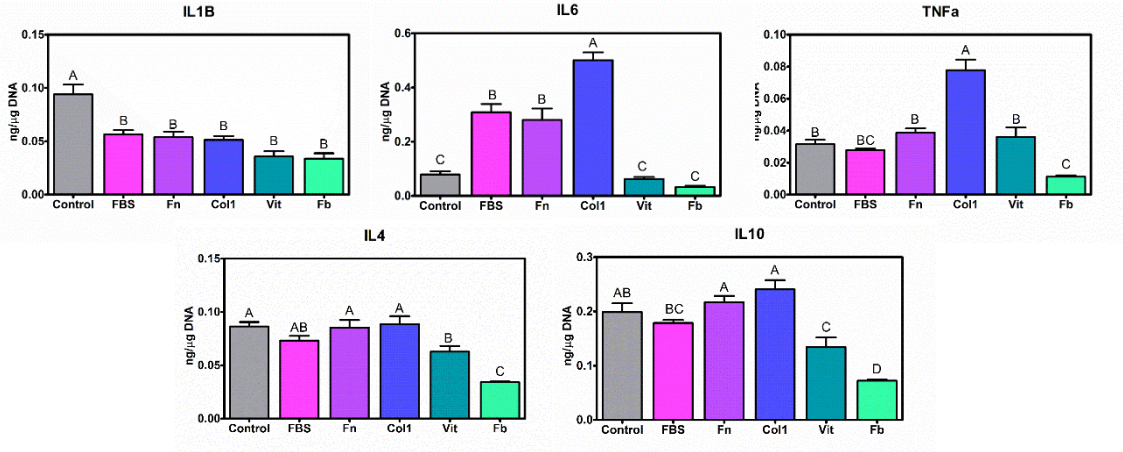

Figure 6.3.1: Macrophage cytokine release in response to protein coatings. Different letters denote $p<0.05$ significant difference

The presence of different proteins during the stages of wound healing can influence macrophage activation. Other studies have found fibronectin to promote pro-inflammatory factors.

When Ti surfaces were coated with specific proteins the macrophage activation profile changed. Overall a higher level of pro-inflammatory factors were secreted when a single

protein was used to coat the surface. Similar to TCPS there was an overall increase in cytokine release from macrophages cultured on Ti surfaces coated with collagen 1. These results enforce the importance of protein adsorption on the inflammatory cascade. The specific protein adsorption on a material can influence the initial immune activation and subsequent cascade.

Integrin Subunit Expression

After 12 hours, *Itgb1* and *Itgb2* gene expression was upregulated in macrophages plated on rough Ti. Rough hydrophilic mSLA induced the highest fold change of *Itgb3* (Figure 6.3.2). Changes in integrin subunit profiles have been linked to different stages of monocyte-macrophage activation [90]. Integrin expression at the surface was analyzed by flow cytometry. The highest percent of macrophages on TCPS had integrin β2 on the surface, the beta subunit associated with CD11b in Mac-1 [10], [91]. This integrin is essential for macrophage migration and classically known to be expressed on all leukocytes [92], [93]. Exposing macrophages to inflammatory proteins TNFα and INFγ will induce an up-regulation of the β2 subunit, similarly to the upregulation we found on smooth PT and rough SLA surfaces [90]. The differences seen between the PCR and flow cytometry characterization could indicate a change in activation or differentiation state initiated by the Ti surfaces. The increase gene expression of integrin subunits will eventually lead to changes in the surface receptors themselves. Additionally,

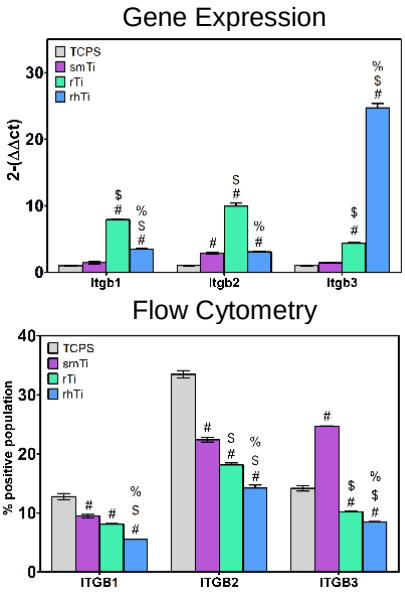

Figure 6.3.2: Changes in macrophage integrin β subunit profile after culture on Ti surfaces. #p<0.05 vs. TCPS, $ vs. smTi, % vs. rTi.

to the beta subunits, we also measured changes in gene expression of integrin alpha subunits. The hydrophilic mSLA surface induced the greatest changes in gene expression, with increased fold changes in *Itga4*, *Itgam*, *Itgav*, and *Itgax* (Figure 6.3.3). Interestingly, there was a reduced level of alpha subunit message expressed in macrophages on smooth PT surfaces. Hydrophilic Ti increased expression of subunits characteristic of both macrophages, Itgam (CD11b), and dendritic cells, Itgax (CD11c),[93] which may suggest an increased antigen presenting ability of cells grown on the hydrophilic surfaces. Studies have found CD18, the β2 subunit of integrin, was shown to be main regulator of adhesion to collagen 1, while CD11b, (Itgam) was not involved [94]. This corresponds to our results where we see an increase in Itgam on the anti-inflammatory hydrophilic surface but not the β2 subunit which is associated with the "inflammatory" collagen 1.

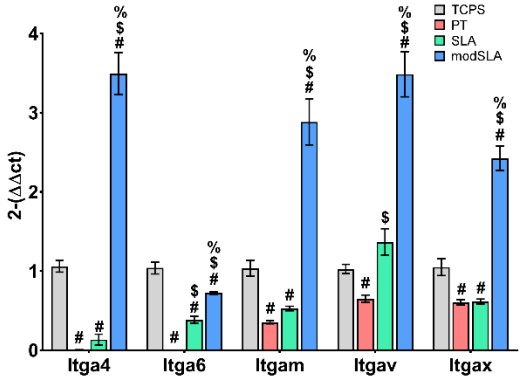

Figure 6.3.3: Changes in macrophage integrin α subunit profile after culture on Ti surfaces. #p<0.05 vs. TCPS, $ vs. PT, % vs. SLA.

In previous studies (Chapter 5) we found macrophage activation on Ti surfaces to be dynamic and change over time. This change in activation could be explained by either changes in protein adsorption over time or changes in macrophage surface receptors over time. Proteins from blood or FBS will immediately adsorb to the surface of a material. Which proteins adsorb and in what conformation is dependent on material properties and the proteins themselves [65], [95]. Initially, protein adsorption is strongly influenced by diffusion and the ability of the protein to reach the surface first, but overtime the affinity of

a particular protein for a surface will play a larger role. This dynamic nature of protein mixtures can lead to different epitopes exposed for cell activation and differentiation[96].

Integrin β-subunit Antibody Blocking

Treatment with IgG control blocking antibody did not alter the number of cells attached to TCPS or Ti surfaces compared to control. However, blocking antibodies specific for the β 1, 2, and 3 subunits did reduce cell attachment to Ti surfaces but not differentially on TCPS (Figure 6.3.4). Greater changes were evident in gene expression than in protein secretion, which may indicate that a greater change in protein secretion would be measured at later time points.

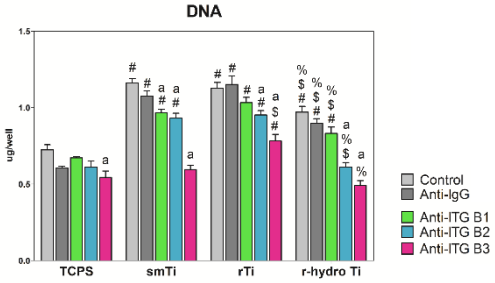

Figure 6.3.4: Changes cell attachment after antibody blocking #p<0.05 vs. TCPS, $ vs. smTi, % vs. rTi. a p<0.05 vs. control.

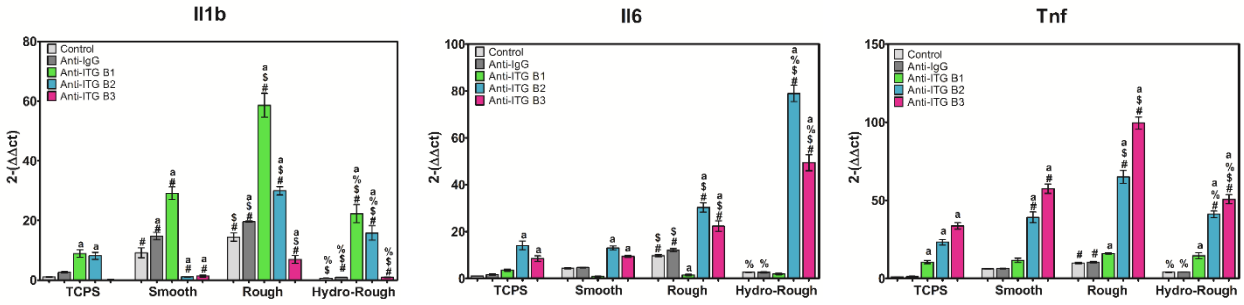

Figure 6.3.5: Changes pro-inflammatory gene expression after antibody blocking #p<0.05 vs. TCPS, $ vs. smTi, % vs. rTi. a p<0.05 vs. control.

Blocking integrin β1 increased gene expression of IL1β, while maintaining TNFa and reducing IL6. The highest fold change of IL1β was measured after blocking integrin B1 binding on rough Ti (SLA) surfaces. The β1 antibody blocking removed the changes in IL6 and TNFa gene expression across the Ti surfaces. A reduced level of anti-

inflammatory *Il10* gene expression was measured in each group following β1 blocking (Figure 6.3.6). A similar trend was seen in protein secretion with integrin β1 blocking having the greatest effect on the release of IL1β. Conversely to gene expression, the highest level of each pro-inflammatory protein measured was secreted from macrophages on smooth Ti (PT). Blocking integrin β1 eliminated differences in secretion of IL4 between Ti surfaces. The level of IL10 released was also increased on smooth Ti and rough hydrophilic Ti compared to control macrophages. Other studies have found β1 to be associated with section of pro-inflammatory cytokines such as IL1β, specifically when coupled with VLA-4.

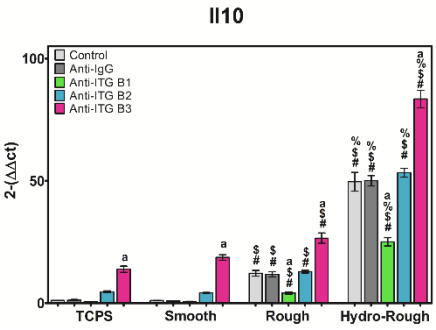

Figure 6.3.6: Changes *Il10* gene expression after antibody blocking #p<0.05 vs. TCPS, $ vs. smTi, % vs. rTi. A p<0.05 vs. control.

After blocking integrin β2 there was an overall increase in gene expression of pro-inflammatory Il1b, Il6, and Tnfa, while still maintaining the profile generated by changes

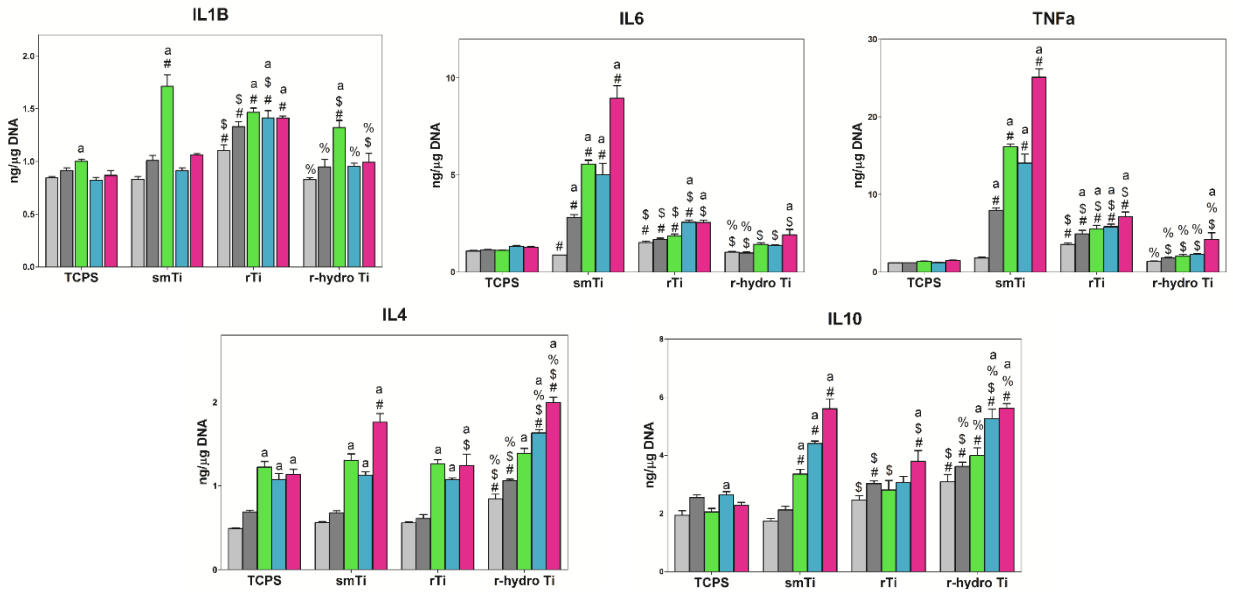

Figure 6.3.7: Changes in pro- (IL1B, IL6, TNFa) and anti- (IL4, IL10) inflammatory protein release after antibody blocking #p<0.05 vs. TCPS, $ vs. smTi, % vs. rTi. A p<0.05 vs. control.

in surface properties. Preventing β2 binding did not alter gene expression of Il10. Protein secretion followed the same trend as gene expression, with β2 blocking increasing overall protein secretion but still following the same trend as control cells (Figure 6.3.7). Another study using nonporous polytetrafluoroethylene materials found β2 blocking to be instrumental in the production of IL1β from adherent macrophages [97]. The differences between these two studies could be attributed to a different protein adsorption to Ti and polytetrafluoroethylene. Other studies have shown the β2 integrin to be instrumental in macrophage activation and localization to sites of injury or inflammation[66], [91]. This may validate our results which suggest this integrin subunit is not the main regulator in macrophage response to implant surface characteristics.

Blocking integrin β3 resulted in the greatest changes in macrophage activation induced by Ti surface properties. Macrophages on smooth Ti had the highest level of Il6 and Tnfα when β3 was blocked. While integrin β3 is commonly considered to be associated with osteoclasts[98], this study shows a potential role in macrophage inflammation. Similarly to another study focused on muscle regeneration [99], we found elevated levels of initial IL4 and IL10 secretion from macrophages when β3 was not able to bind. Integrin β3 KO mice had impaired muscle regeneration, which could be attributed to increased inflammation and cytokine production by macrophages [99]. The β3 integrin may be integral in the transition from M1 to M2-like activated macrophages.

Interestingly, the smooth Ti surface showed the greatest changes when integrin β subunits were blocked suggesting less binding leads to increased inflammation. On smooth substrates macrophages will be more elongated and make more contact points with the surface. This stretched out phenotype allows for a greater number of integrin

interactions with the substrate and the potential for more integrin surface receptors. This coincides with the increase in integrin subunits measured through flow cytometry on smooth surfaces compared to rough. Blocking surface receptors on a macrophage interacting with a smooth surface will have a larger impact than a rough because there are more contact points.

Integrin β1-subunit Silencing

Integrin beta subunits were knocked down using shRNA lentiviral particles. Short hairpin RNA is able to integrate into DNA to continue to reduce expression overtime. Additionally, the folded shape of shRNA results in fewer pro-inflammatory effects that siRNA which may be recognized as danger signals by

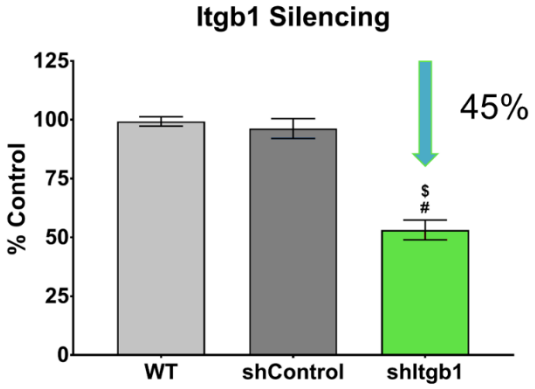

Figure 6.3.8: Successful Itgb1 silencing in RAW264.7 cells. # p<0.05 vs. WT, $ vs. shControl

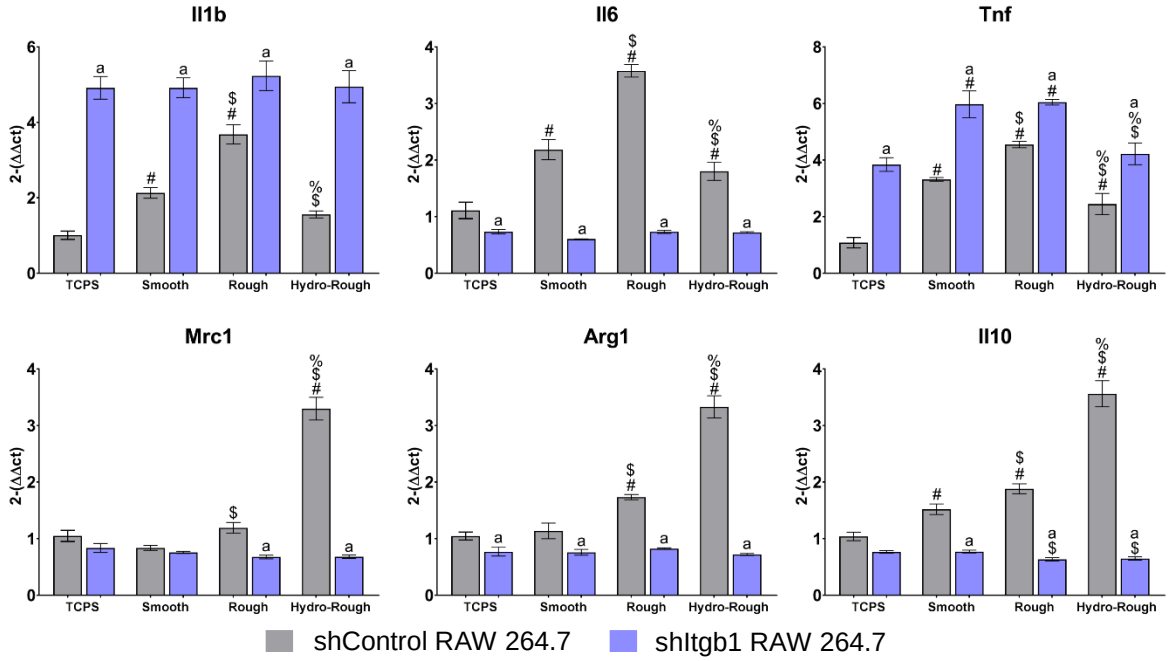

Figure 6.3.9: Changes in gene expression following Itgb1 knockdown in RAW264.7 cells. # p<0.05 vs. TCPS, $ vs. Smooth, % vs. Rough. a p<0.05 vs. shControl cells

inflammatory cells. Treatment of RAW 264.7 macrophage-like cells with Itgb1 shRNA lentiviral particles resulted in an overall knock down of 45% in Itgb1 expression (Figure 6.3.8). Cells silenced for Itgb1 showed the greatest increase in Il1b gene expression, similarly to when ITGB1 antibodies were used to prevent integrin β1 binding. Integrin β1 silenced cells showed lowered levels of pro-inflammatory *Il6*, and anti-inflammatory cytokine *Il10* and markers *Mrc1* and *Arg1*. (Figure 6.3.9)

Integrin β3-subunit Silencing

shRNA lentiviral particles were used to knockdown expression of integrin β3 subunit expression in RAW 264.7 cells. After selection an impressive 99% reduction in integrin β3 was achieved (Figure 6.3.10). Knockdown of Itgb3 resulted in reduced Il1b expression on TCPS and each Ti surface compared to WT and shControl cells. The reduction followed a similar trend to ITG-B3 antibody blocking, but to a lesser extent. Macrophages with reduced Itgb3 expression produced higher gene expression of both pro-inflammatory Tnf and anti-inflammatory Il10 genes when cultured on Ti surfaces for 12 hours. Tgfb1 levels were similar across each surface group in shItgb3 RAW 264.7 cells, but increased in control cells on SLA and mSLA surfaces. Silencing of both Itgb1 and Itgb3 altered RAW 264.7 response to Ti surfaces. Overall, the β1 subunit appeared to be important in the modulating the production on IL1β, and β3 controlling both pro- and anti-inflammatory gene markers (Figure 6.3.11).

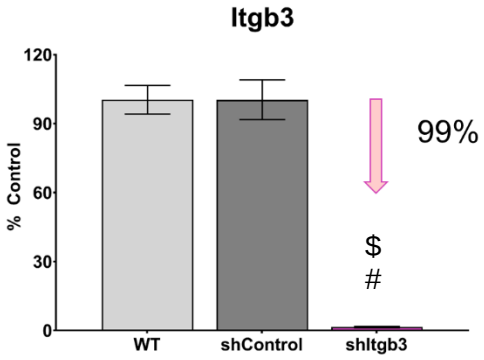

Figure 6.3.10: Successful Itgb3 silencing in RAW264.7 cells. # p<0.05 vs. WT, $ vs. shControl

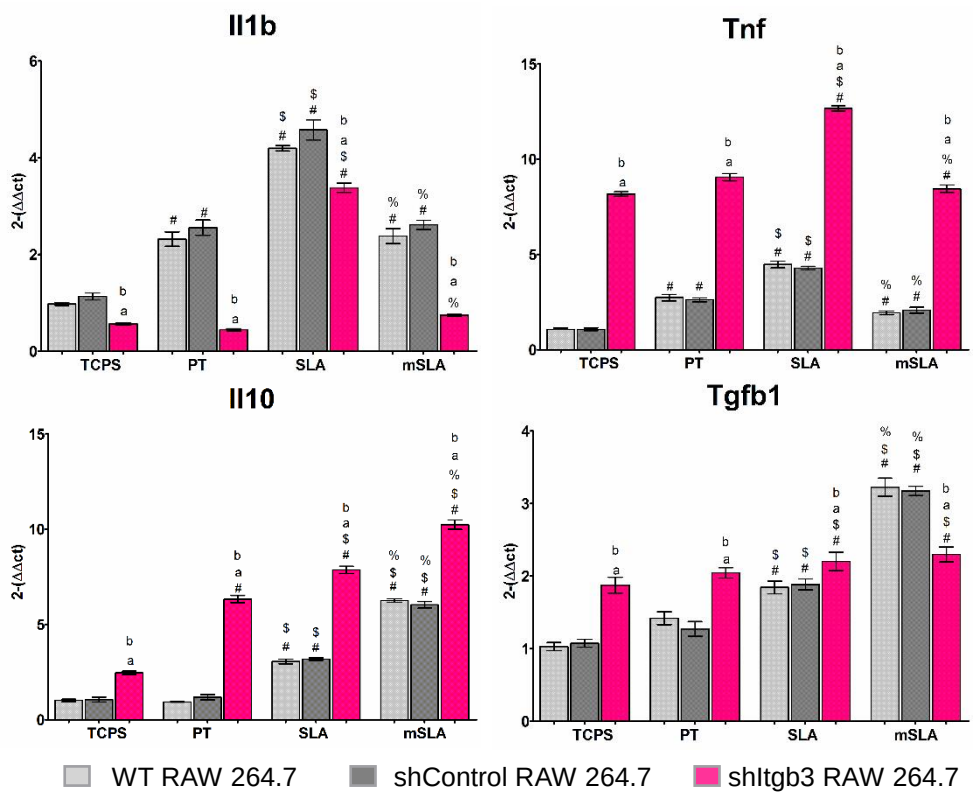

Figure 6.3.11: Changes in gene expression following Itgb3 knockdown in RAW264.7 cells. # p<0.05 vs. TCPS, $ vs. PT, % vs. SLA. a p<0.05 vs. WT, b vs. shControl cells

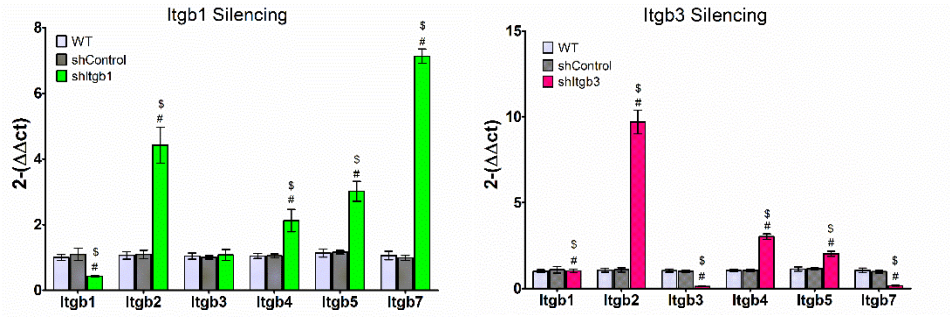

Figure 6.3.12: Changes in integrin beta subunit gene expression following Itgb1 and Itgb3 knockdown in RAW264.7 cells. # vs. WT, $ vs. shControl.

An increase in alternative integrin beta subunit expression was observed following the knockdown of select β1 and β3 subunits. Reducing both Itgb1 and Itgb3 resulted in an increase in Itgb2 expression, which suggests the cells may be maintained in a more naïve phenotype with higher levels of the migratory β2 subunit (Figure 6.3.12). Additionally, Itgb4 and Itgb5 were increased in both

silencing groups, but shItgb1 treatment increased Itgb7 expression while Itgb3 reduced this marker.

6.4| Determine if cell shape and force in the cytoskeleton is important in macrophage activation.

As cells come into contact with a biomaterial they may attach in different shapes and with different strengths. A smooth surface can facilitate a spread out phenotype, while patterned surface roughness can control the shape of cells. Different surface chemistry and wettability will change the protein arrangement and potential stiffness felt in cell cytoskeleton. Here we aimed to correlate cell shape and cytoskeletal force with macrophage activation.

Materials and Methods

Cell staining

Naïve macrophages were plated at 20,000 cells/cm^2 on different surfaces to visualize potential differences in cell shape and attachment. Cells were plated for 24 hours then rinsed with warm DPBS without calcium and magnesium (Life Technologies) before fixation with 4% paraformaldehyde in PBS for 30 minutes at room temperature. Fixed cell membranes were then permeabilized with 0.1% Triton X 100 (Sigma Aldrich) in PBS to facilitate intracellular staining. Cytoskeleton was stained with 0.165µM Alexa Fluor 488 conjugated phalloidin in PBS and nuclei stained with 2.5ng/mL of Hoechst 34580 (Life Technologies).

FAK and Podosome inhibition

Naïve macrophages were plated and allowed to attach to 24-well plate or Ti surfaces for 2 hours before treatment with FAK inhibitor or Wiskostatin at either 5 or 10 μM concentration (Torcis, location).

Results and Discussion

Cell staining

Cells on smooth Ti (PT) and glass surfaces appeared more elongated and spread out than on rough surfaces. Macrophages appeared similar in number and morphology on smooth Ti surfaces and the glass substrate control. Cells on rough surfaces had a less elongated morphology. No multinucleated cells were detected under visual assessment of cells attached to the surfaces.

FAK Inhibition

In the next study we wanted to inhibit focal adhesion kinase (FAK) which is immediately downstream of integrin binding. By treating cells with FAK inhibitor the force

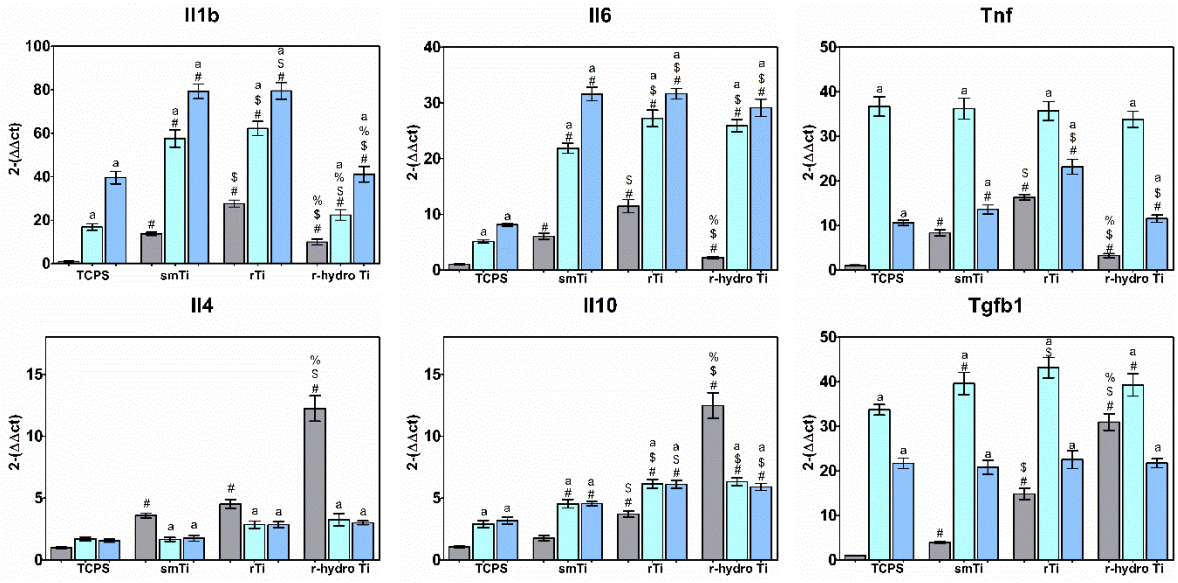

Figure 6.4.1: Changes in gene expression following FAK inhibition in macrophages. # p<0.05 vs. TCPS, $ vs. smTi, % vs. rTi. a p<0.05 vs. control

and signal transduction induced by integrin binding will be blocked. When cells were treated with 5µM and 10µM of FAK inhibitor changes in inflammatory gene expression was measured. When FAK was inhibited there was an increase in pro-inflammatory Il1b, Il6, and Tnfa (Figure 6.4.1). No difference was measured in Tnfa expression across the surfaces. FAK inhibition also reduced expression of anti-inflammatory Il4 and Il10. Fewer changes were evident in protein secretion than in gene expression (Figure 6.4.2).

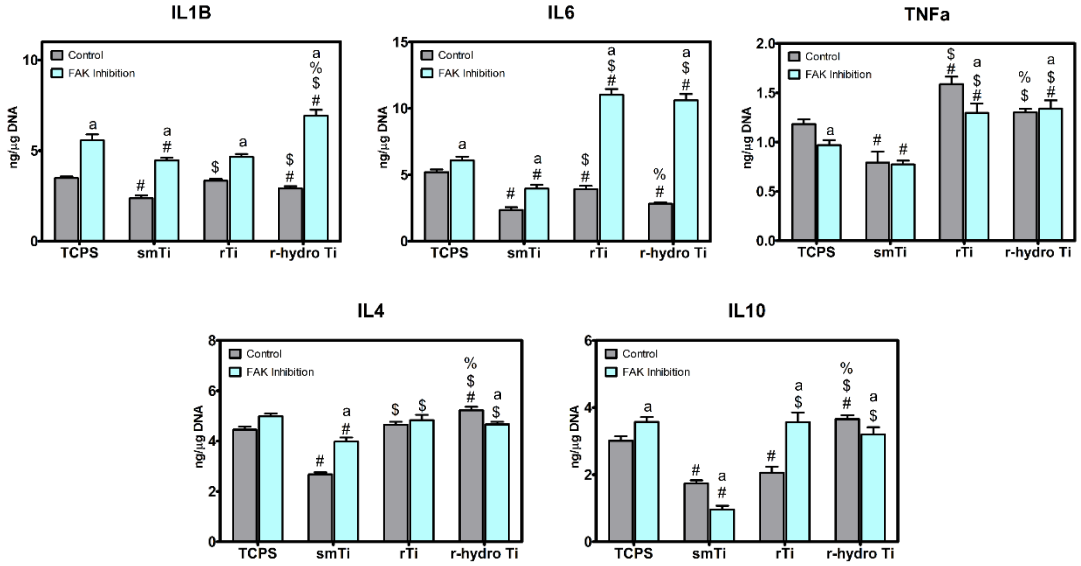

Figure 6.4.2: Changes in protein secretion following FAK inhibition in macrophages. # p<0.05 vs. TCPS, $ vs. smTi, % vs. rTi. a p<0.05 vs. control

Podosome Inhibition

When macrophages were treated with Wiskostatin to inhibit podosome formation gene expression of pro- and anti-inflammatory cytokines were also reduced. Podosome inhibition led similar levels of Il1b, Il12 and Tnf gene expression across the surface groups (Figure 6.4.3). There were also similar levels of anti-inflammatory fold change of Il4, Il10 and Tgfb1 from macrophages treated with Wiskostatin. These results suggest that while

podosomes are classically considered to be important in immune cell migration[72], [100] they may also be important in the recognition of biomaterial surface properties.

Other studies have outlined the role of substrate stiffness in macrophage activation[94], [101]–[103], with lower stiffness materials promoting a more M2-like anti-

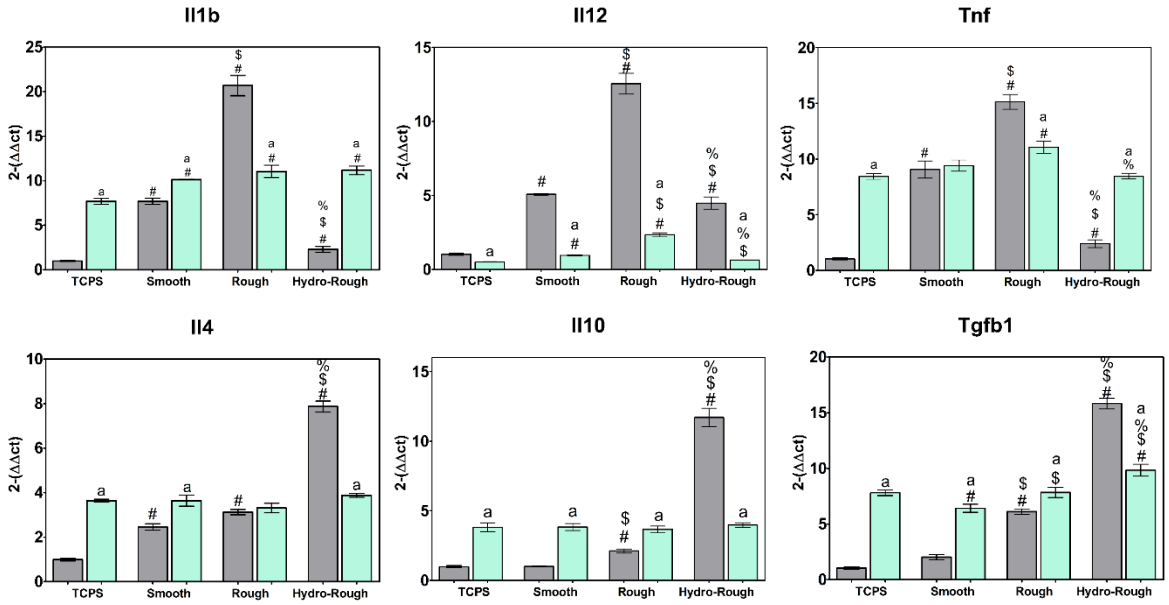

Figure 6.4.2: Changes in gene expression following 5μM Wiskostatin treatment in macrophages. # p<0.05 vs. TCPS, $ vs. smTi, % vs. rTi. a p<0.05 vs. control

inflammatory macrophage activation. A softer substrate will prevent cell elongation at attachment and may reduce forces felt in the cytoskeleton. We found a similar cell morphology between macrophages on both rough surfaces, SLA and mSLA, which contradicted the different activation profiles measured between the two. Cells on each rough surface appeared smaller and less spread than cells on smooth surfaces. While it has been well established that an M1 activated macrophage will appear round and flattened and M2 cells are elongated[48] on smooth stiff tissue culture plastic, cell shape after interaction with a biomaterial may not be an accurate indicator of activation state. Blot clots formed on hydrophilic mSLA implant surfaces have been characterized as

thicker and less stiff than on hydrophobic SLA. The change in protein layer stiffness may play an instrumental role in macrophage activation after contact with the material surface.

6.5| Conclusion

From this study we determined that many factors are important in macrophage activation to biomaterial properties. The disruption of one or more binding molecules can elevated macrophage activation and increase the production of pro-inflammatory factors. Reducing macrophage attachment points, specifically by preventing integrin binding and podosome formation resulted in the greatest pro-inflammatory macrophage activation. This study correlated integrin β subunit binding with specific IL secretion from macrophages on Ti surfaces.

Chapter 7 | Aim 3

Role of material surface induced macrophage activation in the response to implanted materials

7.1| Introduction

Our group has shown that macrophages can respond to differences in titanium (Ti) surface properties such as roughness, wettability, and chemistry [53], [54]. Changes in these properties can control the polarization of naïve macrophages towards either a pro-inflammatory phenotype (M1-like) or an anti-inflammatory phenotype (M2-like) [45]–[47], [50]. Anti-inflammatory macrophage activation was generated on rough-hydrophilic implants. These results correlate with higher success rates and reduced healing times of rough-hydrophilic metallic implants in clinical settings, which also promote stem cell osteogenesis *in vitro* [2], [19], [28], [55].

It is well established that the adaptive immune system determines how xenografts and allografts are accepted after implantation. However, it is not clear whether elements of the adaptive immune system, especially T-helper cells, contribute to the healing and regenerative response after biomaterial implantation. The outcome of these procedures is determined by an interaction between the host and the implanted object. While it is known that biological implants may be rejected if the immune system becomes activated after antigen processing and presentation, many of these principles have been under-studied in the context of synthetic biomaterials.

The aim of this study was to examine whether implant surface properties influence initial events following placement including T-cell activation and MSC recruitment. Based on our previous work with macrophage activation, we hypothesized that higher surface roughness and wettability would have an immunomodulatory effect and promote stem cell recruitment at the implant site.

Materials and Methods

Ti Implants

Implants for *in vivo* studies were generated from 1mm diameter grade 4 Ti rods and surface modifications were created following the same procedure as disks. All Ti materials were sterilized by γ-irradiation.

Characterization of Ti materials

Qualitatively, a higher surface roughness is evident in both rough Ti and rough-hydrophilic Ti compared to smTi in SEM imaging. The increase in roughened appearance was confirmed by quantification of LSCM images for average surface roughness (S_a). Both rough Ti materials had greater S_a values (rTi: S_a=3.58μm and r-hydro Ti: S_a=3.55μm) compared to smooth surfaces (smTi: S_a=0.59μm), but were not different from each other. Smooth and rough hydrophobic Ti showed greater contact angle measurements and increased carbon present in the oxide layer compared to rough-hydrophilic Ti.

Animals and Surgical Procedure

For each study, 10-week male mice (The Jackson Laboratory, Bar Harbor, ME) were used. Animal handling procedures were performed under the approval of the Virginia Commonwealth University Institutional Animal Care and Use Committee (Protocol:

AD10001108). Surgeries were performed between 8am and 12pm with mice randomly assigned to groups. 1mm diameter Ti implants were inserted into the right femoral medullary canal of mice via a medial parapatellar arthrotomy as previously described [104]. Prior to procedures, mice were anesthetized by inhalation of 5% isoflurane gas in O_2 and weighed (weight range 22-26g). Legs were prepared by shaving and cleaned with isopropanol and chlorhexidine. Mice were maintained under anesthesia by isoflurane gas during preparation and surgical procedures. To place the implant, an 8 mm incision was made with a scalpel over the distal side of the knee. The knee ligaments and patella were then moved aside to expose the intercondylar notch of the femur. A 1 mm round dental burr was used to penetrate into the bone and access the medullary canal. Penetration into the canal was confirmed by x-ray. Cylindrical Ti implants were then placed in the medullary canal. Six successful implants were performed for each surface type. After implant placement, periosteal tissue was replaced and closed using resorbable sutures and surgical incisions closed with wound clips. Animals were treated with 0.01mg/kg buprenorphine SR LAB prior to recovery from anesthesia to relieve post-operative pain. Animals were monitored until initial ambulation and every 24 hours for the first 3 days following surgery. All animals were single housed following surgical procedure, with standard 12 hour light dark cycle and access to food and water *ad libitum* for the duration of the study. No signs of infection were present in these studies.

7.2| Determine if improved cell response achieved from hydrophilicity in vitro translates in vivo.

Materials and Methods

Animals

Male 10 week C57Bl/6 mice were purchased from Jackson Laboratory under IACUC approval (AD10001108) for this study.

Flow Cytometry Analysis

Changes in local T-cell populations were quantified by flow cytometry of single cell suspension of cells adherent to the implant after 3 or 7 days. Systemic changes were measured in contralateral leg bone marrow and spleens. Prior to staining, Fc receptors were blocked by incubation with CD16/32 (Biolegend, San Diego, CA) and membranes permeabilized for transcription factor staining. Cell populations were identified by antibodies against T-helper cell marker CD4 (APC-CD4, Biolegend), as well as transcription factors of specific T-cell populations [Th1 (PE-Tbet), Th2 (Alexa 488-Gata3), Th17 (PE-RORγT, BD Biosciences), and Treg (Alexa 488-Foxp3)] (Biolegend). Antibody concentrations were added based on manufacturer's protocol. A total of 10,000 cellular events were measured with three replicates for each measurement. Results were analyzed using guava Soft 3.1.1 InCyte software.

PCR Array

RNA from cells adherent to implant surface was extracted using TRIzol Reagent (Life Technologies, Carlsbad, CA, USA) and quantified using a NanoDrop spectrophotometer (Thermo Fisher Scientific, Waltham, MA). cDNA was generated by reverse transcription

of 500 ng RNA (iSCRIPT, BioRad, Hercules, CA). Custom PCR arrays were designed (BioRad) to assess cytokine markers for T-cell activation and transcription factors associated with T-helper cells. Differences were determined by $2^{-\Delta\Delta CT}$ analysis calculated using endogenous housekeeping genes (Gapdh, Rps18, Tbp, Hbrt) and naïve control mice as controls.

Circulating Inflammation

Blood was harvests by cardiac puncture at 1, 3 and 7 days post material implantation and placed in 4% EDTA to prevent clotting. Samples were then centrifuged at 10,000 RPM for 15 mins and plasma removed. Cytokine levels were quantified by custom designed express Bioplex assay (Biorad) for pro-inflammatory (IL1β, IL6, IL12p40, TNFα) and anti-inflammatory (IL4 and IL10) factors.

Statistical Analysis

Animal studies were performed with six animals per implant group. Flow cytometry samples were run in three technical replicates. Statistical analyses were performed using Prism GraphPad 5.0 software. A one-factor, equal-variance analysis of variance (ANOVA) was used to test the null hypothesis that the group means were equal, against an alternative hypothesis that at least two of the group means were different, at the $\alpha=0.05$ significance level. Once a p-value resulting from the ANOVA model was determined to be less than 0.05, multiple comparisons between the group means were made using the Tukey-HSD method.

Results and Discussion

Local changes: Implant surface properties induce changes in local inflammatory and chemotaxis gene expression

Small (1mm) diameter rods were placed in the femoral canal of C57Bl/6 mice. To determine how material implantation may affect gene expression in the bone marrow immediately surrounding in implants, tissue was removed at 3 and 7 days post-operation and analyzed by quantitative real-time polymerase chain reaction (qPCR). Changes in gene expression in cells and tissue surrounding the implant were compared to bone marrow of un-operated control mice. The greatest change of cytokine genes associated with inflammation was measured at 3 days. Levels of *Il4, Il10*, and *Il13* were elevated on hydrophilic implants in the first 3 days. By seven days, changes in cytokine genes were still evident compared to control animals, with the highest fold change found around rough Ti implant. The highest level of pro-inflammatory Il6 was seen on rough Ti at both time points (Figure 7.2.1, A).

Increased levels of immune cell chemokines (*Ccl2, Ccl4, Ccl7*) were detected in bone marrow surrounding implant and sham surgeries after three days. The highest level of *Ccl2* was measured around the rough Ti implant. By seven days chemokine markers were reduced closer to control bone marrow and an increase in stem cell chemokine, *Cxcl12*, was measured with the highest level on the rough hydrophilic implant. (Figure 7.2.1, B)

Additionally, it was noted that changes in gene expression surrounding implanted Ti and sham surgeries coincided with T-helper cell sub populations. An upregulation of Th1-associated genes (*Tbx21* and *Ifnγ*) was measured in sham-operated animals 3 days after

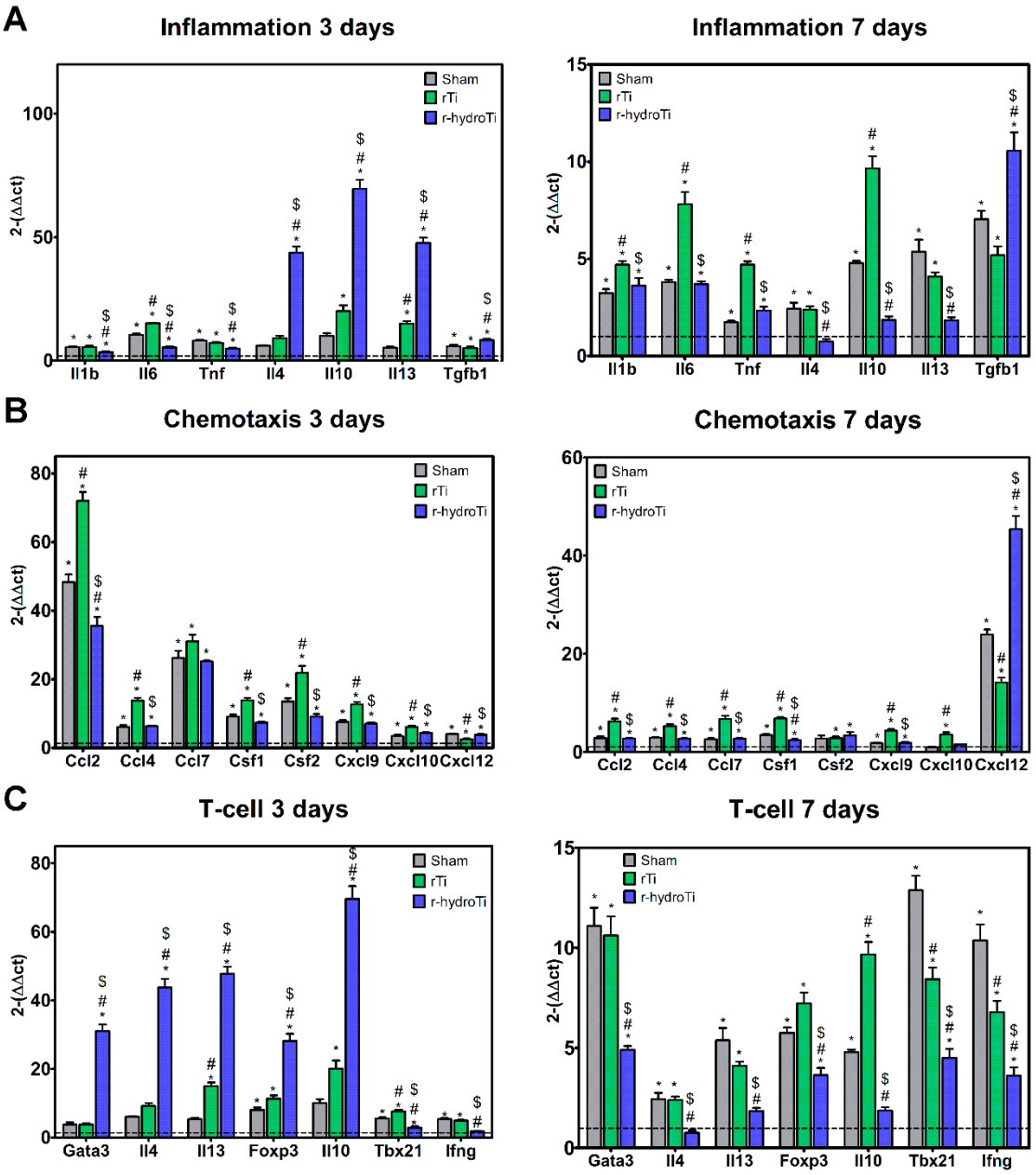

Figure 7.2.1: Changes in mRNA expression surrounding sham, rTi, and r-hydro Ti implants compared to untouched control mice. A. Inflammatory cytokines, B. Chemokines, C. T-cell associated genes. The highest fold regulation of anti-inflammatory cytokines and T-helper cell markers was measured on r-hydro Ti implants. *p<0.05 vs. control, # vs. sham, $ vs. rTi.

surgery, with no change in Th2-linked genes (*Gata3, Il4,* and *Il13*). Rough hydrophobic Ti implants induced elevated Th1 as well as Th2 and Treg phenotype factors compared to control. Rough-hydrophilic Ti generated the greatest up-regulation of Th2 and Treg genes, while simultaneously reducing Th1 genes at day 3. After 7 days, the largest up-

regulation of Th1-associated genes was present in the bone marrow of sham-operated animals. Rough Ti reduced these levels compared to sham, while still being increased compared to control. Finally, bone marrow surrounding rough-hydrophilic implants showed reduced Th1 markers compared to sham and hydrophobic implants. Levels of Th2 and Treg markers continued to be increased compared to control in sham and hydrophobic implants, while levels in hydrophilic implant mice were similar to levels in control mice. (Figure 7.2.1, C)

Local changes: Surface modifications change cell populations at implant surface

Changes in cell populations were quantified by flow cytometry from single cell suspensions generated from cells adherent to the implant surface or bone marrow in sham and control animals. A higher percent of CD45+CD11b+ macrophages were present on rough hydrophilic Ti implants one day following implant placement compared to rough Ti. By three days, similar levels of macrophages were attached on each implant, and at seven days a higher percent of macrophages were on rough Ti compared to the hydrophilic implant. (Figure 7.2.2, B)

All surgical procedures resulted in changes to the T-helper cell profiles compared to baseline three and seven days after the operations (data not shown). Few changes and the lowest percentage of Th1 populations were measured at 3 or 7 days in our surgical groups. A reduced percentage of pro-inflammatory Th17 cells were found surrounding Ti implants compared to sham operation at 3 days. Few differences were found in Th17 populations by day 7. The greatest changes in T-cell populations were observed within anti-inflammatory associated Th2 and Treg populations after 3 days. Increased percentages of Th2 cells were found on Ti implants, with more on rough Ti and greatest

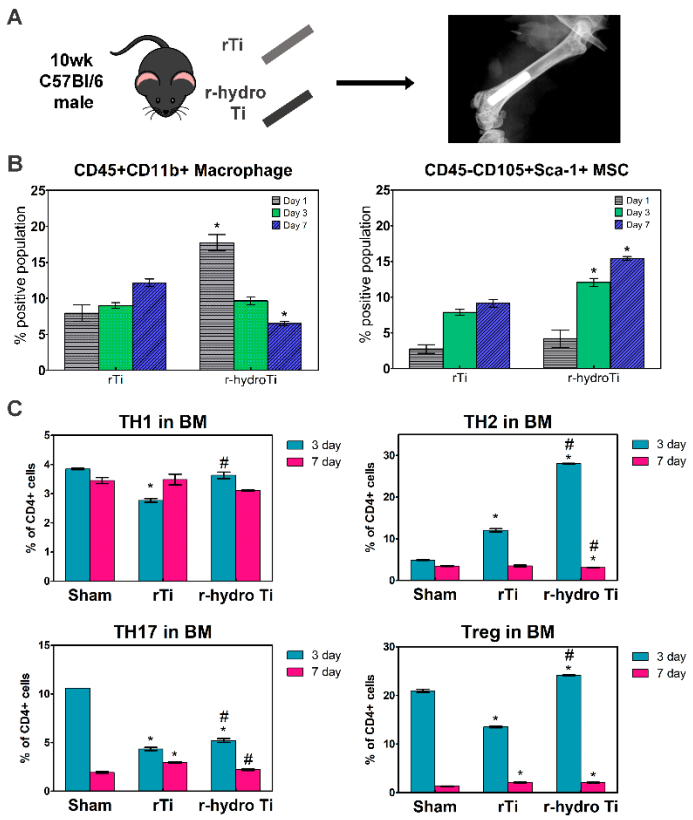

Figure 7.2.2: Local changes in cell populations adherent to implant surface within first 7 days. A. Schematic of surgery B. CD45+CD11b+ Macrophages adhered to implant. Changes in CD45-CD90+Sca-1+ MSCs at implant surface *p<0.05 vs. rTi. C. Changes in T-cell populations at implant, (n=6) The greatest changes in T-helper cell populations with surface properties was found in anti-inflammatory Th2 and Treg populations. The greatest percent of these populations were found on r-hydro Ti implants. *p<0.05 vs. sham, # vs. rTi

on rough-hydrophilic Ti. An initial reduction in Treg populations was measured on smooth and rough Ti at 3 days compared to the sham. Alternatively, an increased level of Tregs was found on rough-hydrophilic Ti compared to all other groups. By 7 days, lower percentages of Th2 and Tregs were measured in surgical groups with few differences between them. Increased Tregs were found on rough and rough-hydrophilic Ti after 7 days. (Figure 7.2.2, C)

Stem cells present at the implant site varied between surface hydrophilicity. At both 3 and 7 days following implantation, a greater percent of CD45-CD90+Sca-1+ stem cells were present on rough hydrophilic Ti implants compared to rough Ti. The highest percent of MSCs were quantified on rough hydrophilic Ti after seven days.

Systemic changes: Changes in T-cell populations extended to contralateral leg bone marrow and spleens

Differing levels of cytokines were measured in circulating plasma based on implant surface properties. We detected an increased level of pro-inflammatory IL12p40 in circulation of mice receiving the rough hydrophilic implant compared to rough Ti after 24 hours. (Figure 7.2.3, A) There was also a higher level of anti-inflammatory IL10 in mice with rough hydrophilic Ti. After 3 days levels of IL12p40 were reduced in hydrophilic groups compared to hydrophobic and IL10 was still higher in hydrophilic. Finally, at 7 days

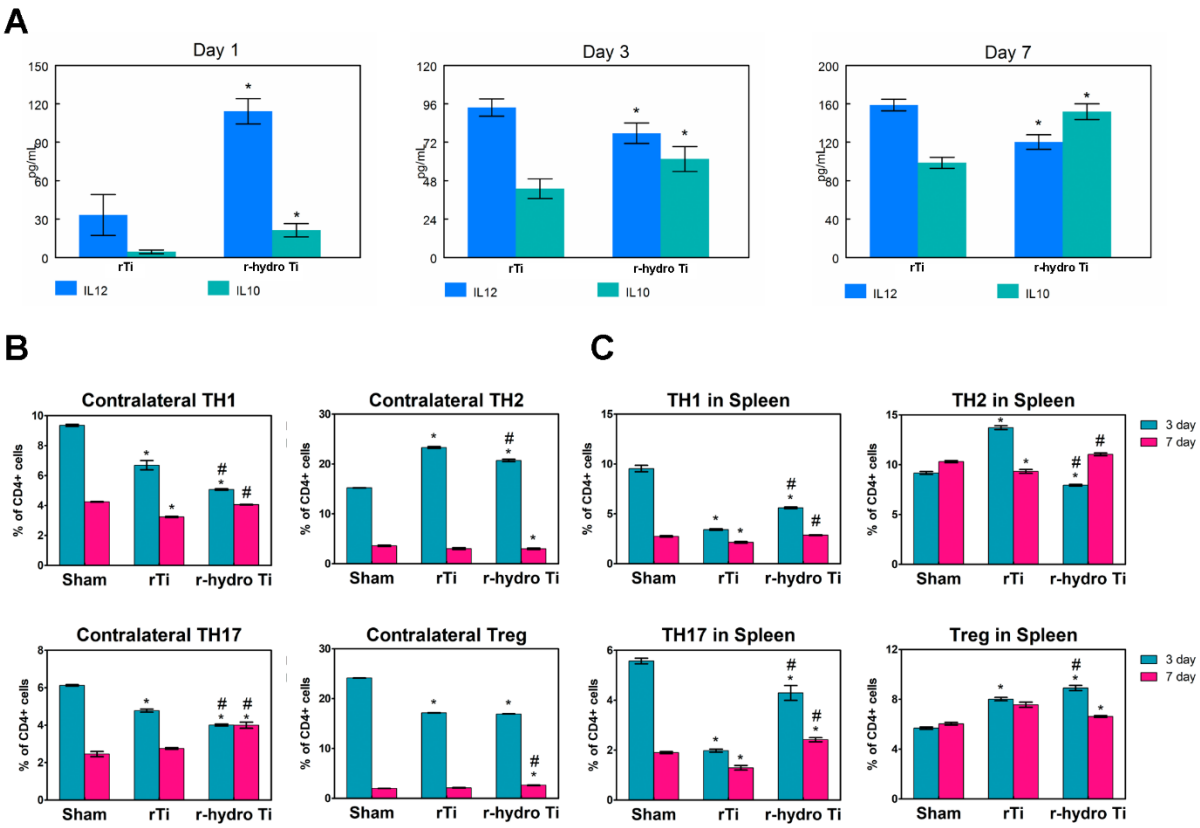

Figure 7.2.3: Systemic changes in inflammatory state. A. Changes in cytokine levels in circulating plasma. (n=6) *p<0.5 vs, rTi. B. Systemic changes in T-helper cell populations in the contralateral leg bone marrow at 3 and 7 days. C. Changes in T-helper cell populations in the spleen. (n=6) *p<0.05 vs. sham, # vs. smTi, $ vs. rTi.

there was a further increase in IL10 and still lower levels of IL12p40 in mice with hydrophilic implants.

Similar to changes in T-cell populations at the implant site, we found the greatest variation in levels of Th2 and Treg cells in the contralateral leg bone marrow at 3 days. Population percentages of Th1 and Th17 cells were reduced in animals receiving Ti implants compared to sham in the opposite leg. Lower levels of these cells were present in bone marrow of rough-hydrophilic implanted mice. An increased percentage of Th2 cells were found in the contralateral bone marrow of rough and rough-hydrophilic implanted mice at 3 days. Few differences were found after 7 days. A reduced level of Treg cells was quantified in the contralateral bone marrow of all Ti implant mice compared to sham at 3 days. (Figure 7.2.3, B)

All experimental animals had altered percentages of helper T-cell populations compared to the baseline spleen at day three of unoperated controls at days 3 and 7 (data not shown). Reduced percentages of Th1 and Th17 cells were found in spleens from animals receiving Ti implants compared to sham mice at 3 days. The highest percentages of both Th1 and Th17 cells in implant groups were found in the spleen of rough-hydrophilic implanted mice. By day 7, changes in percent populations were reduced in pro-inflammatory associated T-cell populations compared to day 3. The highest percentage of Th2 cells was found in animals receiving rTi implants at 3 days, which is reduced to lowest levels at 7 days. The highest percentage of Tregs was measured in spleens of mice with rough-hydrophilic implants at 3 days.

The inflammatory process following synthetic biomaterial implantation has traditionally thought to be modulated by the cells of the innate immune system. We and others have

shown that biomaterial surface characteristics affect the innate immune response and activate macrophages and dendritic cells into pro- or anti-inflammatory phenotypes depending on surface properties [53], [83], [100], [105]. However, growing evidence from healing and regenerative models suggests that the adaptive immune system may also actively participate in the biomaterial integration process [88], [106]. Our results demonstrate that intramedullary implantation of titanium rods results in local and systemic increases in Th2 and Treg populations.

The traditional tissue healing process has been divided into overlapping biological processes that include inflammation, repair, and remodeling [31], [32], [42]. After tissue injury by surgery or trauma, disrupted blood vessels cause hematoma formation. Immune cells are a significant constituent of the hematoma and secrete pro-inflammatory molecules that attract additional immune cells to the injury site [1], [32]. In normal healing, the initial inflammatory reaction subsides and is followed by a regenerative phase characterized by anti-inflammatory cells and molecules, which promote recruitment of progenitor and endothelial cells [44], [104]. Therefore, the tightly controlled pro- and anti-inflammatory events generated by the immune cells are critical to creating the necessary environment for a successful tissue healing and repair. This coordinated cascade of events can be affected by many local and systemic factors, but also can be affected by the nature of the material in the case of biomaterial implants. Therefore, it is important to understand how cells of the innate and adaptive immune system interact to create better materials that are not only biocompatible but also have the ability to influence the immune system to generate the desired response.

In this study, we saw an initial increase in local and systemic pro-inflammatory markers and elevated macrophage markers one day following placement of the rough hydrophilic implant compared to the hydrophobic with matching surface topography. By three days the greatest differences in cells populations and circulating cytokines were measured. At day 3 elevated inflammation had already begun to resolve surrounding the rough hydrophilic group and is still increasing in the rough Ti group, as evident by the prolonged increase in cytokines and macrophages present at the implant. This suggests that the hydrophilic implant surface is triggering cells, most likely macrophages, to secrete factors to resolve inflammation and begin recruiting tissue forming cells. In this study, macrophages appeared particularly important in modulating levels of IL12 and IL10. When macrophages were reduced lower levels of both proteins were found in circulation and no difference was found between implant groups. Alternatively, when macrophages were reduced there was an increase in the production of other cytokines. This suggests that other immune cells, such as natural killer or neutrophils may be playing a role and not strongly affected by ablation procedures. While macrophages may not be solely responsible for the rapid resolution, they are important for activating cells of the adaptive system.

The role of the immune system, both innate and adaptive, has been established as necessary in bone formation and repair [107]. Adaptive immune cells, like T-cells, are known to migrate to the site of bone injury at around 3 days and remain until callus formation begins. This time frame aligns with changes in T-helper cell activation seen in this study where we found the greatest changes locally and systemically at 3 days which were reduced by the end of the week. The increased anti-inflammatory T-cell populations

may have helped to promote resolution of the initial phase. Classically following the inflammatory phase will be tissue formation where MSCs will migrate to the site. The driving factor of stem cell migration is the release of cytokines and chemokines from resident and migratory immune cells, particularly *Cxcl12* which was increased on rough hydrophilic Ti implants. Once MSCs arrive at the implant site they will not only regenerate tissue but act to control and resolve the immune response by suppressing the release of immune cell recruitment factors, such as *Ccl2*, *Ccl4*, and *Ccl9* [107], [108] (Figure 7.2.1).

Synthetic materials that lacked potential epitopes for antigen presentation have previously been considered unable to engage the adaptive immune system. However, our results demonstrate a clear modulation of the T-helper cell response to biomaterial surface properties through activation of the innate immune response. Our study suggests that this initial effect on the innate immune system, specifically on macrophage activation, is extended into the adaptive immune system. Our results showed that T-helper cell profile changed in the immediate microenvironment surrounding the implant as early as 3 days post implantation. Moreover, gene expression from bone marrow adjacent to rough-hydrophilic implants showed a significant increase in *Gata3, Il4, Il13, Foxp3*, and *Il10*, genes central in Th2 and Treg activation and function [36]. It is important to note is that we used the same raw material to produce implants employed in this study and that the implants only differ at the surface level as a result of the modifications (sand blasting and acid etching) and the storage conditions (atmospheric vs. saline solution). These results demonstrate that surface properties like roughness and wettability play a vital role in immune cell activation.

Our results showed that rough-hydrophilic implants sharply increased Th2 cytokines in the bone marrow adjacent to the implant when compared to sham operation or the other implanted materials within the first 3 days. This effect may be the result of the initial macrophage activation in response to surface modifications that we have previously characterized [53], [54], with a macrophage activation resembling an M2-like phenotype on rough-hydrophilic surfaces and an M1-like phenotype on smooth or rough-hydrophobic surfaces. We saw changes in systemic cytokines measured in the serum, with an increase in pro- and anti-inflammatory cytokines. This systemic effect was also evident in changes in the CD4+ cells profile in the spleen and in the bone marrow of the contralateral limb. Ti implants with rough and rough-hydrophilic surface modifications changed the T-helper cell profile by decreasing Th1, Th17, and Treg populations and increasing Th2 cells in bone marrow from the contralateral leg. Interestingly, changes in T-helper cell population was also noticed in the spleen, with a decrease in Th1 and Th17 cells and increase in Treg population. These results suggest that either soluble factors produced from cells in contact or adjacent to the implant reach the circulatory system and affect other T-cells systemically or antigen presenting cells travel from the implantation site and re-enter the lymph.

The T-helper cell population changed dramatically by day 7 locally and systemically (Figure 7.2.2 and Figure 7.2.3). Locally, rough-hydrophilic surfaces decreased Th2 and increased Treg population, while rough-hydrophobic increased Th17 and Treg population. Similar results were observed in systemic T-helper cells from the contralateral bone marrow and spleen with most of the implants having a lower T-helper cell population when compared to sham animals. The polarization towards a Th2 response in the study

reflects what our group has seen in previous studies with alternative macrophage activation. Interestingly, it has been recently shown that a Th2 response increases wound healing of the skin [9], and we saw a similar effect in the bone microenvironment. Previous studies have shown that rough-hydrophilic implants have a faster rate of integration into bone compared to rough-hydrophobic titanium [17], [41], [109], [110]. In line with the previous study, we observed a significant Th2 skew in both the splenic helper T cell population and in the bone microenvironment surrounding rough-hydrophilic Ti implants. The Th2 polarized response may be directly correlated to wound healing time and is of interest for future studies.

7.3| Determine how soluble factors released from cells in contact with biomaterials will effect cells in the microenvironment.

In order to confirm the effect of macrophages on T-helper cell activation, we established a direct and indirect co-culture model. Our results showed that macrophages cultured on rough-hydrophilic titanium surfaces preferentially activated CD4+ cells into Th2 and decreased Th1 polarization. The *objective* of this study is to determine if contact with biomaterials following surface modification procedures will induce cells to influence cells within the local environment. We *hypothesize* that macrophages cultured on rough, hydrophilic surfaces will release factor to increase chemotaxis and promote survival and differentiation of stem cells. We also hypothesize that factors released from MSCs will reduce the production of inflammatory factors seen on rough, hydrophobic surfaces.

Materials and Methods

Cell Isolation and culture

Primary macrophages and MSCs were isolated from femurs of 8-12 week-old male C57BL/6 mice (The Jackson Laboratory, Bar Harbor, ME) under VCU IACUC approval based on previously established protocols. Briefly, bone marrow cells were flushed from the femurs using Dulbecco's phosphate-buffered saline (Life Technologies, Carlsbad, CA). Red blood cells were removed from flushed bone marrow by addition of ACK Lysing Buffer (Quality Biological, Inc., Gaithersburg, MD). Cells were counted (TC20™ Automated Cell Counter, Bio-Rad Laboratories, Hercules, CA) and plated in a 175 cm^2 flask at a density of 500,000 cells/mL in 30mL RPMI 1640 media (Life Technologies) supplemented with 10% fetal bovine serum (Life Technologies), 50U/mL penicillin-50 µg/mL streptomycin (Life Technologies), and 30ng/mL macrophage colony-stimulating factor (M-CSF, PeproTech, Rocky Hill, NJ). Cells were cultured at 37°C, 5% CO_2, and 100% humidity. Fresh media supplemented with M-CSF was added after four days. After seven days of exposure to growth factors, macrophages were passaged with Accutase (Life Technologies) at room temperature for 1 hour and seeded onto Ti surfaces for each experiment. Hydrophilic surfaces were removed from the saline solution and rinsed with ultrapure water prior to cell seeding.

Primary T cells were isolated from spleens removed from the same 10 week-old male C57Bl/6 mice. Naïve CD4+ T cells were then separated by negative selection using isolation columns (Milteny Biotec, San Diego CA). Briefly, spleens were crushed between two sterilized microscope slides to release cells, and red blood cells were lysed (ACK Lysing Buffer, Quality Biological, Inc.). A single cell suspension was magnetically labeled

using a cocktail of biotinylated monoclonal antibodies and anti-biotin microbeads labeling agents to deplete non-CD4+ splenocytes. Untouched isolated CD4+ T cells were then cultured in complete RPMI 1640 containing 10% FBS, 1% L-Glutamine, 1% penicillin-streptomycin, and 0.1% 2-mercaptoethanol and activated for 48 hours in plates pre-coated with 5μg/mL anti-CD3e mAb (Biolegend) and treated by 2μg/mL anti-CD28 to promote proliferation before being used in experiments.

In Vitro Co-Culture Model

Stem cell migration was assessed by pre-labeling mouse MSCs (mMSC) with 1μM Calcein AM (BD Pharmingen), then 20,000 cells per well were plated in 1% FBS DMEM in the top chamber of a BD invasion assay. Activated M1 (20ng/mL IFNγ (PeproTech) and 50ng/mL LPS (Sigma), M2 (20ng/mL IL4 and IL13 (PeproTech)), naïve, and macrophages on each smooth, rough and rough-hydrophilic Ti surfaces were on the bottom of the chamber. Additionally, macrophage activation in the presence of MSCs was established using 1μm pore size transwell inserts in a 6 well plate. mMSCs were plated at 10,000 cells/cm^2 in the lower portion and macrophages plated on Ti surfaces or sterilized glass covers slips at 50,000 cells/cm^2. Cells were incubated together for 24 hours, then separated and media replaced for 12 hours. Harvested media from macrophages were analyzed for secreted ILs by ELISA as previously mentioned.

Interactions between T-cells and macrophages were examined using direct and indirect co-culture experiments. In indirect co-culture experiments, macrophages were cultured on Ti surfaces for 24 hours at a density of 100,000 cells/well. Media and secreted factors were then collected and used to treat activated T-cells in a separate 24 well plate. For direct culture experiments, macrophages were grown on Ti surfaces for 24 hours and

then activated T-cells were added to the culture in a 1:1 ratio. These cells were allowed to interact for an additional 24 hours before media, and non-adherent T-cells were collected for analysis. To assess proliferation, CD4+ T-cells were treated with carboxyfluorescein succinimidyl ester (CFSE, Molecular Probes, ThermoFisher) at the time of either direct or indirect co-culture with macrophages. After 24 hours of interaction, cells were collected and analyzed by flow cytometry. Changes in CD4+ T-helper subsets were determined by flow cytometry using PE-Tbet, Alexa 488-Gata3, PE-RoRγt, or Alexa 488-Foxp3 positive populations.

Results and Discussion

Macrophage modulation of T-cell proliferation and activation

To determine the importance of macrophages in T-cell proliferation and population changes, we conducted two different *in vitro* culture experiments between T-cells and macrophages. The first was an indirect co-culture of T-cells treated with conditioned medium from macrophages, and the second was a direct contact co-culture with macrophages and Ti biomaterial surface. Activated T-cells treated with conditioned media from macrophages plated on different surfaces with different surface properties maintained the ability to proliferate. In addition, the media and secreted proteins from macrophages on each Ti surface enhanced the number of cells that proliferated 3 or more times compared to T cells exposed to conditioned media from macrophages on TCPS. Naïve T-helper cells plated at a 1:1 ratio with macrophages on the different surfaces all proliferated. Both rough Ti surfaces had significantly more T-cells doubling 3 or more times (CFSE low) than T cells plated on smooth Ti surfaces. T-cells co-cultured on

hydrophilic rough Ti had greater proliferative capability than T-cells co-cultured with macrophages on TCPS and smooth Ti.

Direct contact with macrophages resulted in greater changes in percentages of each T-helper cell population on Ti surfaces compared to treatment with soluble factors in conditioned media. A higher percent of Th1 cells was present in all groups of direct culture compared to indirect. Within the direct culture group, Ti surfaces reduced percentages of Th1 cells compared to TCPS, with rough-hydrophilic Ti having the lowest level. Indirect culture on Ti surfaces also reduced Th1 populations compared to TCPS. Direct co-culture

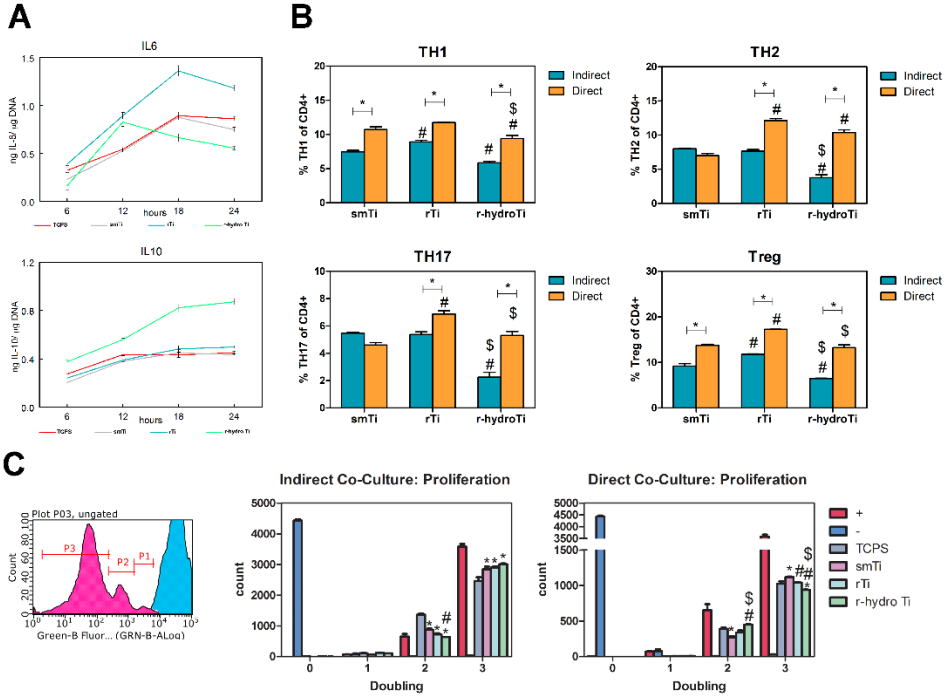

Figure 7.3.1: Ti surfaces induces inflammatory changes *in vitro.* A. Time course of macrophage activation on surface. B. Direct and indirect *in vitro* cultures between macrophages on Ti surfaces and CD4+ cells. (n=6) #p<0.05 vs. smTi, $ vs. rTi. Bracket* p<0.05 vs. indirect culture. C. Representative histogram showing cell doubling times. B. Bar graph quantification of T-cell proliferation (n=6). C. Changes in activated T-cell proliferation with indirect and direct co-culture with macrophages. (n=6) *p<0.05 vs. TCPS, # vs. smTi, $ vs. rTi. + denotes CD4+ cells in contact with anti-CD3e treated with anti-CD28, - CD4+ cells in contact with anti-CD3e.

on rough surface resulted in higher percentages of Th2 cell compared to indirect, while smooth Ti reduced the percent of Th2 in both culture conditions. Similar levels of Th2

cells were present between rough Ti and TCPS with direct culture, but treatment with conditioned media reduced the Th2 population on rough Ti compared to TCPS. Direct culture with macrophages resulted in increased Th17 populations compared to indirect. A greater percent of Treg cells was found in direct culture with macrophages compared to indirect. The lowest level of Treg was measured in T cells cultured with conditioned media from macrophages on hydrophilic surfaces. (Figure 7.3.1)

Macrophage-induced stem cell recruitment and activation

A greater number of tagged MSCs migrated toward wells where macrophages were present compared to matching well with only media. The highest level of MSC recruitment was measured toward M2 activated and macrophages on rough hydrophilic Ti disks. While naïve and M1 activated macrophages on TCPS recruited the lowest level of MSCs and were not different from media or media with LPS, respectively (Figure 7.3.2). Next, we wanted to establish how MSC presence would alter macrophage activation either

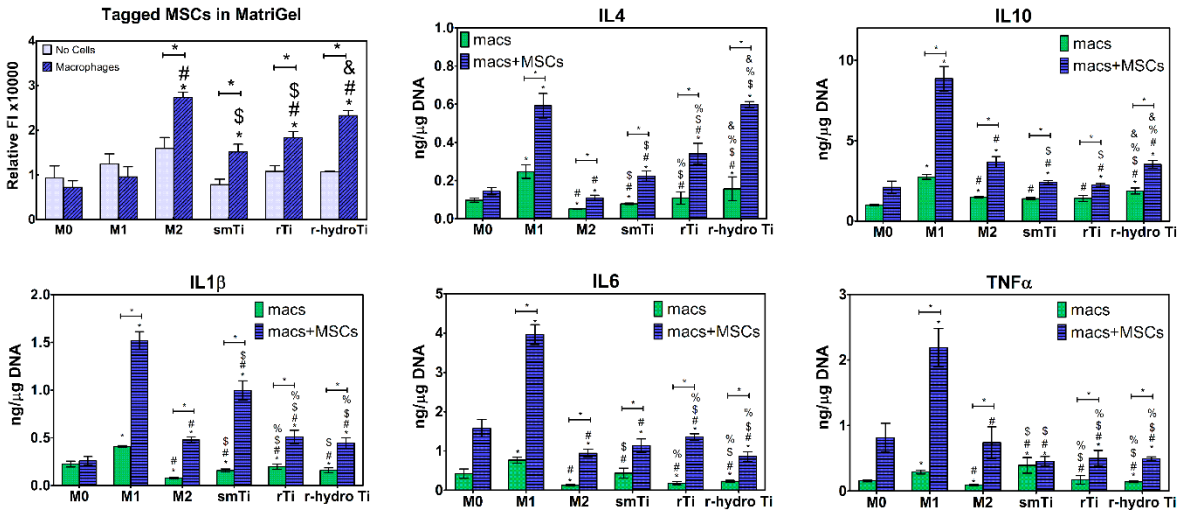

Figure 7.3.2: Ti surface properties alter macrophage activation induces stem cell recruitment and resulting phenotype. A. MSC migration through matrigel toward macrophages classically activated or by Ti surface properties. (n=6) *p<0.05 vs. M0, # vs. M1, $ vs. M2, % vs. smTi, & vs. rTi. Bracket*p<0.05 vs. no cell control. B. Macrophage activation with and without stem cell co-culture. (n=6) *p<0.05 vs. M0, # vs. M1, $ vs. M2, % vs. smTi, & vs. rTi. Bracket*p<0.05

classically or on the Ti surfaces. We found that when cultured in the presence of MSCs for 24 hours macrophages consistently released a greater amount of cytokines than when cultured alone. Overall, classically activated M1 macrophages secreted the highest level of all cytokines.

We also found distinct differences in levels of MSC migration to the hydrophilic implant *in vitro.* When macrophages were reduced *in vivo* the changes in T-cell and stem cell populations were also reduced. Stem cells have also been found to promote an M2-macrophage phenotype in direct co-culture models as well as from conditioned media [111]. While similar cell ratios were used in this study, 1:5 MSCs to macrophages, the presence of stem cells did not induce a less inflammatory phenotype in activated macrophages. This study differed from others in that the cells were separated and media replaced following co-culture, which allowed for only cytokines from macrophages to be collected and not mixed with stem cell secreted factors.

7.4| Evaluate the response to implanted metallic materials without macrophages.

Materials and Methods

Animals and Surgical Procedure

For each study, 10-week male C57Bl/6 mice (The Jackson Laboratory, Bar Harbor, ME) or MaFIA (C57BL/6-Tg(Csf1r-EGFP-NGFR/FKBP1A/TNFRSF6)2Bck/J) (The Jackson Laboratory) were used.

Macrophage Ablation

Macrophages and macrophage precursors were ablated in MaFIA mice by 50µL IP injections of AP20187 (Takara Bio USA) (5mg/kg in 1% DMSO + 10% PEG-400 + 2% Tween-80 in sterile water) beginning 3 days prior to surgery and continuing every 48 hours until endpoint. Mature phagocytic cells were ablated in wild-type C57Bl/6 mice with clodronate liposomes following published procedures [56]. Mice were injected with 200uL of clodronate (40µg/kg), or PBS filled liposomes (ClondronateLiposomes.org, Netherlands) for three consecutive days prior to implant placement and every 48 hours for the duration of the study to maintain ablation.

Flow Cytometry Analysis

Changes in local cell populations were quantified by flow cytometry of implant-adherent cells after 1, 3 or 7 days. Systemic changes were measured in spleens. Prior to staining, Fc receptors were blocked by incubation with CD16/32 (BioLegend, San Diego, CA) and membranes permeabilized for transcription factor staining. The ratio of stem cell and macrophage population was determined in bone marrow (MSC: PE-Sca-1, PE/Cy7-CD90, APC-CD29, APC-CD105, PE/Cy7-CD105; Macrophage: FITC-CD11b, PE-CD45, CD68-PE/Cy7) (Biolegend). T cell populations were identified by antibodies against T-helper cell marker CD4 (APC-CD4, Biolegend), as well as transcription factors of specific T-cell populations [Th1 (PE-Tbet), Th2 (Alexa 488-Gata3), Th17 (PE-RORγT, BD Biosciences), and Treg (Alexa 488-Foxp3)] (Biolegend). Cells were fixed and permeabalized for intracellular staining using Foxp3 Transcription Factor Staining Kit (eBiosciences, Thermofisher). Antibody concentrations were added based on manufacturer's protocol. Stained cell suspensions were analyzed using the Guava®

easyCyte 6-2L Benchtop Flow Cytometer (MilliporeSigma) instrument with a total of 10,000 events were measured with three replicates for each measurement. Results were analyzed using guava Soft 3.1.1 InCyte software and FCS Express software (Figure S2).

Circulating Inflammation

Circulating plasma was isolated from blood collected 1, 3 and 7 days post material implantation by cardiac puncture. Cytokine levels were quantified by custom-designed BioPlex assay (BioRad) for pro-inflammatory (IL1β, IL6, IL12p40, TNFα) and anti-inflammatory (IL4 and IL10) factors.

Statistical Analysis

Animal studies were performed with six animals per implant group. Flow cytometry samples were run in three technical replicates. Statistical analyses were performed using Prism GraphPad 5.0 and JMP Pro software. A one-factor, equal-variance analysis of variance (ANOVA) was used to test the null hypothesis that the group means were equal, against an alternative hypothesis that at least two of the group means were different, at the $\alpha=0.05$ significance level. Once a p-value resulting from the ANOVA model was determined to be less than 0.05, multiple comparisons between the group means were made using the Tukey-HSD method.

Results and Discussion

Macrophage ablation reduced changes in T-helper cell populations and systemic inflammation

To assess whether changes in systemic inflammation would be present in our model without macrophages, clodronate liposomes were used to ablate mature macrophages or MaFIA mice to remove macrophage precursors. In our first study macrophages and macrophage precursors were removed with MaFIA mice. There was a reduced level of circulating pro-inflammatory IL12p40 following macrophage ablation at 1, 3 and 7 days compared to wild-type mice. Lower levels of IL10 were measured in macrophage ablated MaFIA mice compared to C57Bl/6 mice with matching implants at 1 and 3 days, while levels were similar at 7 days. In our second study, mature phagocytes were ablated with clodronate liposome injections. Control mice with rough hydrophilic implants had higher levels of circulating IL10 compared to mice with rough implants. Hydrophilic implants also resulted in lower levels of pro-inflammatory IL-12p40. (Figure 7.4.1, A) Following macrophage ablation, circulating inflammatory factors were similar between implant groups and reduced compared to non-macrophage ablated mice. In contrast, there was a higher level of IL1β, IL6, and IL4 in circulating plasma from macrophage ablated mice compared to control with matching implants.

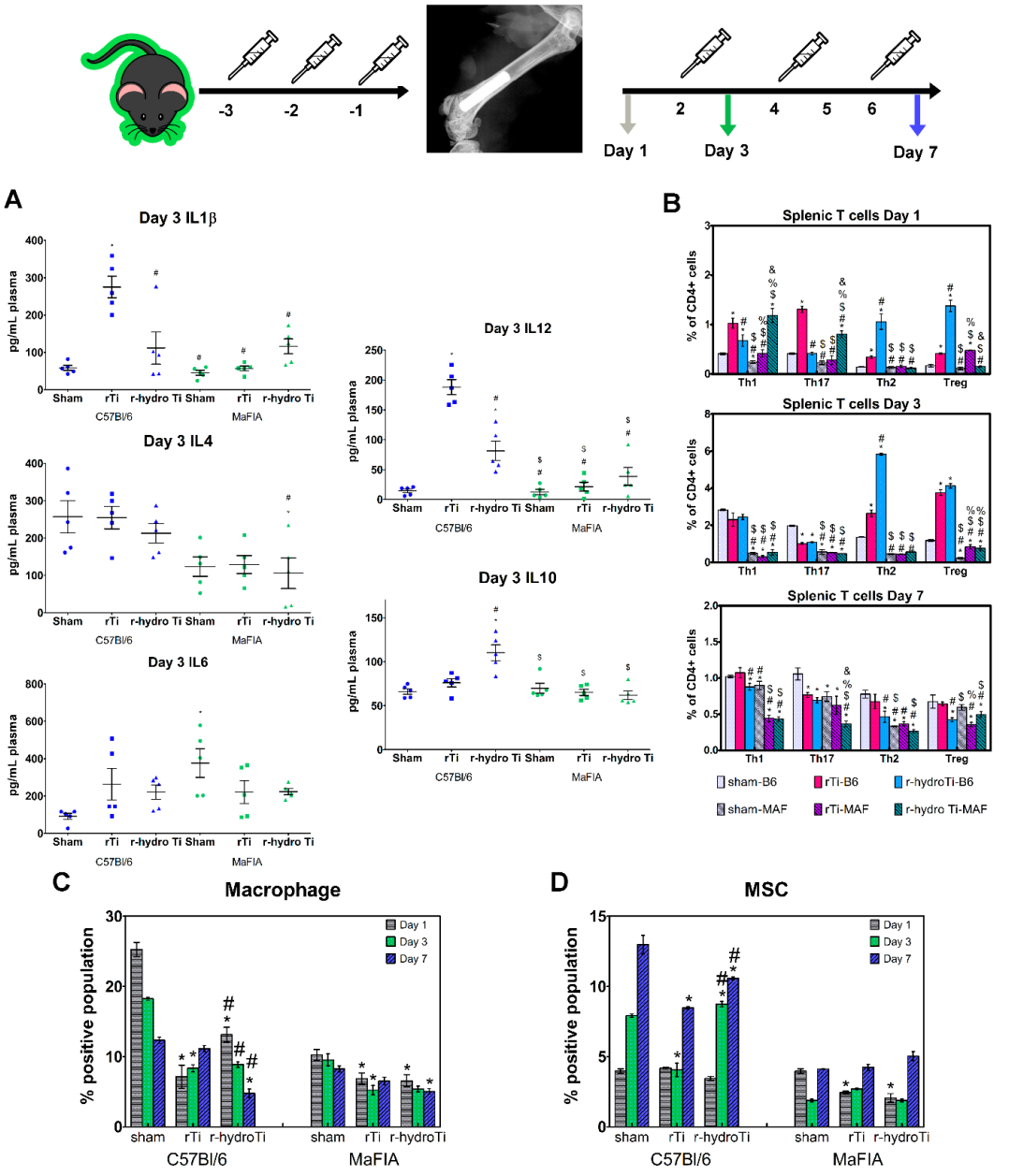

Figure 7.4.1: Inflammation and cell populations changes with macrophage ablation in MaFIA mice A. Injection and harvest time table. B. Changes in circulating inflammation were greatest at day 3, (n=6) * p<0.05 vs. C57Bl/6-sham, # vs. C57Bl/6-rTi, $ vs. C57Bl/6-r-hydro Ti. B. Splenic T-cell populations at 1, 3 and 7 days post-surgery. (n=6) stats completed within cell populations *p<0.05 vs. C57Bl/6-sham, # vs. C57Bl/6-rTi, $ vs. C57Bl/6-r-hydro-Ti, % vs. MaFIA-sham, & vs. MaFIA-rTi. C. Reduced levels of macrophage populations at surgery site with AP20187 injections in MaFIA mice. Stats completed within mouse species *p<0.05 vs. sham, # vs. rTi. D. Stem cell populations are reduced at implant site at days 1, 3 and 7 with AP20187 injections in MaFIA mice. (n=6) *p<0.05 vs. sham, # vs. rTi.

The highest percent of activated T-cells was measured at 3 days post-surgery in the first study. A greater percent of Th2 cells were found in wild-type mice receiving rough

hydrophilic implants compared to sham and rough implants at 1 and 3 days. A higher level of regulatory T cells was also found in spleens of mice at 1 and 3 days in mice receiving either implant compared to sham (Figure 7.4.1, C). When macrophages were ablated in the MaFIA mouse model, a reduced level of all T-helper cell populations was found in spleens at each time point. Because the greatest changes were measured in anti-inflammatory T-helper cell populations, these were focused on in the second study with mature macrophage ablation. Similarly, higher percentages of anti-inflammatory associated T-helper cell populations, Th2 and Treg, were found in spleens of no injection and PBS liposome control animals receiving the hydrophilic implant compared to rough Ti. When macrophages were ablated with clodronate liposomes, no difference in T-helper cell populations was detected between the rough and rough-hydrophilic Ti implant groups.

Macrophage ablation reduces stem cell population at the implant surface

MaFIA mice showed a 47% reduction in macrophage population following ablation at day 1 and only 35% at day 7 (data not shown). At day 1 there was the highest percentage of macrophages found in the C57Bl/6 sham group (Figure 7.4.1, C). The percent of macrophages in the sham group decreased over time. We again found a higher initial level of macrophages on rough hydrophilic implants compared to hydrophobic in C57Bl/6 mice. The level reduced over time on hydrophilic implants and increased on hydrophobic. In MaFIA mice following macrophage ablation, there were lower levels of macrophages in sham groups, which again reduced overtime. The lowest level of macrophages was found on rough hydrophilic implants at day 7. The level of stem cells increased in each C57Bl/6 group over time, with a higher level present on hydrophilic Ti at day 3 compared to both sham and rough Ti.

Clodronate liposome injections successfully removed 74% of macrophages following injections. In wild-type control mice, the number of MSCs at the implant surface increased over the first week, with the highest percent present at 7 days (Figure 7.4.2). Higher numbers were present on rough hydrophilic Ti at 3 and 7 days compared to rough Ti

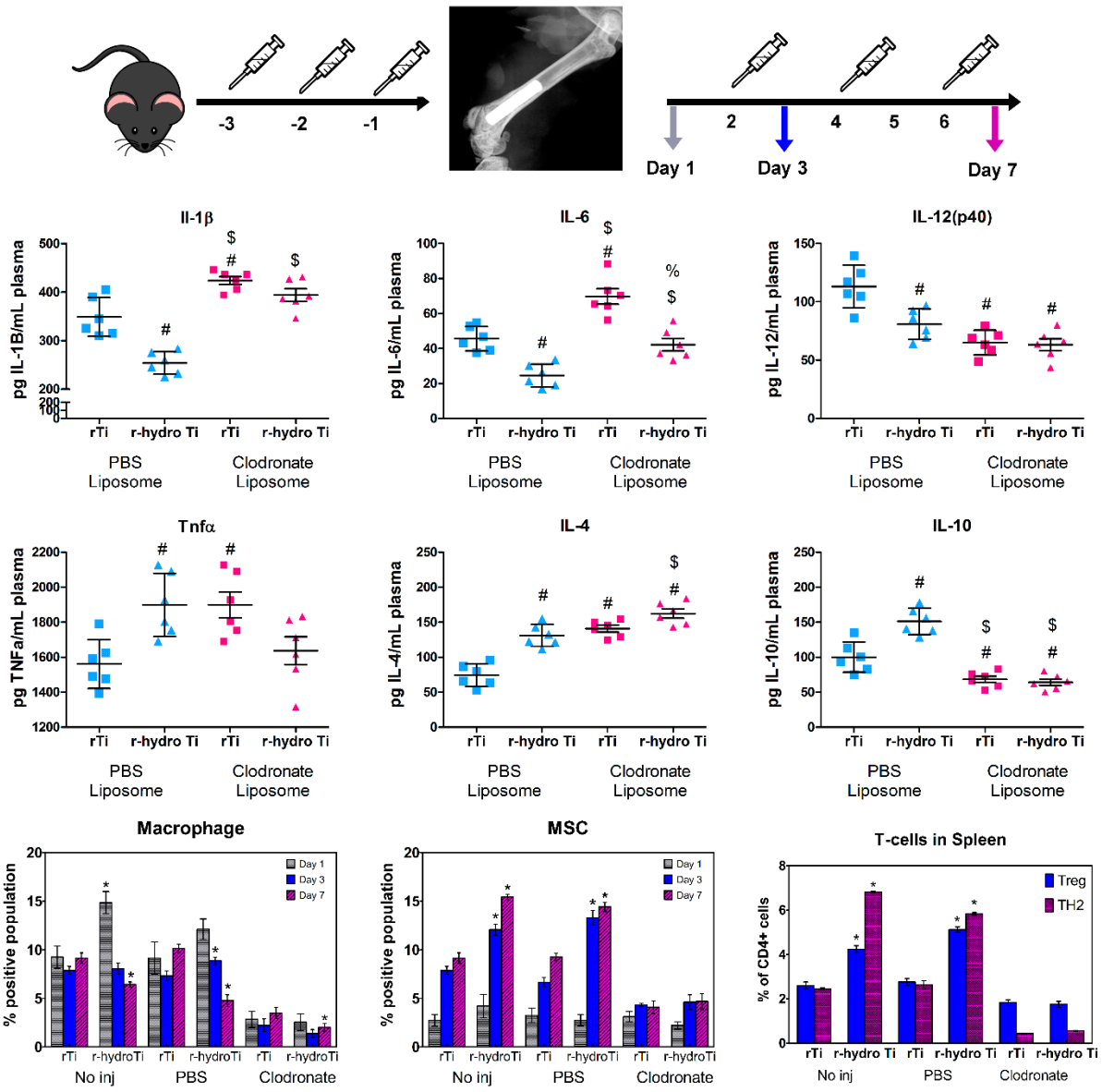

Figure 7.4.2: Macrophage ablation with clodronate liposomes reduced changes in inflammatory response between implant types. A. Time table of injections and harvest. B. Greater levels of IL-10 with hydrophilic implants and reduces changes in circulating inflammation without macrophages. #p<0.05 vs. PBS-Liposome rTi, $ vs. PBS-Liposome r-hydro Ti. B. Lower levels of macrophages and stem cells at implant site following clodronate liposome injection. (n=6) *p<0.05 vs. rTi. Reduced changes in T-helper cell populations in the spleen following macrophage ablation. *p<0.05 vs. rTi.

implants. When mature macrophages were removed with clodronate liposome injections, fewer stem cells were at the implant surface, and no difference was found between surface properties.

The specific removal of macrophages through chemical or transgenic modification has shown to alter bone formation following tibia fracture in mice [33, 34]. Studies have demonstrated the importance of tissue resident macrophages (termed osteomacs) macrophages on fracture repair and have highlighted the actions of macrophages in the deposition of collagen matrix and the formation of new bone. Both circulating and tissue resident macrophages can be activated along the gradient from M1 to M2 and have differing effects on the wound healing cascade. The increased level of anti-inflammatory factors produced on rough, hydrophilic surfaces in this study may allow for faster resolution of inflammation and initiation of tissue regeneration.

Successful integration of biomaterials is typically accessed by interaction with surrounding tissue after at least one month. In this study, we assessed modulation of the initial inflammatory and cell recruitment process by material surface properties and macrophages during the first week. The inflammatory process following synthetic biomaterial implantation has traditionally thought to be modulated by the cells of the innate immune system. We and others have shown that biomaterial surface characteristics affect the innate immune response and activate macrophages and dendritic cells into pro- or anti-inflammatory phenotypes depending on surface properties [53], [83], [100], [105]. However, growing evidence from healing and regenerative models suggests that the adaptive immune system may also actively participate in the biomaterial integration process [88], [106]. Our results demonstrate that intramedullary implantation

of titanium rods results in local and systemic changes in inflammatory profile. We also found changes in macrophage levels surrounding implants depending on implant wettability. Increased initial macrophage populations could be correlated with increases in Th2 and Treg populations and greater levels of stem cells at the implant. Moreover, we were able to reproduce this activation *in vitro*, demonstrating that biomaterial-activated macrophages can selectively activate CD4+ cells into Th2 and Treg populations depending on material surface characteristics.

For these studies, we aimed to establish the importance of macrophages in changes seen in stem cell recruitment and inflammatory cell populations using two separate models of macrophage ablation. The first was the MaFIA mouse model which uses a suicide gene activating ligand (AP20187) to induce apoptosis in cells with the CSF1R. This receptor is located on other cell populations including monocytes, dendritic cells, and osteoclasts, which may lead to effects not evaluated in this study. We lost 3 of 6 mice in initial studies using a 10mg/kg dose given for the total 10 days necessary for these studies. To ensure the survival of MaFIA mice receiving AP20187 injections throughout the study, we chose to use a lower dose (5mg/kg) than that used by others (>10 mg/kg) [57]. These studies used macrophage ablation to confirm their involvement in callus formation following fracture. Our second model of macrophage ablation used the injection of specifically sized liposomes containing clodronate. The size of these liposomes ensured that only phagocytic cells would be affected, therefore not altering monocytes and osteoclasts as with the MaFIA mouse model. Similar to other studies, we were able to establish macrophage importance in changes in systemic inflammation and local MSC recruitment. A greater reduction in stem cell recruitment and change in T-helper cell

populations were found in the clodronate liposome ablation model compared to the MaFIA model. This may have been due to one of two reasons. The first is that we were able to achieve a greater macrophage ablation in this model while still maintaining animal survival. The second being that mature phagocytes play a more prominent role in the initial healing stages following implant placement. Immature myeloid cells present at the injury site may not be responsible for recruiting tissue healing stem cells. Following macrophage ablation in both models, a lower percent of stem cells were present at the implant site, and surface properties did not induce changes. Macrophages were not entirely ablated in either of our models but were reduced.

Since T-helper cells are unlikely to recognize proteins adsorbed on the biomaterial surface or attach to the surface directly and immune cells will likely interact with the material prior to stem cells, we used the two established models of macrophage ablation with clodronate liposomes [56] and MaFIA mice [57] to determine macrophage importance in changes found in T-helper cell populations in our animal model. After macrophage ablation with clodronate liposomes, CD4+ cell populations were not changed between biomaterial surface modifications tested. There was a decrease in all T-helper cell populations, suggesting that macrophages are responsible for the initial changes in T-cell response. We and others have previously reported that macrophages are among the first cells to interact with implanted biomaterials and that this initial interaction affects the activation and phenotype of naïve macrophages [41], [64]. In order to confirm the effect of macrophages on T-helper cell activation, we established a direct and indirect co-culture model. Our results showed that macrophages cultured on rough-hydrophilic titanium surfaces preferentially activated CD4+ cells into Th2 and decreased Th1

polarization. Alternatively activated macrophages on hydrophilic Ti will condition the microenvironment through secretion of cytokines, IL4 and IL10, which can promote Th2 activation. Interestingly, T-helper cell population changed dramatically by day 7 locally and systemically. Locally, rough-hydrophilic surfaces decreased Th2 and increased Treg population, while rough-hydrophobic increased Th17 and Treg population. Similar results were observed in systemic T-helper cells from the contralateral bone marrow and spleen with most of the implants having a lower T-helper cell population when compared to sham animals.

7.5| Conclusion

In Aim 3 the importance of macrophage activation to biomaterial surface properties in healing events over the first week following implant placement was confirmed using mouse models. When macrophages are present, the hydrophilic mSLA surface promoted a faster switch from a pro-inflammatory to anti-inflammatory microenvironment immediately surrounding the implant compared to hydrophobic SLA. Increased levels of anti-inflammatory associated T-cell populations, Th2 and Treg, were found locally at day 3 and systemically in spleens at day 7 in mice receiving hydrophilic implants. While stem cells were present surrounding both SLA and mSLA implants, a higher number of cells surrounding the hydrophilic implant were stem cells. When macrophages were reduced changes in T-cell populations in the spleen were no longer different between the surfaces and were lower. Additionally, without macrophages there were fewer stem cells present at the implant site at days 3 and 7 following implantation and no difference was found between the rough hydrophobic SLA and rough hydrophilic Tim SLA implants.

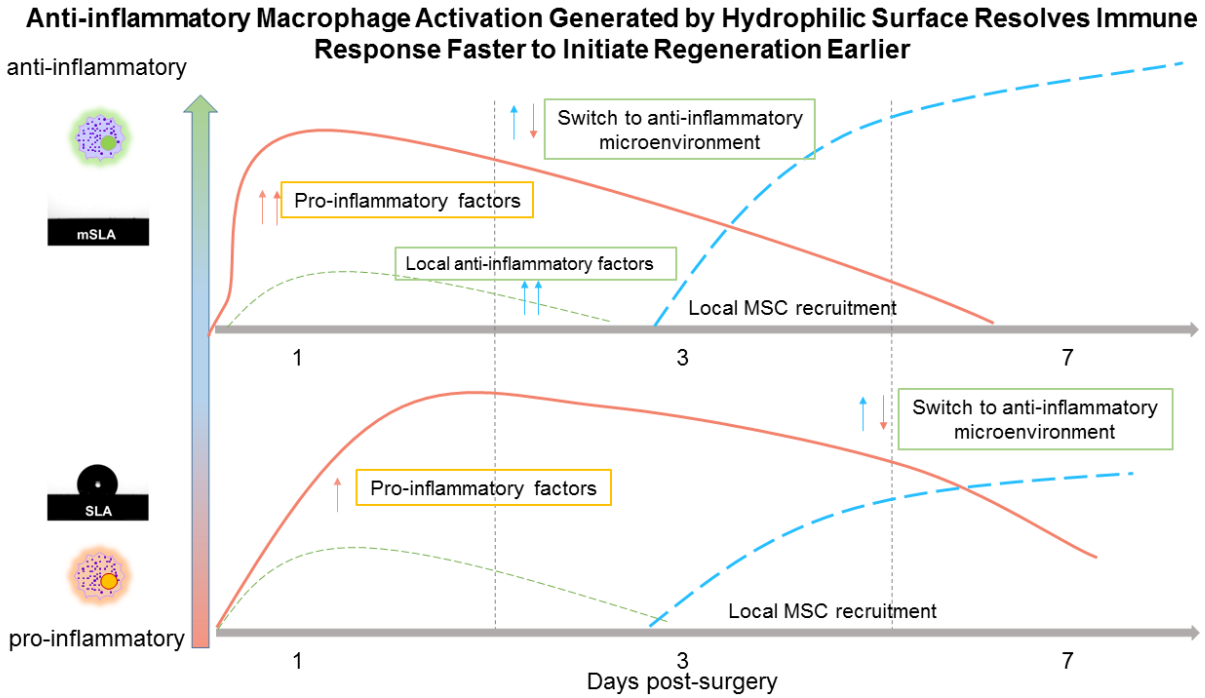

Figure 7.5.1: Summary figure for Aim 3. Macrophage activation on Ti implants regulates inflammation both locally and systemically as well as stem cell recruitment to the implant site.

Chapter 8 | Limitations, Implications & Future Directions

Studies conducted throughout this Ph.D. dissertation show the ability of macrophages to be differentially activated by biomaterial surface properties. Changes in Ti surface characteristics, specifically wettability, were able to consistently modify macrophage activation both in *in vitro* and *in vivo* mouse models. Increased wettability on hydrophilic implants generated a more anti-inflammatory, M2-like. Each of these studies were performed in mice which allow for a wide range of genetic tools for analysis and animals for specific removal of cells types. While hydrophilic surfaces promoted anti-inflammatory macrophage activation and reduced healing times in the clinical setting following implant placement it will also be interesting to confirm the effect on macrophage activation using cells sampled from different human populations.

Overall, a greater understanding of how immune cells recognize and respond to materials can help both engineers and physicians to design and select implants for patients with compromised healing. Blocking interaction between specific integrin surface receptors and protein adsorption on biomaterial surfaces will increase inflammatory activation of macrophages. While these studies showed increased anti-inflammatory cell activation with an increase in hydrophilicity across different Ti and Ti alloys, non-metallic and degradable materials were not studied. Determining if increasing hydrophilicity of other commonly used biomaterials, such as polyether-ether-ketone and poly-lactic-acid, could help in the development and selection of materials for tissue regeneration procedures.

References

[1] C. Gretzer, L. Emanuelsson, E. Liljensten, and P. Thomsen, “The inflammatory cell influx and cytokines changes during transition from acute inflammation to fibrous repair around implanted materials.,” *J. Biomater. Sci. Polym. Ed.*, vol. 17, no. 6, pp. 669–87, Jan. 2006.

[2] M. Esposito, M. G. Grusovin, M. Willings, P. Coulthard, and H. V Worthington, “The effectiveness of immediate, early, and conventional loading of dental implants: a Cochrane systematic review of randomized controlled clinical trials.,” *Int. J. Oral Maxillofac. Implants*, vol. 22, no. 6, pp. 893–904, Jan. 2007.

[3] C. von Wilmowsky, T. Moest, E. Nkenke, F. Stelzle, and K. A. Schlegel, “Implants in bone: Part I. A current overview about tissue response, surface modifications and future perspectives,” *Oral Maxillofac. Surg.*, vol. 18, no. 3, pp. 243–257, Sep. 2014.

[4] L. L. Hench and J. M. Polak, “Third-generation biomedical materials.,” *Science*, vol. 295, no. 5557, pp. 1014–7, Feb. 2002.

[5] C. A. Custódio, R. L. Reis, and J. F. Mano, “Engineering Biomolecular Microenvironments for Cell Instructive Biomaterials,” *Adv. Healthc. Mater.*, vol. 3, no. 6, pp. 797–810, Jun. 2014.

[6] C. Castells-Sala and C. E. Semino, “Biomaterials for stem cell culture and seeding for the generation and delivery of cardiac myocytes,” *Curr. Opin. Organ Transplant.*, vol. 17, no. 6, pp. 681–687, Dec. 2012.

[7] M. D’Este, D. Eglin, M. Alini, and L. Kyllonen, “Bone regeneration with biomaterials and active molecules delivery.,” *Curr. Pharm. Biotechnol.*, vol. 16, no. 7, pp. 582–605, 2015.

[8] A. Sculean, D. Nikolidakis, G. Nikou, A. Ivanovic, I. L. C. Chapple, and A. Stavropoulos, “Biomaterials for promoting periodontal regeneration in human intrabony defects: a systematic review,” *Periodontol. 2000*, vol. 68, no. 1, pp. 182–216, Jun. 2015.

[9] K. Sadtler, K. Estrellas, B. W. Allen, M. T. Wolf, H. Fan, A. J. Tam, C. H. Patel, B. S. Luber, H. Wang, K. R. Wagner, J. D. Powell, F. Housseau, D. M. Pardoll, and J. H. Elisseeff, “Developing a pro-regenerative biomaterial scaffold microenvironment requires T helper 2 cells,” *Science (80-.).*, vol. 352, no. 6283, pp. 366–370, 2016.

[10] L. Tang, T. P. Ugarova, E. F. Plow, and J. W. Eaton, “Molecular determinants of acute inflammatory responses to biomaterials.,” *J. Clin. Invest.*, vol. 97, no. 5, pp. 1329–34, Mar. 1996.

[11] M. Navarro, A. Michiardi, O. Castaño, and J. A. Planell, “Biomaterials in orthopaedics.,” *J. R. Soc. Interface*, vol. 5, no. 27, pp. 1137–58, Oct. 2008.

[12] C. von Wilmowsky, T. Moest, E. Nkenke, F. Stelzle, and K. A. Schlegel, “Implants in bone: Part I. A current overview about tissue response, surface modifications and future perspectives,” *Oral Maxillofac. Surg.*, vol. 18, no. 3, pp. 243–257, Sep. 2014.

[13] M. Quirynen, B. Al-Nawas, H. J. A. Meijer, A. Razavi, T. E. Reichert, M. Schimmel, S. Storelli, and E. Romeo, “Small-diameter titanium Grade IV and titanium-zirconium implants in edentulous mandibles: three-year results from a double-blind, randomized controlled trial.,” *Clin. Oral Implants Res.*, vol. 26, no. 7, pp. 831–40, Jul. 2015.

[14] B. Wen, F. Zhu, Z. Li, P. Zhang, X. Lin, and M. Dard, “The osseointegration behavior of titanium-zirconium implants in ovariectomized rabbits.,” *Clin. Oral Implants Res.*, vol. 25, no. 7, pp. 819–25, Jul. 2014.

[15] C. A. Simmons, N. Valiquette, and R. M. Pilliar, “Osseointegration of sintered porous-surfaced and plasma spray-coated implants: An animal model study of early postimplantation healing response and mechanical stability.,” *J. Biomed. Mater. Res.*, vol. 47, no. 2, pp. 127–38, Nov. 1999.

[16] X. Liu, R. W. . Poon, S. C. . Kwok, P. K. Chu, and C. Ding, “Plasma surface modification of titanium for hard tissue replacements,” *Surf. Coatings Technol.*, vol. 186, no. 1–2, pp. 227–233, Aug. 2004.

[17] L. Le Guéhennec, A. Soueidan, P. Layrolle, and Y. Amouriq, “Surface treatments of titanium dental implants for rapid osseointegration.,” *Dent. Mater.*, vol. 23, no. 7, pp. 844–54, Jul. 2007.

[18] X. LIU, P. CHU, and C. DING, “Surface modification of titanium, titanium alloys, and related materials for biomedical applications,” *Mater. Sci. Eng. R Reports*, vol. 47, no. 3–4, pp. 49–121, Dec. 2004.

[19] S. L. Hyzy, R. Olivares-Navarrete, D. L. Hutton, C. Tan, B. D. Boyan, and Z. Schwartz, “Microstructured titanium regulates interleukin production by osteoblasts, an effect modulated by exogenous BMP-2.,” *Acta Biomater.*, vol. 9, no. 3, pp. 5821–9, Mar. 2013.

[20] G. Zhao, Z. Schwartz, M. Wieland, F. Rupp, J. Geis-Gerstorfer, D. L. Cochran, and B. D. Boyan, “High surface energy enhances cell response to titanium substrate microstructure.,” *J. Biomed. Mater. Res. A*, vol. 74, no. 1, pp. 49–58, Jul. 2005.

[21] A. Wennerberg, L. M. Svanborg, S. Berner, and M. Andersson, “Spontaneously formed nanostructures on titanium surfaces.,” *Clin. Oral Implants Res.*, vol. 24, no. 2, pp. 203–9, Feb. 2013.

[22] S. Sista, C. Wen, P. D. Hodgson, and G. Pande, “The influence of surface energy of titanium-zirconium alloy on osteoblast cell functions in vitro.,” *J. Biomed. Mater.*

Res. A, vol. 97, no. 1, pp. 27–36, Apr. 2011.

[23] J. Gottlow, M. Dard, F. Kjellson, M. Obrecht, and L. Sennerby, “Evaluation of a new titanium-zirconium dental implant: a biomechanical and histological comparative study in the mini pig.,” *Clin. Implant Dent. Relat. Res.*, vol. 14, no. 4, pp. 538–45, Aug. 2012.

[24] M. M. Bornstein, B. Schmid, U. C. Belser, A. Lussi, and D. Buser, “Early loading of non-submerged titanium implants with a sandblasted and acid-etched surface. 5-year results of a prospective study in partially edentulous patients.,” *Clin. Oral Implants Res.*, vol. 16, no. 6, pp. 631–8, Dec. 2005.

[25] D. L. Cochran, P. V Nummikoski, F. L. Higginbottom, J. S. Hermann, S. R. Makins, and D. Buser, “Evaluation of an endosseous titanium implant with a sandblasted and acid-etched surface in the canine mandible: radiographic results.,” *Clin. Oral Implants Res.*, vol. 7, no. 3, pp. 240–52, Sep. 1996.

[26] B. Lethaus, J. Kälber, G. Petrin, A. Brandstätter, and D. Weingart, “Early loading of sandblasted and acid-etched titanium implants in the edentulous mandible: a prospective 5-year study.,” *Int. J. Oral Maxillofac. Implants*, vol. 26, no. 4, pp. 887–92, Jan. .

[27] M. Roccuzzo, M. Aglietta, M. Bunino, and L. Bonino, “Early loading of sandblasted and acid-etched implants: a randomized-controlled double-blind split-mouth study. Five-year results.,” *Clin. Oral Implants Res.*, vol. 19, no. 2, pp. 148–52, Feb. 2008.

[28] A. Wennerberg, Albrektsson, and Galli, “Current knowledge about the hydrophilic and nanostructured SLActive surface,” *Clin. Cosmet. Investig. Dent.*, vol. Volume 3, pp. 59–67, Sep. 2011.

[29] E. Eisenbarth, J. Meyle, W. Nachtigall, and J. Breme, “Influence of the surface structure of titanium materials on the adhesion of fibroblasts.,” *Biomaterials*, vol. 17, no. 14, pp. 1399–403, Jul. 1996.

[30] A. C. Wu, L. J. Raggatt, K. A. Alexander, and A. R. Pettit, “Unraveling macrophage contributions to bone repair.,” *Bonekey Rep.*, vol. 2, p. 373, Jan. 2013.

[31] T. J. Koh and L. A. DiPietro, “Inflammation and wound healing: the role of the macrophage.,” *Expert Rev. Mol. Med.*, vol. 13, p. e23, Jan. 2011.

[32] P. Martin and S. J. Leibovich, “Inflammatory cells during wound repair: the good, the bad and the ugly.,” *Trends Cell Biol.*, vol. 15, no. 11, pp. 599–607, Nov. 2005.

[33] S. Lucke, A. Hoene, U. Walschus, A. Kob, J.-W. Pissarek, and M. Schlosser, “Acute and chronic local inflammatory reaction after implantation of different extracellular porcine dermis collagen matrices in rats.,” *Biomed Res. Int.*, vol. 2015, p. 938059, 2015.

[34] V. Lazarevic, L. H. Glimcher, and G. M. Lord, “T-bet: a bridge between innate and adaptive immunity,” *Nat. Rev. Immunol.*, vol. 13, no. 11, pp. 777–789, Oct. 2013.

[35] X. Song, H. Gao, and Y. Qian, “Th17 Differentiation and Their Pro-inflammation Function,” in *Advances in experimental medicine and biology*, vol. 841, 2014, pp. 99–151.

[36] K. Hirahara and T. Nakayama, “CD4+ T-cell subsets in inflammatory diseases: beyond the Th1/Th2 paradigm.,” *Int. Immunol.*, vol. 28, no. 4, pp. 163–71, Apr. 2016.

[37] M. O. Li and A. Y. Rudensky, “T cell receptor signalling in the control of regulatory T cell differentiation and function,” *Nat. Rev. Immunol.*, vol. 16, no. 4, pp. 220–233, Mar. 2016.

[38] H. Lei, K. Schmidt-Bleek, A. Dienelt, P. Reinke, and H.-D. Volk, “Regulatory T cell-mediated anti-inflammatory effects promote successful tissue repair in both indirect and direct manners.,” *Front. Pharmacol.*, vol. 6, p. 184, 2015.

[39] S. Schiaffino, M. G. Pereira, S. Ciciliot, and P. Rovere-Querini, “Regulatory T cells and skeletal muscle regeneration,” *FEBS J.*, vol. 284, no. 4, pp. 517–524, Feb. 2017.

[40] F. Lebre, C. H. Hearnden, and E. C. Lavelle, “Modulation of Immune Responses by Particulate Materials,” *Adv. Mater.*, vol. 28, no. 27, pp. 5525–5541, Jul. 2016.

[41] A. F. Mavrogenis, R. Dimitriou, J. Parvizi, and G. C. Babis, “Biology of implant osseointegration.,” *J. Musculoskelet. Neuronal Interact.*, vol. 9, no. 2, pp. 61–71, Jan. 2009.

[42] “Wound Healing and Growth Factors: Overview, Types of Wound Healing, Phases of Wound Healing.” [Online]. Available: http://emedicine.medscape.com/article/1298196-overview. [Accessed: 08-Jan-2016].

[43] M. L. Novak and T. J. Koh, “Macrophage phenotypes during tissue repair.,” *J. Leukoc. Biol.*, vol. 93, no. 6, pp. 875–81, Jun. 2013.

[44] S. K. Brancato and J. E. Albina, “Wound macrophages as key regulators of repair: origin, phenotype, and function.,” *Am. J. Pathol.*, vol. 178, no. 1, pp. 19–25, Jan. 2011.

[45] D. M. Mosser and J. P. Edwards, “Exploring the full spectrum of macrophage activation.,” *Nat. Rev. Immunol.*, vol. 8, no. 12, pp. 958–69, Dec. 2008.

[46] Y. S. Schwartz and A. V Svistelnik, “Functional phenotypes of macrophages and the M1-M2 polarization concept. Part I. Proinflammatory phenotype.,” *Biochem. Moscow*, vol. 77, no. 3, pp. 246–60, Mar. 2012.

[47] A. Sica and A. Mantovani, “Macrophage plasticity and polarization: in vivo veritas.,” *J. Clin. Invest.*, vol. 122, no. 3, pp. 787–95, Mar. 2012.

[48] F. Y. McWhorter, T. Wang, P. Nguyen, T. Chung, and W. F. Liu, “Modulation of macrophage phenotype by cell shape,” *Proc. Natl. Acad. Sci.*, vol. 110, no. 43, pp. 17253–17258, Oct. 2013.

[49] R. Olivares-Navarrete, S. L. Hyzy, R. A. Gittens, J. M. Schneider, D. A. Haithcock, P. F. Ullrich, P. J. Slosar, Z. Schwartz, and B. D. Boyan, “Rough titanium alloys regulate osteoblast production of angiogenic factors.,” *Spine J.*, vol. 13, no. 11, pp. 1563–70, Nov. 2013.

[50] F. O. Martinez and S. Gordon, “The M1 and M2 paradigm of macrophage activation: time for reassessment.,” *F1000Prime Rep.*, vol. 6, p. 13, Jan. 2014.

[51] A. Mantovani, S. K. Biswas, M. R. Galdiero, A. Sica, and M. Locati, “Macrophage plasticity and polarization in tissue repair and remodelling.,” *J. Pathol.*, vol. 229, no. 2, pp. 176–85, Jan. 2013.

[52] J. Pajarinen, V.-P. Kouri, E. Jämsen, T.-F. Li, J. Mandelin, and Y. T. Konttinen, “The response of macrophages to titanium particles is determined by macrophage polarization.,” *Acta Biomater.*, vol. 9, no. 11, pp. 9229–40, Nov. 2013.

[53] K. M. Hotchkiss, G. B. Reddy, S. L. Hyzy, Z. Schwartz, B. D. Boyan, and R. Olivares-Navarrete, “Titanium surface characteristics, including topography and wettability, alter macrophage activation,” *Acta Biomater.*, vol. 31, pp. 425–434, Feb. 2016.

[54] K. M. Hotchkiss, N. B. Ayad, S. L. Hyzy, B. D. Boyan, and R. Olivares-Navarrete, “Dental implant surface chemistry and energy alter macrophage activation in vitro.,” *Clin. Oral Implants Res.*, Mar. 2016.

[55] G. N. Thalji, S. Nares, and L. F. Cooper, “Early molecular assessment of osseointegration in humans.,” *Clin. Oral Implants Res.*, vol. 25, no. 11, pp. 1273–85, Nov. 2014.

[56] K. A. Alexander, M. K. Chang, E. R. Maylin, T. Kohler, R. Müller, A. C. Wu, N. Van Rooijen, M. J. Sweet, D. A. Hume, L. J. Raggatt, and A. R. Pettit, “Osteal macrophages promote in vivo intramembranous bone healing in a mouse tibial injury model.,” *J. Bone Miner. Res.*, vol. 26, no. 7, pp. 1517–32, Jul. 2011.

[57] L. J. Raggatt, M. E. Wullschleger, K. A. Alexander, A. C. K. Wu, S. M. Millard, S. Kaur, M. L. Maugham, L. S. Gregory, R. Steck, and A. R. Pettit, “Fracture healing via periosteal callus formation requires macrophages for both initiation and progression of early endochondral ossification.,” *Am. J. Pathol.*, vol. 184, no. 12, pp. 3192–204, Dec. 2014.

[58] B. P. Sinder, A. R. Pettit, and L. K. McCauley, “Macrophages: Their Emerging Roles in Bone,” *J. Bone Miner. Res.*, vol. 30, no. 12, pp. 2140–2149, Dec. 2015.

[59] C. Schlundt, T. El Khassawna, A. Serra, A. Dienelt, S. Wendler, H. Schell, N. van Rooijen, A. Radbruch, R. Lucius, S. Hartmann, G. N. Duda, and K. Schmidt-Bleek, “Macrophages in bone fracture healing: Their essential role in endochondral ossification,” *Bone*, vol. 106, pp. 78–89, Jan. 2018.

[60] S. Franz, S. Rammelt, D. Scharnweber, and J. C. Simon, “Immune responses to implants - a review of the implications for the design of immunomodulatory biomaterials.,” *Biomaterials*, vol. 32, no. 28, pp. 6692–709, Oct. 2011.

[61] O. Veiseh, J. C. Doloff, M. Ma, A. J. Vegas, H. H. Tam, A. R. Bader, J. Li, E. Langan, J. Wyckoff, W. S. Loo, S. Jhunjhunwala, A. Chiu, S. Siebert, K. Tang, J. Hollister-Lock, S. Aresta-Dasilva, M. Bochenek, J. Mendoza-Elias, Y. Wang, M. Qi, D. M. Lavin, M. Chen, N. Dholakia, R. Thakrar, I. Lacík, G. C. Weir, J. Oberholzer, D. L. Greiner, R. Langer, and D. G. Anderson, "Size- and shape-dependent foreign body immune response to materials implanted in rodents and non-human primates.," *Nat. Mater.*, vol. 14, no. 6, pp. 643–51, Jun. 2015.

[62] R. F. Diegelmann and M. C. Evans, "Wound healing: an overview of acute, fibrotic and delayed healing.," *Front. Biosci.*, vol. 9, pp. 283–9, Jan. 2004.

[63] C. J. Wilson, R. E. Clegg, D. I. Leavesley, and M. J. Pearcy, "Mediation of biomaterial-cell interactions by adsorbed proteins: a review.," *Tissue Eng.*, vol. 11, no. 1–2, pp. 1–18, Jan. .

[64] J. M. Anderson, A. Rodriguez, and D. T. Chang, "Foreign body reaction to biomaterials.," *Semin. Immunol.*, vol. 20, no. 2, pp. 86–100, Apr. 2008.

[65] M. Rabe, D. Verdes, and S. Seeger, "Understanding protein adsorption phenomena at solid surfaces.," *Adv. Colloid Interface Sci.*, vol. 162, no. 1–2, pp. 87–106, Feb. 2011.

[66] A. J. García, "Get a grip: integrins in cell-biomaterial interactions.," *Biomaterials*, vol. 26, no. 36, pp. 7525–9, Dec. 2005.

[67] S. Gronthos, P. J. Simmons, S. E. Graves, and P. G. Robey, "Integrin-mediated interactions between human bone marrow stromal precursor cells and the extracellular matrix.," *Bone*, vol. 28, no. 2, pp. 174–81, Feb. 2001.

[68] F. G. Giancotti and E. Ruoslahti, "Integrin signaling.," *Science*, vol. 285, no. 5430, pp. 1028–32, Aug. 1999.

[69] A. R. de Fougerolles and V. E. Koteliansky, "Regulation of monocyte gene expression by the extracellular matrix and its functional implications," *Immunol. Rev.*, vol. 186, no. 1, pp. 208–220, Aug. 2002.

[70] R. O. Hynes, "IntegrinsBidirectional, Allosteric Signaling Machines," *Cell*, vol. 110, no. 6, pp. 673–687, Sep. 2002.

[71] W. J. Hu, J. W. Eaton, T. P. Ugarova, and L. Tang, "Molecular basis of biomaterial-mediated foreign body reactions.," *Blood*, vol. 98, no. 4, pp. 1231–8, Aug. 2001.

[72] Y. Calle, S. Burns, A. J. Thrasher, and G. E. Jones, "The leukocyte podosome," *Eur. J. Cell Biol.*, vol. 85, no. 3, pp. 151–157, 2006.

[73] J. Monypenny, H.-C. Chou, I. Bañón-Rodríguez, A. J. Thrasher, I. M. Antón, G. E. Jones, and Y. Calle, "Role of WASP in cell polarity and podosome dynamics of myeloid cells," *Eur. J. Cell Biol.*, vol. 90, no. 2, pp. 198–204, 2011.

[74] K. T. Keylock, V. J. Vieira, M. A. Wallig, L. A. DiPietro, M. Schrementi, and J. A. Woods, "Exercise accelerates cutaneous wound healing and decreases wound

inflammation in aged mice.," *Am. J. Physiol. Regul. Integr. Comp. Physiol.*, vol. 294, no. 1, pp. R179-84, Jan. 2008.

[75] A. Gosain and L. A. DiPietro, "Aging and wound healing.," *World J. Surg.*, vol. 28, no. 3, pp. 321–6, Mar. 2004.

[76] S. H. Burnett, B. J. Beus, R. Avdiushko, J. Qualls, A. M. Kaplan, and D. A. Cohen, "Development of peritoneal adhesions in macrophage depleted mice.," *J. Surg. Res.*, vol. 131, no. 2, pp. 296–301, Apr. 2006.

[77] E. F. Redente, R. C. Keith, W. Janssen, P. M. Henson, L. A. Ortiz, G. P. Downey, D. L. Bratton, and D. W. H. Riches, "Tumor Necrosis Factor-α Accelerates the Resolution of Established Pulmonary Fibrosis in Mice by Targeting Profibrotic Lung Macrophages," *Am. J. Respir. Cell Mol. Biol.*, vol. 50, no. 4, pp. 825–837, Apr. 2014.

[78] N. van Rooijen, A. Sanders, and T. K. van den Berg, "Apoptosis of macrophages induced by liposome-mediated intracellular delivery of clodronate and propamidine.," *J. Immunol. Methods*, vol. 193, no. 1, pp. 93–9, Jun. 1996.

[79] C. L. Elsegood, C. W. Chan, M. A. Degli-Esposti, M. E. Wikstrom, A. Domenichini, K. Lazarus, N. van Rooijen, R. Ganss, J. K. Olynyk, and G. C. T. Yeoh, "Kupffer cell-monocyte communication is essential for initiating murine liver progenitor cell-mediated liver regeneration," *Hepatology*, vol. 62, no. 4, pp. 1272–1284, Oct. 2015.

[80] P. Alzuguren, S. Hervas-Stubbs, G. Gonzalez-Aseguinolaza, J. Poutou, P. Fortes, U. Mancheno, M. Bunuales, C. Olagüe, N. Razquin, N. Van Rooijen, M. Enguita, and R. Hernandez-Alcoceba, "Transient depletion of specific immune cell populations to improve adenovirus-mediated transgene expression in the liver," *Liver Int.*, vol. 35, no. 4, pp. 1274–1289, Apr. 2015.

[81] M. Davarpanah, H. Martinez, J. F. Tecucianu, R. Celletti, and R. Lazzara, "Small-diameter implants: indications and contraindications.," *J. Esthet. Dent.*, vol. 12, no. 4, pp. 186–94, Jan. 2000.

[82] N. Saulacic, D. D. Bosshardt, M. M. Bornstein, S. Berner, and D. Buser, "Bone apposition to a titanium-zirconium alloy implant, as compared to two other titanium-containing implants.," *Eur. Cell. Mater.*, vol. 23, pp. 273-86–8, Jan. 2012.

[83] S. Hamlet, M. Alfarsi, R. George, and S. Ivanovski, "The effect of hydrophilic titanium surface modification on macrophage inflammatory cytokine gene expression.," *Clin. Oral Implants Res.*, vol. 23, no. 5, pp. 584–90, May 2012.

[84] R. D. Stout, "Editorial: Macrophage functional phenotypes: no alternatives in dermal wound healing?," *J. Leukoc. Biol.*, vol. 87, no. 1, pp. 19–21, Jan. 2010.

[85] H. Terheyden, N. P. Lang, S. Bierbaum, and B. Stadlinger, "Osseointegration--communication of cells.," *Clin. Oral Implants Res.*, vol. 23, no. 10, pp. 1127–35, Oct. 2012.

[86] R. Trindade, T. Albrektsson, P. Tengvall, and A. Wennerberg, "Foreign Body

Reaction to Biomaterials: On Mechanisms for Buildup and Breakdown of Osseointegration.," *Clin. Implant Dent. Relat. Res.*, Sep. 2014.

[87] P. W. Kämmerer, V. Palarie, E. Schiegnitz, S. Hagmann, A. Alshihri, and B. Al-Nawas, "Vertical osteoconductivity and early bone formation of titanium-zirconium and titanium implants in a subperiosteal rabbit animal model.," *Clin. Oral Implants Res.*, vol. 25, no. 7, pp. 774–80, Jul. 2014.

[88] D. S. Thoma, A. A. Jones, M. Dard, L. Grize, M. Obrecht, and D. L. Cochran, "Tissue integration of a new titanium-zirconium dental implant: a comparative histologic and radiographic study in the canine.," *J. Periodontol.*, vol. 82, no. 10, pp. 1453–61, Oct. 2011.

[89] S. F. Badylak, J. E. Valentin, A. K. Ravindra, G. P. McCabe, and A. M. Stewart-Akers, "Macrophage phenotype as a determinant of biologic scaffold remodeling.," *Tissue Eng. Part A*, vol. 14, no. 11, pp. 1835–42, Nov. 2008.

[90] J. Prieto, A. Eklund, and M. Patarroyo, "Regulated Expression of Integrins and Other Adhesion Molecules during Differentiation of Monocytes into Macrophages," *Cell. Immunol.*, vol. 156, no. 1, pp. 191–211, Jun. 1994.

[91] T. D. Zaveri, J. S. Lewis, N. V Dolgova, M. J. Clare-Salzler, and B. G. Keselowsky, "Integrin-directed modulation of macrophage responses to biomaterials.," *Biomaterials*, vol. 35, no. 11, pp. 3504–15, Apr. 2014.

[92] A. Mócsai, C. L. Abram, Z. Jakus, Y. Hu, L. L. Lanier, and C. A. Lowell, "Integrin signaling in neutrophils and macrophages uses adaptors containing immunoreceptor tyrosine-based activation motifs," *Nat. Immunol.*, vol. 7, no. 12, pp. 1326–1333, Dec. 2006.

[93] C. Ammon, S. P. Meyer, L. Schwarzfischer, S. W. Krause, R. Andreesen, and M. Kreutz, "Comparative analysis of integrin expression on monocyte-derived macrophages and monocyte-derived dendritic cells.," *Immunology*, vol. 100, no. 3, pp. 364–9, Jul. 2000.

[94] S. Féréol, R. Fodil, B. Labat, S. Galiacy, V. M. Laurent, B. Louis, D. Isabey, and E. Planus, "Sensitivity of alveolar macrophages to substrate mechanical and adhesive properties," *Cell Motil. Cytoskeleton*, vol. 63, no. 6, pp. 321–340, Jun. 2006.

[95] D. R. Schmidt, H. Waldeck, and W. J. Kao, "Protein Adsorption to Biomaterials," in *Biological Interactions on Materials Surfaces*, New York, NY: Springer US, 2009, pp. 1–18.

[96] K. K. Chittur, "FTIR/ATR for protein adsorption to biomaterial surfaces," *Biomaterials*, vol. 19, no. 4–5, pp. 357–369, Mar. 1998.

[97] A. M. B. Collie, P. C. S. Bota, R. E. Johns, R. V. Maier, and P. S. Stayton, "Differential monocyte/macrophage interleukin-1β production due to biomaterial topography requires the β2 integrin signaling pathway," *J. Biomed. Mater. Res. Part A*, vol. 96A, no. 1, pp. 162–169, Jan. 2011.

[98] E. J. Brown, “Integrins of Macrophages and Macrophage-Like Cells,” Springer, Berlin, Heidelberg, 2003, pp. 111–130.

[99] L. Zhang, Y. Dong, Y. Dong, J. Cheng, and J. Du, “Role of integrin-β3 protein in macrophage polarization and regeneration of injured muscle.,” *J. Biol. Chem.*, vol. 287, no. 9, pp. 6177–86, Feb. 2012.

[100] T. H. Rogers and J. E. Babensee, “The role of integrins in the recognition and response of dendritic cells to biomaterials.,” *Biomaterials*, vol. 32, no. 5, pp. 1270–9, Feb. 2011.

[101] A. K. Blakney, M. D. Swartzlander, and S. J. Bryant, “The effects of substrate stiffness on the in vitro activation of macrophages and in vivo host response to poly(ethylene glycol)-based hydrogels.,” *J. Biomed. Mater. Res. A*, vol. 100, no. 6, pp. 1375–86, Jun. 2012.

[102] T. Okamoto, Y. Takagi, E. Kawamoto, E. J. Park, H. Usuda, K. Wada, and M. Shimaoka, “Reduced substrate stiffness promotes M2-like macrophage activation and enhances peroxisome proliferator-activated receptor γ expression,” *Exp. Cell Res.*, Apr. 2018.

[103] M. L. Previtera and A. Sengupta, “Substrate Stiffness Regulates Proinflammatory Mediator Production through TLR4 Activity in Macrophages.,” *PLoS One*, vol. 10, no. 12, p. e0145813, 2015.

[104] R. Olivares-Navarrete, A. L. Raines, S. L. Hyzy, J. H. Park, D. L. Hutton, D. L. Cochran, B. D. Boyan, and Z. Schwartz, “Osteoblast maturation and new bone formation in response to titanium implant surface features are reduced with age,” *J. Bone Miner. Res.*, vol. 27, no. 8, pp. 1773–1783, Aug. 2012.

[105] M. A. Alfarsi, S. M. Hamlet, and S. Ivanovski, “Titanium surface hydrophilicity modulates the human macrophage inflammatory cytokine response.,” *J. Biomed. Mater. Res. A*, vol. 102, no. 1, pp. 60–7, Jan. 2014.

[106] R. Sridharan, A. R. Cameron, D. J. Kelly, C. J. Kearney, and F. J. O’Brien, “Biomaterial based modulation of macrophage polarization: a review and suggested design principles,” *Mater. Today*, vol. 18, no. 6, pp. 313–325, Jul. 2015.

[107] J. J. El-Jawhari, E. Jones, and P. V. Giannoudis, “The roles of immune cells in bone healing; what we know, do not know and future perspectives,” *Injury*, vol. 47, no. 11, pp. 2399–2406, Nov. 2016.

[108] Z. Julier, A. J. Park, P. S. Briquez, and M. M. Martino, “Promoting tissue regeneration by modulating the immune system,” *Acta Biomater.*, vol. 53, pp. 13–28, Apr. 2017.

[109] M. Wong, J. Eulenberger, R. Schenk, and E. Hunziker, “Effect of surface topology on the osseointegration of implant materials in trabecular bone.,” *J. Biomed. Mater. Res.*, vol. 29, no. 12, pp. 1567–75, Dec. 1995.

[110] T. W. Oates, P. Valderrama, M. Bischof, R. Nedir, A. Jones, J. Simpson, H.

Toutenburg, and D. L. Cochran, “Enhanced implant stability with a chemically modified SLA surface: a randomized pilot study.,” *Int. J. Oral Maxillofac. Implants*, vol. 22, no. 5, pp. 755–60, Jan. 2007.

[111] L. Chiossone, R. Conte, G. M. Spaggiari, M. Serra, C. Romei, F. Bellora, F. Becchetti, A. Andaloro, L. Moretta, and C. Bottino, “Mesenchymal Stromal Cells Induce Peculiar Alternatively Activated Macrophages Capable of Dampening Both Innate and Adaptive Immune Responses,” *Stem Cells*, vol. 34, no. 7, pp. 1909–1921, Jul. 2016.

Vita

Kelly Morgan Hotchkiss was born on January 19th, 1990, in Williamsburg, Virginia, and is an American citizen. She graduated from Lee Davis High School in Mechanicsville, Virginia in 2008. Kelly received her bachelors of science in Materials Science and Engineering with minors in Chemistry and Engineering Science and Mechanics from Virginia Polytechnic Institute and State University in 2013.